



Final report from 2 November 2025

---

## DemoUpStorage

Demonstration and Upscaling of Carbon Dioxide storage for a net zero Switzerland

---



Source: Alba Zappone, 2023



# DEMO UP STORAGE

**Date:** 02.11.2025

**Location:** Bern

**Publisher:**

Swiss Federal Office of Energy SFOE  
Energy Research and Cleantech  
CH-3003 Berne  
[www.energy-research.ch](http://www.energy-research.ch)

**Subsidy recipients:**

Eidgenössische Technische Hochschule Zürich  
CH-8092 Zurich  
[www.ethz.ch](http://www.ethz.ch)

Ecole Polytechnique Fédérale de Lausanne  
CH-1015 Lausanne  
[www.epfl.ch](http://www.epfl.ch)

University of Geneva  
CH-1211, Geneve  
[www.unige.ch](http://www.unige.ch)

Eidgenössische Anstalt für Wasserversorgung, Abwasserreinigung und Gewässerschutz  
Oberlandstrasse 133, 8600 Dubendorf,  
[www.eawag.ch](http://www.eawag.ch)

**Authors:**

Alba Zappone, ETHZ, [alba.zappone@SED.ethz.ch](mailto:alba.zappone@SED.ethz.ch)  
Stefan Wiemer ETHZ, [stefan.wiemer@SED.ethz.ch](mailto:stefan.wiemer@SED.ethz.ch)  
Matthias Brennwald, EAWAG, [matthias.brennwald@eawag.ethz.ch](mailto:matthias.brennwald@eawag.ethz.ch)  
Irina Dallo, ETHZ, [irina.dallo@sed.ethz.ch](mailto:irina.dallo@sed.ethz.ch)  
Ovie Eruteya University of Geneva, [ovie.eruteya@unige.ch](mailto:ovie.eruteya@unige.ch)  
Jonas Simon Junker, ETHZ, [jonas.junker@sed.ethz.ch](mailto:jonas.junker@sed.ethz.ch)  
Rolf Kipfer, EAWAG, [rolf.kipfer@eawag.ch](mailto:rolf.kipfer@eawag.ch)  
Lyesse Laloui, EPFL, [lyesse.laloui@epfl.ch](mailto:lyesse.laloui@epfl.ch)  
Michèle Marti, [michele.marti@sed.ethz.ch](mailto:michele.marti@sed.ethz.ch)  
Andrea Moscariello, University of Geneva, [andrea.moscariello@unige.ch](mailto:andrea.moscariello@unige.ch)  
Anne Obermann, ETHZ, [anne.obermann@sed.ethz.ch](mailto:anne.obermann@sed.ethz.ch)  
Antonio Pio Rinaldi, [antonio.pio.rinaldi@sed.ethz.ch](mailto:antonio.pio.rinaldi@sed.ethz.ch)  
Katinka Tuinsra, [katinka.tuinstra@sed.ethz.ch](mailto:katinka.tuinstra@sed.ethz.ch)  
Eleni Stavropoulou, EPFL, [eleni.stavropoulou@epfl.ch](mailto:eleni.stavropoulou@epfl.ch)  
Stefanie Zeller, ETHZ, [stefanie.zeller@sed.ethz.ch](mailto:stefanie.zeller@sed.ethz.ch)

**SFOE project coordinators:**

Men Wirz, [Men.Wirz@bfe.admin.ch](mailto:Men.Wirz@bfe.admin.ch)  
Florence Bégue, [Florence.Begue@bfe.admin.ch](mailto:Florence.Begue@bfe.admin.ch)

**SFOE contract number:** SI/502429-01

**The authors bear the entire responsibility for the content of this report and for the conclusions drawn therefrom.**



## Summary

The DemoUpStorage project, entitled “Demonstration and Upscaling of Solutions for CO<sub>2</sub> Storage for a Net-Zero Switzerland”, aims to test advanced geophysical monitoring techniques combined with geochemical observations at the Carbfix injection site in Helgúvík, Iceland. Helgúvík serves as a field-scale demonstration site trialling the injection of CO<sub>2</sub> dissolved in saline groundwater similar to seawater into basalt formations and mineral storage. This is an important step towards overcoming the major limitation associated with freshwater use of this method, opening new perspectives for offshore and nearshore CO<sub>2</sub> storage. The in-situ operations are supported by numerical modelling and laboratory experiments. By conducting CO<sub>2</sub> storage research where suitable basalt formations exist, DemoUpStorage provides Switzerland with the scientific, technical, and social foundations, urgently needed to scale from pilot testing to full-scale industrial deployment of transnational carbon storage.

DemoUpStorage was conceived as a multidisciplinary pilot project, combining geosciences (site characterization, laboratory work), engineering (monitoring tools), and social sciences (acceptance, communication) within the broader Swiss DemoUpCARMA project.

While no observations during the project indicated barriers to injections of CO<sub>2</sub> dissolved in saline groundwater, the limited volume of CO<sub>2</sub> injected precluded conclusive observations on subsurface processes such as mineralization during the DemoUpStorage project duration. Renewed injections at this site by Carbfix from October 2025 as part of a different project continue to support the project's main objectives.

Rock physics modelling and synthetic crosshole seismic studies defined the amount of mineral precipitation required to produce detectable seismic changes and identified the appropriate survey geometries. These results help determine the conditions under which time-lapse geophysical monitoring is feasible and guide the optimal design for industrial-scale sites. Laboratory experiments carried out within the project showed measurable reductions in porosity and permeability along with potential rapid precipitation of carbonates or other secondary minerals. These findings contribute to defining realistic boundary conditions and design guidelines for injectivity management, including targeting high-permeability flow paths, staged injection strategies, and contingency measures.

DemoUpStorage enabled a comprehensive characterization of the Helgúvík basalt reservoir, providing a detailed geological, mineralogical, and geophysical baseline of the injection site as well as improved understanding of porosity, permeability, and fracture networks. The project developed and validated new monitoring approaches, integrating on-site dissolved gas analysis (miniRUEDI), electrical resistivity tomography (ERT), and crosshole seismic tomography to observe CO<sub>2</sub> migration and mineralization over time. Numerical simulations established detection limits and improved understanding of how these methods can track CO<sub>2</sub> transport, reactions, and mineralization in real time. Laboratory experiments on basalt samples from the injection site quantified the geochemical and hydromechanical effects, showing how CO<sub>2</sub>-enriched saline water alters basalt flow properties (e.g., permeability reduction, pore clogging, pressure variations). These data enabled the correlation between laboratory and field scales.

DemoUpStorage generated transferable knowledge for future projects, documenting lessons learned in reservoir characterization, injection logistics, and monitoring. It also provided open datasets and methods that can guide future Swiss or international in-situ mineral storage initiatives. The project makes a significant contribution to Switzerland's net-zero roadmap by developing a real-world experimental platform within the DemoUpCARMA project, linking Swiss CO<sub>2</sub> capture with geological storage abroad.

## Zusammenfassung

Das DemoUpStorage-Projekt, mit dem Titel „Demonstration und Hochskalierung von Lösungen für die CO<sub>2</sub>-Speicherung für ein Netto-Null-Schweiz“, hat zum Ziel, moderne geophysikalische Überwachungstechniken in Kombination mit geochemischen Beobachtungen an der Carbfix-Injektionsanlage in



Helguvík (Island) zu erproben. Helguvík dient als Demonstrationsstandort im Feldmassstab, an dem die Injektion von in salzhaltigem Grundwasser (ähnlich Meerwasser) gelöstem CO<sub>2</sub> in Basaltformationen und dessen mineralische Speicherung getestet wird. Dies stellt einen wichtigen Schritt dar, um die wesentliche Einschränkung durch die Nutzung von Süswasser bei dieser Methode zu überwinden und eröffnet neue Perspektiven für die CO<sub>2</sub>-Speicherung im Offshore- und Küstenbereich. Die Vor-Ort-Arbeiten werden durch numerische Modellierungen und Laboruntersuchungen unterstützt. Durch die Durchführung von CO<sub>2</sub>-Speicherungsforschungen in Gebieten mit geeigneten Basaltformationen liefert DemoUpStorage der Schweiz die dringend benötigten wissenschaftlichen, technischen und gesellschaftlichen Grundlagen, um von Pilotversuchen zur vollständigen industriellen Umsetzung der transnationalen Kohlenstoffspeicherung zu gelangen.

DemoUpStorage wurde als multidisziplinäres Pilotprojekt konzipiert, das Geowissenschaften (Standortcharakterisierung, Laborarbeiten), Ingenieurwissenschaften (Überwachungstechnologien) und Sozialwissenschaften (Akzeptanz, Kommunikation) innerhalb des übergeordneten Schweizer DemoUpCARMA-Programms vereint. Obwohl während der Projektlaufzeit keine Beobachtungen auf Hindernisse für die Injektion von in salinem Grundwasser gelöstem CO<sub>2</sub> hindeuteten, liess das begrenzte injizierte CO<sub>2</sub>-Volumen keine abschliessenden Aussagen über unterirdische Prozesse wie die Mineralisierung während der Dauer des DemoUpStorage-Projekts zu. Erneute Injektionen an diesem Standort durch Carbfix ab Oktober 2025 im Rahmen eines anderen Projekts unterstützen weiterhin die Hauptziele des Projekts.

Gesteinsphysikalische Modellierungen und synthetische (numerische) seismische Crosshole-Studien bestimmen die Menge der Mineralfällung, die erforderlich ist, um seismische Veränderungen nachweisen zu können, und identifizierten geeignete Untersuchungsgeometrien. Diese Ergebnisse helfen, die Bedingungen zu bestimmen, unter denen zeitabhängige geophysikalische Überwachung möglich ist, und liefern Hinweise für das optimale Design industrieller Standorte. Laboruntersuchungen innerhalb des Projekts zeigten eine rasche Karbonatfällung sowie messbare Reduktionen von Porosität und Permeabilität. Diese Erkenntnisse tragen dazu bei, realistische Randbedingungen und Gestaltungsrichtlinien für das Injektivitätsmanagement zu definieren, einschliesslich der Fokussierung auf hochpermeable Fliesspfade, gestufte Injektionsstrategien und Notfallmassnahmen. DemoUpStorage ermöglichte eine umfassende Charakterisierung des Basaltreservoirs in Helguvík und lieferte eine detaillierte geologische, mineralogische und geophysikalische Ausgangsbasis des Injektionsstandorts sowie ein verbessertes Verständnis von Porosität, Permeabilität und Klufnetzwerken. Das Projekt entwickelte und validierte neue Überwachungsansätze, die Vor-Ort Gasanalyse (miniRUEDI), elektrische Widerstandstomographie (ERT) und seismische Crosshole-Tomographie integrieren, um die CO<sub>2</sub>-Migration und -Mineralisierung über die Zeit zu beobachten. Numerische Simulationen legten Nachweisgrenzen fest und verbesserten das Verständnis darüber, wie diese Methoden den CO<sub>2</sub>-Transport, chemische Reaktionen und Mineralisierung in Echtzeit verfolgen können. Laborversuche an Basaltproben des Injektionsstandorts quantifizierten die geochemischen und hydromechanischen Effekte und zeigten, wie CO<sub>2</sub>-angereichertes Salzwasser die Flieseigenschaften des Basalts verändert (z. B. Permeabilitätsreduktion, Porenverstopfung, Druckschwankungen). Diese Daten ermöglichten die Korrelation zwischen Labor- und Feldmassstab.

DemoUpStorage generierte übertragbares Wissen für zukünftige Projekte, dokumentierte die gewonnenen Erkenntnisse in der Reservoircharakterisierung, Injektionslogistik und Überwachung und stellte offene Datensätze und Methoden bereit, die künftige Schweizer oder internationale In-Situ-Mineralisierungsspeicherungsinitiativen leiten können. Das Projekt leistet einen bedeutenden Beitrag zur Netto-Null-Roadmap der Schweiz, indem es im Rahmen des DemoUpCARMA-Programms eine reale experimentelle Plattform entwickelt, die die CO<sub>2</sub>-Abscheidung in der Schweiz mit der geologischen Speicherung im Ausland verbindet.



## Résumé

Le projet DemoUpStorage, intitulé « Démonstration et mise à l'échelle de solutions de stockage du CO<sub>2</sub> pour une Suisse neutre en carbone », vise à tester des techniques avancées de surveillance géophysique combinées à des observations géochimiques sur le site d'injection Carbfix à Helgúvík, en Islande. Ce site sert de terrain d'expérimentation pour l'injection de CO<sub>2</sub> dissous dans de l'eau souterraine saline, similaire à l'eau de mer, dans des formations basaltiques afin d'assurer le stockage par minéralisation. Cette étape est importante pour surmonter la principale limitation de cette méthode liée à l'utilisation d'eau douce, ouvrant ainsi de nouvelles perspectives pour le stockage du CO<sub>2</sub> en mer et en zone côtière. Les opérations sur le site sont appuyées par des modélisations numériques et des expériences en laboratoire. En menant des recherches sur le stockage du CO<sub>2</sub> dans des régions où existent des formations basaltiques appropriées, DemoUpStorage fournit à la Suisse les bases scientifiques, techniques et sociales indispensables pour passer de la phase pilote à la mise en œuvre industrielle à grande échelle du stockage transnational du carbone.

DemoUpStorage est un projet pilote multidisciplinaire combinant les géosciences (caractérisation du site, travaux de laboratoire), le travail d'ingénieur (outils de surveillance) et les sciences sociales (acceptation, communication), dans le cadre plus large du projet suisse DemoUpCARMA.

Bien qu'aucune observation au cours du projet n'ait mis en évidence d'obstacles à l'injection de CO<sub>2</sub> dissous dans une eau souterraine saline, le volume limité de CO<sub>2</sub> injecté n'a pas permis d'observations concluantes des processus souterrains tels que la minéralisation durant la durée du projet DemoUpStorage. De nouvelles injections sur ce site par Carbfix à partir d'octobre 2025, dans le cadre d'un autre projet, continuent de soutenir les principaux objectifs du projet.

La modélisation géophysique des roches et les études sismiques synthétiques entre forages « cross-hole » ont permis de déterminer la quantité de précipitation minérale nécessaire pour produire des changements sismiques détectables et d'identifier les géométries de relevé sismique appropriées. Ces résultats contribuent à définir les conditions dans lesquelles la surveillance géophysique en temps différé est réalisable et à guider la conception optimale des sites à l'échelle industrielle. Les expériences de laboratoire menées dans le cadre du projet ont montré une précipitation rapide de carbonates ainsi qu'une réduction mesurable de la porosité et de la perméabilité. Ces résultats aident à définir des conditions limites réalistes et des directives de conception pour la gestion de l'injectivité, notamment en ciblant les zones à forte perméabilité, en prévoyant des stratégies d'injection en plusieurs étapes et en mettant en place des mesures de contingence.

DemoUpStorage a permis de caractériser de manière approfondie le réservoir basaltique d'Helgúvík, fournissant une base géologique, minéralogique et géophysique détaillée du site d'injection, et permettant une meilleure compréhension de la porosité, de la perméabilité et des réseaux de fractures. Le projet a permis de développer et valider de nouvelles approches de surveillance intégrant l'analyse des gaz dissous sur site (miniRUEDI), la tomographie de résistivité électrique (ERT) et la tomographie sismique entre forages (cross-hole), afin d'observer la migration et la minéralisation du CO<sub>2</sub> dans le temps. Les simulations numériques ont permis d'établir les seuils de détection et d'améliorer la compréhension de la manière dont ces méthodes peuvent suivre le transport, les réactions et la minéralisation du CO<sub>2</sub> en temps réel. Les expériences de laboratoire réalisées sur des échantillons de basalte prélevés sur le site d'injection ont permis de quantifier les effets géochimiques et hydromécaniques, et de montrer comment l'eau saline enrichie en CO<sub>2</sub> modifie les propriétés d'écoulement du basalte (par ex. réduction de la perméabilité, colmatage des pores, variations de pression). Ces données ont permis d'établir une corrélation entre les observations à l'échelle du laboratoire et du terrain.

DemoUpStorage a généré des connaissances transférables pour de futurs projets, en documentant les leçons tirées en matière de caractérisation des réservoirs, de la logistique d'injection et de la surveillance. L'ensemble des données et des méthodes sont mis à disposition publiquement pouvant guider de futures initiatives suisses ou internationales de stockage par minéralisation in situ. Le projet apporte une contribution significative à la feuille de route de la Suisse vers la neutralité carbone, en développant



une plateforme expérimentale réelle dans le cadre du projet DemoUpCARMA, qui relie la capture du CO<sub>2</sub> en Suisse au stockage géologique à l'étranger.



## Main findings («Take-Home Messages»)

- Helguvík is a scientifically robust testbed for scaling CO<sub>2</sub> mineral storage in basalts, using seawater. The reservoir characterization highlights strong geological heterogeneity, while the multidisciplinary monitoring innovations (dissolved noble gas + ERT + seismic) suggest, no leakage (after a monitoring period of ten months), and detectability of geochemical and geophysical signatures. Together, these provide a roadmap for safer, more efficient CO<sub>2</sub> storage through in situ mineralization in basalt worldwide. Scaling up will require balancing technical, environmental, and social factors.
- The following aspects have been investigated:
  1. Monitoring innovation: Combining geochemical (gas tracers), geophysical (seismic, ERT), and lab-based approaches provides a robust monitoring toolkit.
  2. Societal dimension: Public acceptance hinges on communication, perceived safety, and integration into broader decarbonization efforts.
- The basalt reservoir characterization at the Helguvík site evidenced a geology dominated by fractured basalt with heterogeneous flow properties, providing both challenges and opportunities for injection and monitoring.
- The rock physics modeling indicated that CO<sub>2</sub> mineralization can increase P-wave velocities due to carbonate precipitation, and synthetic seismic modeling showed that velocity changes as small as 1.5 % are detectable, provided an adequately dense sensors array, making crosshole seismic surveys a viable monitoring tool. This provides a geophysical method to complement chemical monitoring, potentially allowing direct localization of mineralization zones.
- The geophysical site characterization, which combined crosshole seismic and electrical resistivity tomography (ERT), successfully mapped zones of high and low porosity in the Helguvík basalt, in alignment with drill cuttings and well-logging data. These methods establish a baseline model of subsurface structure and potential CO<sub>2</sub> pathways, critical for long-term monitoring and ensuring mineralization efficiency.
- A novel on-site dissolved gas mass spectrometer (miniRuedi) tracked injected CO<sub>2</sub> and helium (inert tracer) in real time. Data showed that CO<sub>2</sub> transport was retarded, relative to the He tracer. No leakage was detected into the overlying freshwater aquifers. ERT showed localized resistivity decreases, indicating basalt dissolution near injection wells. Combined, these tools provide cost-effective and complementary monitoring strategies.
- Laboratory studies on CO<sub>2</sub>-seawater-basalt interactions confirmed that injecting CO<sub>2</sub> dissolved in seawater causes porosity reduction (up to 1.5%) and permeability decreases (up to an order of magnitude) within months, potentially due to carbonate precipitation and/or other secondary mineral formation. While this may indicate mineralization, it also highlights risks of pore clogging, which confirms the necessity to inject in fractured zones to ensure long-term injection capacity.
- Regarding social perceptions (Switzerland Case Study), public familiarity with CCS and CO<sub>2</sub> mineral storage remains low in Switzerland. Acceptance depends strongly on perceived risks/benefits, trust in institutions, and effective communication, with infographics and visual explanations preferred over text-only formats. Support is higher when CO<sub>2</sub> storage is presented as part of a broader climate mitigation strategy, not as a stand-alone solution.
- The main challenges of the project were the repeated delays in completing the injection site—outlined in detail in the DemoUpCARMA final report—and the limited volume of CO<sub>2</sub> injected, which pushed our monitoring system to the limits of its sensitivity.



# Contents

<b>Summary</b> .....	<b>3</b>
<b>Zusammenfassung</b> .....	<b>3</b>
<b>Résumé</b> .....	<b>5</b>
<b>Main findings («Take-Home Messages»)</b> .....	<b>7</b>
<b>Contents</b> .....	<b>8</b>
<b>List of figures</b> .....	<b>10</b>
<b>List of tables</b> .....	<b>12</b>
<b>List of abbreviations</b> .....	<b>13</b>
<b>1 Introduction</b> .....	<b>14</b>
1.1 Context and motivation.....	14
1.2 Overarching objectives .....	16
1.1.1. Identified issues and knowledge gaps.....	16
1.1.2. Implemented Methods.....	17
1.1.3. Initial Results .....	18
<b>2 Approach, method, results and discussion</b> .....	<b>19</b>
2.1 Organization of the Project (Approach).....	19
2.2 Description of the test site.....	20
2.3 Description of ex situ activities .....	24
2.4 Methods .....	25
2.4.1. Feasibility study for time-lapse CO <sub>2</sub> migration monitoring (WP2).....	25
2.4.2. Geophysical Monitoring (WP2) .....	26
2.4.3. Dissolved gases monitoring (WP2). .....	28
2.4.4. Rock typing (WP3).....	29
2.4.5. Reservoir modelling (WP3).....	30
2.4.6. Flow properties characterization and validation of processes (WP4).....	32
2.4.7. Independent investigation of societal acceptance (WP 5).....	32
2.4.8. Injection (Carbfix) .....	34
2.5 Results.....	34
2.5.1. Feasibility study for time-lapse CO <sub>2</sub> migration monitoring (WP2).....	34
2.5.2. Geophysical Baseline Characterization (WP2) .....	35
2.5.3. Rock typing (WP3).....	37
2.5.4. 3D Geological Model (WP3).....	38
2.5.5. Dissolved gases monitoring (WP2).....	43
2.5.6. Timelapse Electrical Resistivity Imaging (WP2) .....	44
2.5.7. Flow properties characterization and validation of processes (WP4).....	45
Societal Acceptance.....	49



2.6	Discussion.....	49
	2.6.1. Combined Geophysical and Geochemical Monitoring (WP2).....	49
	2.6.2. Rock typing (WP3).....	51
	2.6.3. Flow properties characterization and validation of processes (WP4).....	52
	2.6.4. Societal Studies (WP5).....	54
<b>3</b>	<b>Conclusions and outlook.....</b>	<b>55</b>
<b>4</b>	<b>National and international cooperation.....</b>	<b>57</b>
<b>5</b>	<b>Publications and other communications.....</b>	<b>58</b>
<b>6</b>	<b>References.....</b>	<b>59</b>



## List of figures

- Fig. 1: Schematic and simplified representation of the DemoUpStorage monitoring setup
- Fig. 2: DemoUpStorage Organization chart with the leading houses for each WP
- Fig. 3: Location of Helguvik on the Reykjanes Peninsula and position of recent eruption sites and seismicity.
- Fig. 4: Overview of the storage site.
- Fig. 5: Schematic of the geophysical and hydrochemical monitoring at the injection site
- Fig. 6: The arrival of the first monitoring equipment.
- Fig. 7: Plugs of basalts from the Helguvik site
- Fig. 8: Location of the wells and the backbone seismic stations.
- Fig. 9: Schematic of seismic and electrical resistivity surveys.
- Fig. 10: FO data and experimental layout of the DAS acquisition in borehole
- Fig. 11: Helium board layout (© Solexpert A.G).
- Fig. 12: Installation of the mass spectrometer and Ge-MIMS system.
- Fig. 13: Overview of samples used for the compositional, textural and rock property analysis
- Fig. 14: Subsurface database.
- Fig. 15: Experimental setup for flow characterisation.
- Fig. 16: Overview of the research procedure on societal acceptance of CCTS/CCUS.
- Fig. 17: Results of numerical simulation on p-waves ( $V_p$ ) velocity variations.
- Fig. 18: Probabilistic Power Spectral Density (PPSD) of the backbone stations (DC01) 50m from the injection borehole.
- Fig. 19: Seismic tomography
- Fig. 20: Apparent resistivities with depth in CBM-03 for the Wenner (WE), Schlumberger (SL) and Dipole-Dipole configuration.
- Fig. 21: Stratigraphic subdivision based on petrographic description in boreholes CBM-01 and CBM-03.
- Fig. 22: Correlation panel between CBM-03 and CBM-01.
- Fig. 23: 3D conceptual reservoir model of the Helguvík site encompassing the small-scale sector model, outcrop and pseudo boreholes along the cliff and other boreholes in Helguvík.
- Fig. 24: Geological model of the Helguvík storage site.
- Fig. 25: Porosity and Permeability cross plot using conventional core analysis (Helium injection) on core plugs from HB wells.
- Fig. 26: Probabilistic-based static CO<sub>2</sub> storage capacity estimate for the study area - scenario 1.
- Fig. 27: Probabilistic-based static CO<sub>2</sub> storage capacity estimate for the study area - scenario 2.
- Fig. 28: Partial pressures of dissolved He, Ar, Kr, N<sub>2</sub>, O<sub>2</sub> and CO<sub>2</sub> observed at boreholes.
- Fig. 29: Timelapse: Relative changes in electrical resistivity between Summer 2023 and August 2024.
- Fig. 30: Porosity and hydraulic conductivity before and after CO<sub>2</sub> exposure.



- Fig. 31: Pore pressure propagation before and after CO<sub>2</sub> exposure.
- Fig. 32: Geophysical baseline characterization results with logging information along the borehole axis of CBI-01.
- Fig. 33: Cross-section porosity and permeability distribution through the study site with the layering identified in the cross-hole seismic and electrical resistivity data.
- Fig. 34: Magnified locations showing micro-fissure evolution of sample 05-02 before and after CO<sub>2</sub> exposure.



## List of tables

Table 1: The available well logs

Table 2: Parameters used for estimating CO<sub>2</sub> storage potential within the sector model – scenario 1.



## List of abbreviations

CCS	Carbon Capture and Storage
CCTS	Carbon Capture, Transportation, and Storage
CCUS	Carbon Capture, Utilization, and Storage
ERT	Electrical Resistivity Tomography
FO	Fiber Optics
LA- ICP-MS	Laser Ablation Inductively Coupled Plasma Mass Spectrometry
MIP	Mercury Intrusion Porosimetry
ML	Local Magnitude
Q&A	Questions and Answers
SFOE	Swiss Federal Office of Energy
V <sub>p</sub>	Seismic Compressional Waves Velocity
WP	Work Package
XRCT	3D x-ray computed tomography
XRF	X-ray Fluorescence



# 1 Introduction

## 1.1 Context and motivation

To fulfil the climate targets that Switzerland has set itself by 2050, Negative Emission Technologies (NETs) must be accompanied by Carbon Capture, Utilization, and Storage (CCUS), to compensate the hard-to-abate CO<sub>2</sub> emissions. Expanding plans to equip CO<sub>2</sub>-emitting plants with capture facilities are creating an ever-increasing demand for CO<sub>2</sub> storage. The most proven approach for CO<sub>2</sub> storage is compressing it into a liquid-like, supercritical form, and injecting it into porous rock formations, typically at a depth large enough to keep the CO<sub>2</sub> in liquid form and capped by an impermeable layer. The most promising reservoirs in sedimentary geological formations are either depleted oil and gas reservoirs, or deep saline aquifers (e.g. Benson and Cole, 2008), underneath an impermeable formation (caprock). Nevertheless, favourable geological conditions are site specific and might be locally limited, and the storage capacity still remains a general bottleneck in the CCUS chain. As an answer to this challenge, an increasing number of alternative storage methods targeting different geological settings is tested worldwide. Among the storage options that do not target sedimentary environments, the in-situ mineral carbonation in mafic and ultramafic rocks, is developing quite quickly. The technology consists of injection of water-dissolved CO<sub>2</sub> into rock formations that are particularly rich in calcium, iron and magnesium (mafic and ultramafic formations). Once CO<sub>2</sub> is dissolved in water, the acidic solution promotes the dissolution of silicate minerals, such as olivine, basaltic glass, pyroxene, and serpentine, releasing divalent cations such as Ca<sup>2+</sup>, Fe<sup>2+</sup> and Mg<sup>2+</sup> into the aqueous solution (e.g. Matter and Kelemen, 2009). These cations react with CO<sub>2</sub> to form non-toxic, solid and stable carbonate minerals like calcite, magnesite, and siderite within month or years (Gislason et al., 2014; Matter et al., 2016). Therefore, trapping of CO<sub>2</sub> in mineral form is achieved on much faster timescales compared to conventional storage methods where these processes are limited. Furthermore, the injection of water-dissolved CO<sub>2</sub> avoids the reliance on an impermeable caprock that is needed for free-phase CO<sub>2</sub> injections due to buoyance of the CO<sub>2</sub>. This method allows to target relatively shallow (c.a. 300 m) reservoirs, because there is no need to have a confining pressure that keeps CO<sub>2</sub> into supercritical or liquid form (conditions encountered typically at depth higher than 1km).

Despite the many advantages and the abundance of mafic rocks on the Earth's surface (Snæbjörnsdóttir et al., 2020), only a limited number of pilot projects deploying this technology have been or are ongoing (Wallula - USA, Chalk - Oman, Jizan and Fujairah - Saudi Arabia, Elementeita - Kenya), and three sites are commercially operational worldwide (all in Iceland). At the Hellisheiði geothermal power plant in Iceland, the company Carbfix (<https://www.carbfix.com>), injected more than 84,000 tCO<sub>2</sub> between 2014 and 2021 (Gunnarsson et al., 2018), and the injection capacity was recently increased with the new Silverstone capture plant. Furthermore, Carbfix operates two injection sites nearby where CO<sub>2</sub> captured directly from air (DAC) by the company Climeworks (projects Orca and Mammoth) is stored. Since March 2023, the Carbfix project started injecting CO<sub>2</sub> also from the Nesjavellir geothermal power plant, mirroring the mineralization approach used at Hellisheiði. This is part of the GECO (Geothermal Emission Control) project that aims to demonstrate the scalability of the method and the potential for widespread use in geothermal carbon capture and storage (<https://geco-h2020.eu/>). Future upscaling plans of the Carbfix company include the Coda Terminal, a cross-border carbon transport and storage hub for receiving CO<sub>2</sub> from European industrial sites via ships and then injecting it into the basalts. The project aims to store up to 3 million tons of CO<sub>2</sub> per year by 2031 ([https://climate.ec.europa.eu/system/files/2022-12/if\\_pf\\_2022\\_coda\\_en.pdf](https://climate.ec.europa.eu/system/files/2022-12/if_pf_2022_coda_en.pdf)). One main bottleneck of the in-situ carbonation method is the high demand for fresh water (≈ 25–27 tonnes of water are required to dissolve 1 tonne of CO<sub>2</sub> under common conditions); this can quickly become a limiting factor in upscaling the technology. To overcome the problem, in 2023 Carbfix started at Helguvík, on the Reykjanes peninsula, a first-ever field test using seawater to mineralize CO<sub>2</sub> underground. The test, already successful on a laboratory scale (Voigt et al., 2021), has the potential to significantly increase the applicability of the Carbfix method.

Carbfix is a main industrial partner both of the DemoUpStorage, and of the linked project DemoUpCARMA (also led by ETH and funded by the SFOE and by the FOEN) and of the Icelandic project CO<sub>2</sub>SeaStone. While DemoUpCARMA tests the feasibility to transport CO<sub>2</sub> from Switzerland to



Iceland, considering all the technological, economical, regulatory, political, and societal factors, CO<sub>2</sub>SeaStone, led by Carbfix, covers the injection activities and geochemical monitoring at Helgufvirk, complementing the combined geophysical and geochemical monitoring of DemoUpStorage.

Monitoring is a legally required component of injection site management. Today CO<sub>2</sub> geological storage in sedimentary environment is moving from demonstration into early commercial operation, several large hub projects are active, such as Gorgon (Barrow Island, Western Australia), Moomba (Cooper Basin, South Australia), Sleipner (Norway), Boundary Dam CCS (Saskatchewan, Canada) and the recent Northern Lights (Norway) are the largest active injections. Typically, in sedimentary storage projects monitoring uses a multi-tool approach: well logging and pressure/chemistry, repeated seismic surveys ((2D/3D, 4D time-lapse), controlled-source electrical resistivity mapping (EM), geodetic techniques that measure surface deformation, gravity (InSAR, GNSS), microseismic, fiberoptic for deformation and temperature distributed measurements (DAS, DTS), and soil/atmospheric gas sampling. These combined methods contribute to track plume location, reservoir pressure, leakage pathways and surface impacts, and to provide regulatory verification and public accountability. Geophysical methods in particular (time-lapse seismic, EM, gravimetry and DAS/DTS) are powerful for imaging plume movement and detecting mechanical changes. At Sleipner (North Sea) for example repeated 3D seismic since 1996 successfully monitor CO<sub>2</sub> migration and caprock containment (Furre et al., 2017). Crosshole & Vertical Seismic Profiling (VSP) are often complementary to surface seismic surveys gaining higher resolution near the wells, for example at Weyburn, Canada (White, 2013), or at CO<sub>2</sub>CRC, Otway (Yurikov et al., 2022). Microseismic Monitoring is regularly employed to assess the safety of injection operations (e.g., Quest, Canada, Goertz-Allmann et al., 2024; Decatur, Illinois, Kaven et al., 2015). Those methods suffer from limited resolution at depth, non-uniqueness of inversion, high survey and processing costs, dependence on good baseline surveys, and sensitivity thresholds that can miss small or slow leaks (Li et al., 2004). Major practical challenges remain open, such as scaling monitoring economically for many sites, integrating diverse data streams into reliable decision frameworks, quantifying long-term permanence (and associated liability), and managing geomechanical risks such as induced seismicity. These concerns, have prompted recent reappraisals of storage potential and emphasized careful siting and risk management (Gidden et al., 2025).

The monitoring in ultramafic or mafic rocks often rely on different technologies and focuses on different aspects compared to conventional storage, for which several methodologies and guidelines have been developed on this topic (Guidance Documents on EU CCS Directive (2009/31/EC); Guidance for Geological CO<sub>2</sub> Storage, 2024; ). Monitoring of reservoir processes mainly relies on geochemical measurements and sampling at monitoring wells. Methods using non-reactive and reactive tracers and fluid chemistry that track CO<sub>2</sub> dissolution, transport, and subsequent carbonate precipitation, have been proposed and successfully tested as a quantitative tool to confirm conversion to solid carbonates and other species (e.g. Matter et al., 2016). However, even if extremely powerful, these methods give data only at specific monitoring locations. While reservoir models can be used to gain a more comprehensive understanding, geophysical (electric, seismic) would have the advantage to track areal distribution of the carbonation at depth, but their sensitivity and interpretability depend strongly on (a) mineralogy and porosity of the host rock, (b) the scale of carbonate precipitation, and (c) availability of good baseline data and repeated surveys. Mineral trapping gives very high permanence compared with buoyant CO<sub>2</sub> plumes, but it produces weaker geophysical signals than free-phase CO<sub>2</sub>, because carbonation converts dissolved CO<sub>2</sub> into solid phases rather than forming large low-density CO<sub>2</sub> plumes. The petrophysical contrast produced by expected carbonation volumes can be near or below detection thresholds for many geophysical methods, especially at reservoir depths. Small changes in velocity, resistivity, or density can result from multiple causes (fluid changes, temperature, rock alteration, precipitation), so linking geophysical anomalies unambiguously to carbonate precipitation requires integrated hydro-geochemical reactive transport modelling and co-located ground truth (cores, logs, tracers).

Most of the above-mentioned challenges in monitoring with geophysical methods in basalts are tackled at hectometre scale in the pilot project in Helgufvirk. The project tests a complementary monitoring toolkit composed of continuous on-site dissolved-gas monitoring, borehole ERT, and crosshole seismic tomography, quantifying the sensitivity and limitations of each method. That allows to move from conceptual monitoring requirements to concrete, tested monitoring protocols and detection thresholds.



At the Helguvík site, CO<sub>2</sub> captured in Switzerland and transported via train and ships (see DemoUpCARMA Final Report<sup>1</sup>) is mixed with saline water from a nearby borehole and injected at 250-400m depth in a basaltic formation. The fate of the CO<sub>2</sub> was monitored via seismic and electric sensors installed at surface and in three monitoring boreholes a few decameter distance from the injection well. Moreover, gases dissolved in underground water were continuously monitored in shallow and deep aquifers. The field activities were complemented by numerical simulations and lab experiment on permeability variations due to carbon mineralization on basalts similar to the Helguvík reservoir. Societal aspects were also evaluated in cooperation with DemoUpCARMA and Carbfix. The description of the monitoring, of the modelling and of the lab activities are detailed in Chapter 2.2

Summarizing, the science and toolset to detect and image CO<sub>2</sub> exist and are improving rapidly, but limits in terms of sensitivity, cost, data interpretation, and long-term uncertainty mean that monitoring must be carefully designed, site-specific, and complemented by conservative permitting and governance.

One aspect that cannot be overlooked when proposing a new technology is its acceptance by the general public. Carbon Capture and Storage (CCS) and in particular mineral carbonation are technologies about which there is still a great deal of information lacking. It is important to recognize that public perception, acceptance, and support for Carbon Capture, Transportation and Storage (CCTS) and Carbon Capture, Utilization, and Storage (CCUS) initiatives are shaped by a variety of personal, social, and local factors. Higher levels of trust in industry, science, and government are linked to stronger public support (Jobin & Siegrist, 2020). Conversely, perceptions of uncontrollability (Arning et al., 2020), preferences for alternative climate mitigation strategies (Oltra et al., 2010), and concerns about risks or interference with nature (Jobin & Siegrist, 2020) tend to reduce public acceptance. DemoUpCARMA and DemoUpStorage add the novel aspect of onshore storage of CO<sub>2</sub> that was originated in a foreign country. This aspect had to be carefully assessed. For instance, Merk et al. (2022) found that Norwegians tend to show greater acceptance of CCTS/CCUS when the captured CO<sub>2</sub> originates domestically rather than from abroad. The communication of the project results to a wide audience including professional stakeholders and the general public was a key point. To this end, we collaborated closely with the DemoUpCARMA project team, building on their gained expertise. A website ([www.demoupcarma.ethz.ch](http://www.demoupcarma.ethz.ch)) was constantly updated with background information on the project, events and news. We developed also a number of key graphics to explain the concept of DemoUpStorage (see for example Fig. 1).

## 1.2 Overarching objectives

The overarching objective of the project is to demonstrate the safe and permanent storage of CO<sub>2</sub> in Icelandic basalt by complementing the existing Carbfix monitoring program with dense, combined geophysical and geochemical monitoring techniques. The project aims to demonstrate and benchmark geophysical monitoring strategies, complemented by dissolved gas detection methods, in order to improve the ability to track CO<sub>2</sub> migration and mineralization in situ. In addition to technological objectives, the project also seeks to independently assess safety aspects and social acceptance of CO<sub>2</sub> mineral storage, recognizing that public trust and transparency are essential for the deployment of carbon capture and storage technologies

### 1.1.1. Identified issues and knowledge gaps

As noted in previous chapters, geophysical techniques to monitor the carbonation at depth have been applied only to a few in situ- carbonation sites (Wallula – USA) and the need to better understand the limits and the potentialities of these methods is still open.

At Wallula, surface-based seismic surveys successfully imaged basalt layering beneath thin sediment cover and confirmed the absence of major faults. However, they did not produce a clear, direct time-lapse seismic signal that unambiguously tracked mineral carbonation in the reservoir (McGrail et al.,

---

<sup>1</sup> <https://www.aramis.admin.ch/Texte/?ProjectID=49400>



2014; White et al., 2020) and only pre- and post-hydrologic characterization and modelling results succeeded in indicating that approximately 60% of the injected CO<sub>2</sub> was sequestered via mineralization.

Similarly, although Carbfix has injected CO<sub>2</sub> for more than ten years at the Hellisheiði geothermal power plant using formation water as a dissolving fluid and continuously monitoring it using mainly geochemical methods, geophysical methods were not applied in a continuous and combined mode. Mineralization verification relied exclusively on water sampling, geochemical analyses, tracer tests, and interpretation in mass-balance calculations and reservoir models. While scientifically robust, this approach is significantly limited in spatial and temporal resolution of mineralization in the subsurface.

Tracer-based hydrogeological tests using dyes or salts are widely used to constrain mass balances and reactive CO<sub>2</sub> transport models (Rezvani et al., 2008; Ratouis et al., 2022; Matter et al., 2016; Gunnarsson et al., 2018). Reactive tracers provide additional insights, however, at field scale, only the original Hellisheiði experiment has applied direct <sup>14</sup>C labelling to track CO<sub>2</sub> transport and retention (Matter et al., 2016). The radiotoxicity of <sup>14</sup>C, together with the need for frequent groundwater sampling and laboratory analyses, makes such approaches costly, logistically demanding, and associated with delayed data availability.

### 1.1.2. Implemented Methods

Within DemoUpStorage, we implemented both borehole-based and surface-based geophysical monitoring technologies to observe the mineralization process at close. Helguvik represents the first field-scale demonstration where CO<sub>2</sub> dissolved in seawater-like saline groundwater is injected into basalts, directly addressing the major bottleneck for mineral storage: the usage of large quantities of freshwater. This approach also opens prospects for offshore and nearshore storage.

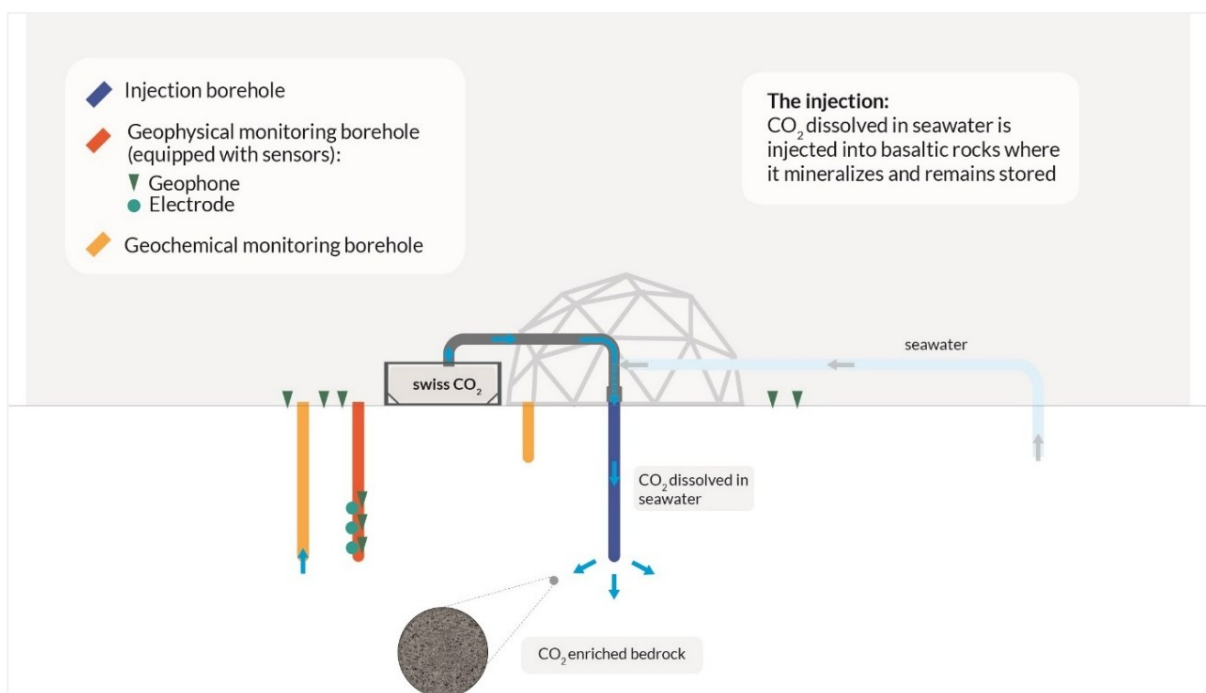


Fig. 1: Schematic and simplified representation of the DemoUpStorage monitoring setup, used for website and communication with public. Please note that the position of the wells and the horizontal and vertical scale do not represent reality. See Fig. 4 for the real experimental setup.



At Helguvík we benchmarked combined borehole- and surface-based monitoring techniques together with computational modelling tools, to reliably track and forecast the migration of CO<sub>2</sub> in difficult geological settings, that can become relevant for future CO<sub>2</sub> injection tests in Switzerland.

The monitoring strategy included seismic and geoelectric resistivity measurements in borehole-based and surface arrays. These observations were linked to continuous measurements of dissolved gasses in shallow and depth aquifers. The project applies a multidisciplinary approach that has already been successfully tested in decameter-scale CO<sub>2</sub> sequestration experimental projects (e.g., Zappone et al., 2021) to investigate whether integrated techniques can visualize fluid migration and carbonate precipitation in the reservoir.

To complement seismic and electrical resistivity methods we implemented gas tracing, using a new technique for autonomous, real-time, on-site monitoring of dissolved CO<sub>2</sub> and other gases in groundwater. A portable mass spectrometer (miniRuedi) coupled with a gas-equilibrium membrane-inlet (GEMIMS, Brennwald et al., 2024) enabled continuous on-site measurement of CO<sub>2</sub>, noble gases, and other species. At Helguvík, CO<sub>2</sub> was injected together with He as an inert tracer, and the partial pressures of CO<sub>2</sub>, He, and other dissolved gases were monitored over a one-year period.

### 1.1.3. Initial Results

Rock-physics modelling and numerical synthetic crosshole seismic studies conducted in DemoUpStorage defined the amount of mineral precipitation required to produce detectable seismic/elastic property changes as well as the survey geometries best suited to track mineralization. These result help to determine when geophysical time-lapse monitoring is feasible and how it should be design for industrial-scale applications.

The results contribute to the definition of realistic constraints and design rules for injectivity management, including the targeting of high-permeability pathways, staged injection strategies, and contingency measures. These insights are exportable also in other geological contexts, especially those pertinent to planned CO<sub>2</sub> injection tests in Switzerland.

Laboratory tests on rock samples performed within this project complement the numerous lab experiments previously conducted on basaltic powders by Carbfix, further demonstrating rapid carbonate precipitation and measurable reductions in porosity and permeability.

Microseismicity was monitored throughout injection operations to assess potential induced seismicity, an essential consideration for any subsurface fluid injection. In addition, possible CO<sub>2</sub> leakage pathways toward the atmosphere or shallow freshwater aquifers were monitored independently of the site operators. This independent monitoring aims to validate safety procedures through an impartial scientific assessment, reducing reputational risks associated with CCS deployment.

Finally, the project addressed societal aspects by independently assessing public perceptions of CO<sub>2</sub> mineral storage. Transparent communication and early stakeholder engagement were adopted to inform the public about both the benefits and risks of the process, recognizing that societal acceptance is a critical factor for successful project implementation (Stauffacher et al., 2015; Dechezleprêtre et al., 2022; Offermann-van Heek et al., 2020).

The Fig. 1 depicts the concept of the whole monitoring elements in a simple graphic form thought to be understandable by the general public, and has been used on our webpages, newsletters and talks.



## 2 Approach, method, results and discussion

### 2.1 Organization of the Project (Approach)

. As part of the DemoUpCARMA project, CO<sub>2</sub> captured from a Swiss biogas plant is transported to Iceland for injection. DemoUpStorage complements DemoUpCARMA by monitoring the CO<sub>2</sub> fate underground. The two projects together aim to evaluate the feasibility of cross-border CO<sub>2</sub> transport and storage (Dallo et al., 2024; Becattini et al., 2022).

The project consists of five components:

- Reservoir characterization, based on detailed geological, mineralogical, geochemical, and stratigraphic studies of the Helgúvík basalt reservoir.
- In situ monitoring using geophysical techniques combined with dissolved gas observations for continuous detection of the CO<sub>2</sub> pathway in the groundwater and in the portion above the layer into which the CO<sub>2</sub> is injected.
- Laboratory tests on rocks from the injection area, in which the effects of mineralization on the microstructure and hydromechanical properties of basalts are observed.
- Numerical simulations of in situ and laboratory tests, both in scoping and validation mode.
- Open, transparent, and continuous communication regarding safety and environmental issues related to storage.

DemoUpStorage was organized into five interlinked work packages:

- WP1 responsible for the organisational framework, the financial and administrative management, the timely implementation of the actions to achieve the objectives, the contribution to the dissemination of the results, the quality control, and the reporting of the results.
- WP2: responsible for mineralization monitoring. The working group was assessing the mobility of CO<sub>2</sub>-enriched water and mineralization processes by measuring changes in seismic velocity, electrical conductivity, and gas analysis of the formation waters near the injection. It provided a high-resolution image of the subsurface at reservoir scale as input to the reservoir model (WP3). The objectives of the WP also included benchmarking and knowledge transfer of monitoring technologies to the Swiss context.
- WP3: responsible for reservoir-scale geophysical and geological modelling, based on the integration of petrophysical properties of the reservoir rocks obtained from the laboratory, and the data collected in WP2.
- WP4: working at laboratory scale, it provided the mineralogical, petrophysical, and hydromechanical characterization of basalt reservoir rocks, evaluated their geomechanical and geochemical response to CO<sub>2</sub>-rich seawater injection, and quantified the time-dependent response of mineral trapping.
- WP5: responsible for independent investigation of the societal acceptance of 'foreign' CO<sub>2</sub> storage in Iceland. It also included knowledge transfer on CO<sub>2</sub> migration monitoring and risk assessment technologies to Swiss conditions and Swiss pilot projects.

The structure of the project is illustrated in Fig. 2.

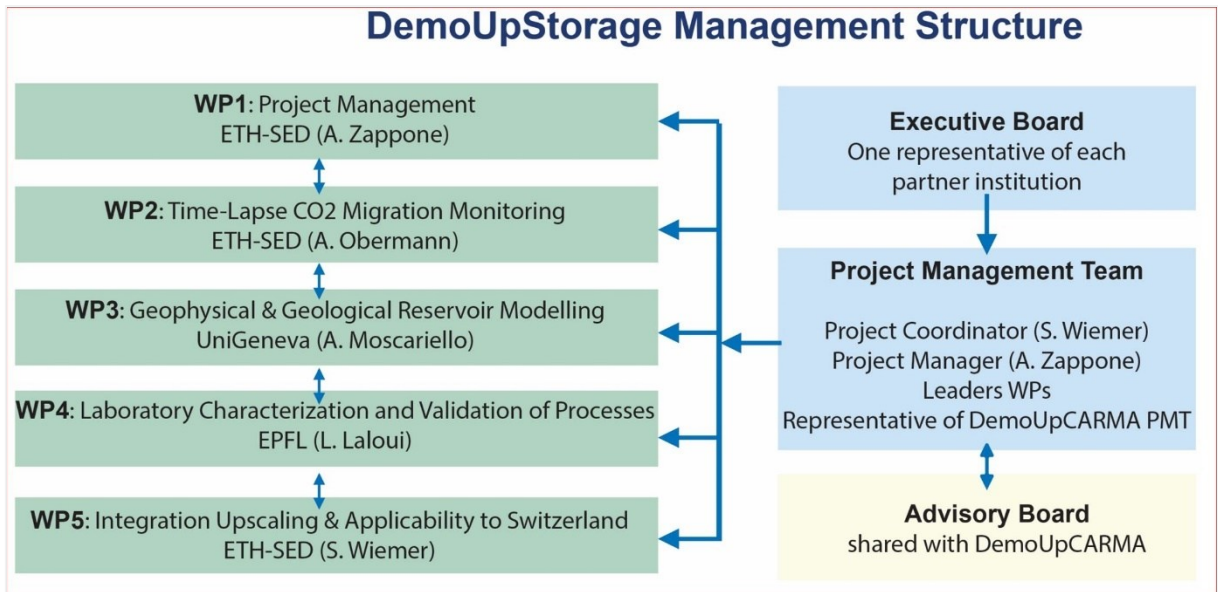


Fig. 2: DemoUpStorage Organization chart with the leading houses for each WP

## 2.2 Description of the test site

The Helguvík site represents the first field-scale demonstration of in-situ carbon mineralization using saline water

Initially an existing well (RH-03) located at Miðnesheiði on the Reykjanes Peninsula was evaluated as injection point for the storage, but after considering infrastructure and monitoring needs, the demonstration site was relocated to Helguvík in spring 2022. The new site offered better scalability and monitoring potential for CO<sub>2</sub> injection.

The site is located 1km northwest of Helguvík industrial harbour, 5 km north of Keflavík International Airport, on the Reykjanes Peninsula (Fig. 3a). It is positioned about 15 km north of the seismically and volcanically active Reykjanes rift zone (Fig. 3 b, c), which is characterised by five main volcanic regions and several tholeiitic lava flows that formed in historical times (875–1340 AD). Approximately 52% of the Reykjanes area is covered by Holocene lava fields, which consist mainly of hyaloclastite, i.e., fragmented, glassy volcanic rocks formed during phreatic (steam-induced) eruptions, often under glaciers, and tholeiitic lava flows. Sedimentary layers of marine origin are also present in the Helguvík area, indicating a rise in sea level during the last deglaciation phase (Moscariello et al., in prep., and references therein). Studies along the sea cliffs north of Helguvík (Vikingsson & Kristinsson, 1982) show that the upper 30 m of the stratigraphic section are cut by cooling-related fractures, mostly vertical joints and horizontal cracks parallel to flow boundaries, with no evidence of tectonic faulting. Since 2021, volcanic and tectonic activity at Fagradalsfjall, about 20 km southeast of the study area, has become more frequent and intense. Major eruptions in December 2023 at Svartsengi and in 2024 at Grindavík produced multi-kilometre fissures and lava flows covering several cubic kilometres, damaging houses and infrastructure. In contrast, the Helguvík area, remains relatively quiet seismically, with earthquakes generally well below magnitude 3 (Panzera et al., 2016; Chatelain, 2024, Fig. 3c).

At the test site, the basalt sequence hosts a freshwater aquifer at the depth of 25 m, with a thickness of ~ 40m, which flows eastwards towards the ocean. The deeper reservoir used for injections (~ 250 m to 400 m depth), contains seawater-derived saline water intruding from the sea shoreline located approx. 800 m east (Myer et al., 2019). Four lithological units, with different mineralogy and hydraulic permeabilities, have been identified, and will be described in detail in section 2.4.4

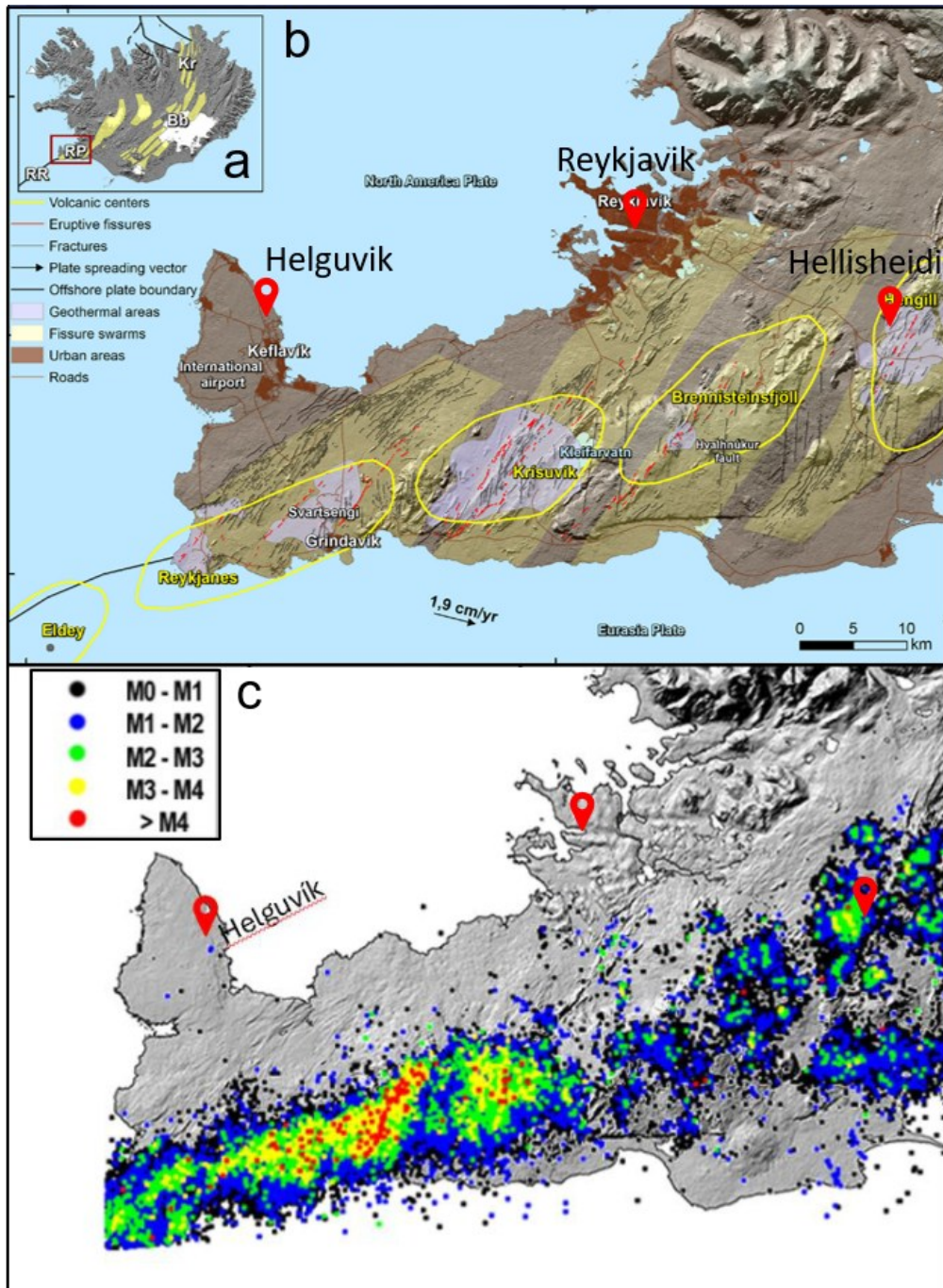


Fig. 3: Location of Helgúvík on the Reykjanes Peninsula and position of recent eruption sites and seismicity. (a) Map of Iceland showing the Reykjanes Ridge (RR) and the Reykjanes Peninsula (RP). (b) Boundaries of the main volcanic centres are marked with yellow lines. Superimposed on the fissure swarms (in black) are northerly strike-slip earthquake fractures (modified from Björnsson et al., 2020). (c) Earthquake localizations in the Reykjanes peninsula recorded between 2009 and 2022 (data from the Skjálfta-Lísa seismic network). The earthquake magnitudes, in local magnitude scale, range from 0 M<sub>L</sub> to 5.6 M<sub>L</sub> (modified from Chatelain, 2024).

Borehole drilling began in August 2022, and by June 2023, five vertical wells were completed. The boreholes, with depths between 32 m and 420 m, were drilled along a NW-SE alignment (Fig 4a). The southernmost well (CBI-1) serves as the CO<sub>2</sub> injection borehole, while the others are equipped for



geochemical and geophysical monitoring or used as groundwater sources (CBW-01). The injection well is open from 250 m depth to 420 m depth and spinner measurements indicate 2 main inflow zones, located at 285 m and 335 m depth where it is expected that the larger inflow occurs. The two monitoring wells CBM-03 and CBM-01, are c.a. 400 m deep, and are drilled respectively at 30 m and 100m distances from CBI-01. The shallow CBM-02 well, slightly out of the alignment and only 10 m from the injection, has the purpose to intercept the uppermost freshwater aquifer. The borehole setting has been designed to allow a combination of surface and borehole-based measurements to characterize the injection site and to monitor the CO<sub>2</sub> injection.

From CBM-01 and CBM-03, available drill-cutting samples allowed mineralogical and stratigraphic analysis. In February 2023, ÍSOR (Iceland Geosurvey) performed optical (CBI-01) and acoustic (CBM-01) televiewer, pressure (CBI-01 & CBM-01), temperature (CBI-01 & CBM-01), conductivity (CBM-01), neutron (CBI-01), calliper (CBM-01) and electrical resistivity (r16 and r64; CBM-01) logs in the boreholes. In addition, ÍSOR carried out a hydraulic spinner test in CBI-01.

The injection system, planned and realized by Carbfix, fits into a container installed on top of the injection well. CO<sub>2</sub> is mixed with saline water and tracers (salt) during injection. The container hosts also a mixing apparatus to add He as a tracer, and the portable mass spectrometer miniRuedi (Gasometrix GmbH, Switzerland, Brennwald et al., 2016), that measures the partial pressure of different gas species dissolved in water. The board that connects the He bottles to the Carbfix mixing system (Fig. 9) has been designed and realised by Solexpert AG (<https://www.solexperts.com/en/home>) and is now permanently used by Carbfix.

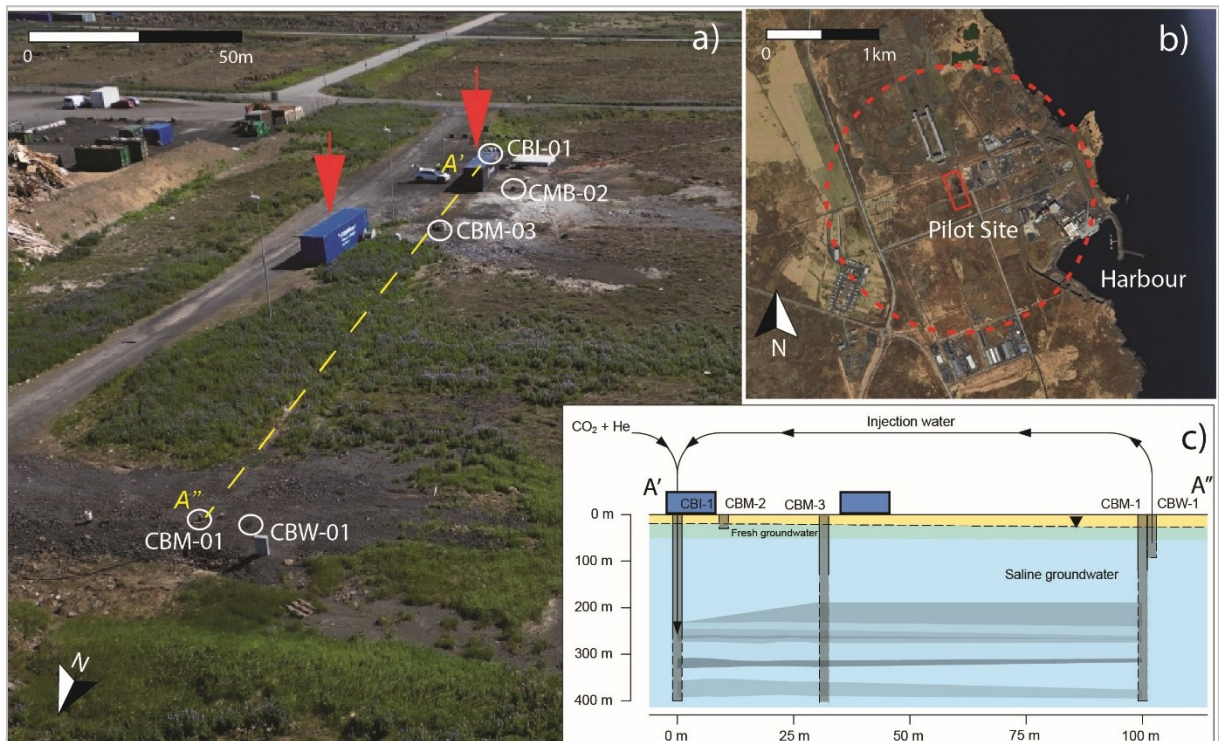


Fig. 4: Overview of the storage site. a) Helguvík study site, corresponding to the red rectangle in b), with the borehole names. The arrows indicate the container for monitoring equipment and the Carbfix injection container above CBI-01. B) Location of the study-site (red rectangle); the red dash line indicates the extension of the monitored area. c) Vertical cross-section diagram of the DemoUpStorage boreholes and injection schematic. The aquifer layers show various hydraulic permeability, and are represented in different tones of blue, ranging approximately from  $10^{-15} \text{ m}^2$  (dark) to  $10^{-13} \text{ m}^2$  (bright). Figure modified after Wiemer et al, 2024 and Brennwald et al., submitted Oct 2025)

The CO<sub>2</sub> and the water pumped from borehole CBW-01 (92 m depth and cased to bottom) are injected in pre-determined proportions into the reservoir through CBI-01 (Fig. 4c) from 250 m depth. The



pressure at 250 m depth is high enough to guarantee complete dissolution of the CO<sub>2</sub> in the water before entering the storage formation.

The first CO<sub>2</sub> injection—dissolved in seawater—occurred in October 2023, marking a global first. Subsequent work focused on optimizing the system, including relocating the tracer setup in December 2023 to improve sampling reliability. Intermittent CO<sub>2</sub> injection from Switzerland began on January 15, 2024, and by September 1, a total of 137 tons had been injected at an average rate of about 4 tons per week. This is well below the planned rate of 20t/week which could not be reached. The operation faced several logistical and technical challenges, including delays in equipment delivery, transportation disruptions, and a temporary halt due to a volcanic eruption. Despite these setbacks, system upgrades, flow tests, and geochemical monitoring were carried out to track changes in the surrounding groundwater and seawater.

The components of the DemoUpStorage monitoring setup were seismic measurements (at surface and downhole), electrical resistivity measurements (downhole), and dissolved gases analyses from the shallow and deep aquifers. Additionally, we installed distributed acoustic sensing (DAS) fiberoptics in all deep monitoring borehole from June to August 2023 and GPR measurements in CBM-03 were tested. A schematic illustration of the monitoring components is in Fig. 5. This monitoring setup supplemented the conventional monitoring carried out by Carbfix that is not described further here.

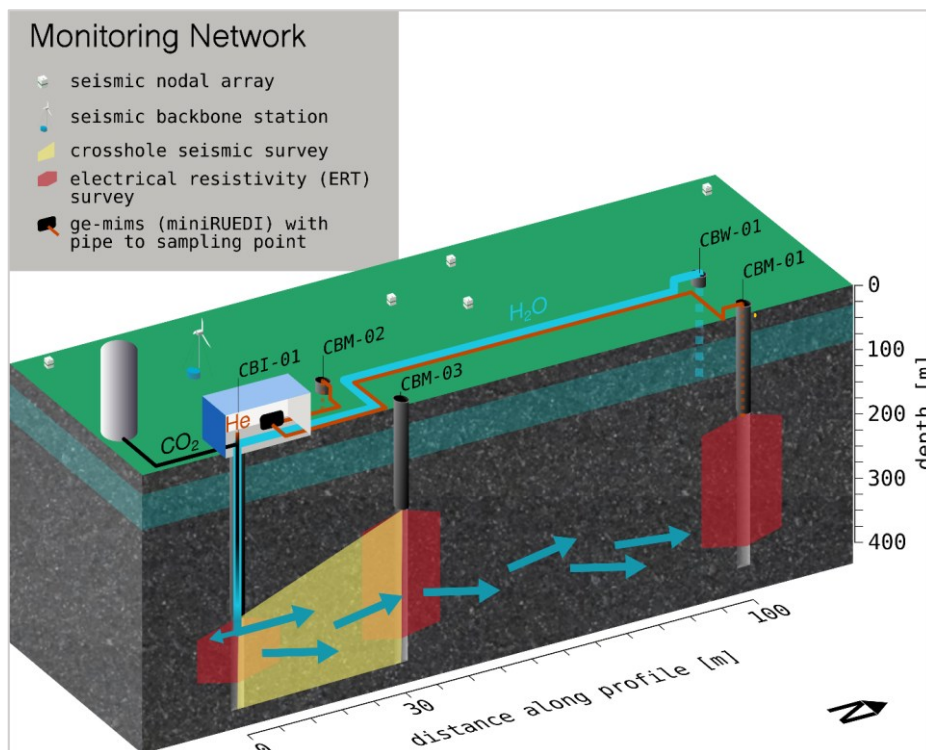


Fig. 5: Schematic of the geophysical and hydrochemical monitoring at the injection site. In yellow we indicate the area illuminated by seismic crosshole survey, in red the areas monitored by electric resistivity. The red lines indicate the connections of the mass spectrometer with the shallow (CMB-02) and deep (CMB-01) aquifers in light blue we schematize the flow of saline water from CBW-01 to the injection CBI-01 and to the deep aquifer. The black line illustrates the CO<sub>2</sub> flow to the head of the injection borehole.

A part of the surface seismic installation was an array of 5 ETH/SED backbone stations (Lennartz 5s seismometers), located around the injection site and collecting data continuously from September 2022 to September 2024. The aim of the seismic network was to monitor the background seismicity and the



seismicity potentially induced by the injection operations. The data were streamed in real-time to ETH Zurich and shared with all the project partners. The surface seismic array included also a mobile nodal seismic network, composed of 43 recording units (SmartSolo 5Hz 3-channel geophones), that were used from June to July 2023 for recording both ambient seismic noise and natural seismicity, and seismicity from energy sources in the boreholes and at the surface. No injections were performed during that period. The details of the measurements are specified in section 2.4.2 The aim was to define a velocity/depth model based on shear waves propagation.

Borehole seismic equipment consisted of a mobile energy source (P-wave sparker source type SBS-42 from Geotomographie GmbH) and a 24-channel BHC-42 hydrophone chain placed alternately in the



CBI-01 and the CBM-03. The electrical resistivity equipment consisted of a 24-electrode chain. We used a 24 channels electrode chain with 2m electrode spacing and a Geolog Geotom MK8E1000 ERT acquisition system, with the electrode chain placed in multiple depth positions to cover most of the open-hole sections. Due to the limited length of the electrode chain, we could only probe depth until 360 m. All these monitoring components were shipped from ETH Zurich and EAWAG Dubendorf, apart from the sparker that was directly shipped from Geotomographie GmbH in Bad Salzdetfurth, Germany. They were located in a container at the pilot side, that became the headquarters of the on-site monitoring operations (Fig. 4a and Fig. 6).

Fig.6. The arrival of the first monitoring equipment on June 14 at the monitoring container in June 2023.

### 2.3 Description of ex situ activities

An essential component of the DemoUpStorage project is being developed ex-situ, in the labs of the University of Geneva and EPFL Lausanne. At the department of Earth Sciences of the University of Geneva, drill-cutting samples from CMB-01 were used to characterize the stratigraphic sequence of the reservoir, in combination with borehole logging data and hydraulic spinner tests. Moreover, seven basalt cores (49 mm diameter) were analysed in the laboratory at EPFL in Lausanne, targeting porosity network and flow properties before and after laboratory exposure to CO<sub>2</sub>-rich saline water. The cores were taken from three shallow boreholes (HB-05, HB-07, and HB-08, Fig 14a) in the Holmsberg cliff near Helguvík, an area with distinct lava flow layers. It should be noted that these wells are shallower (~ 60 m depth) than the injection reservoir and therefore their properties do not necessarily correspond directly those of the reservoir, as especially permeability is often decreasing with depth in similar contexts. Because basalt forms from rapidly cooled lava, the cores display highly variable and visibly porous structures. The cores were chosen to represent different pore characteristics (Fig. 7).

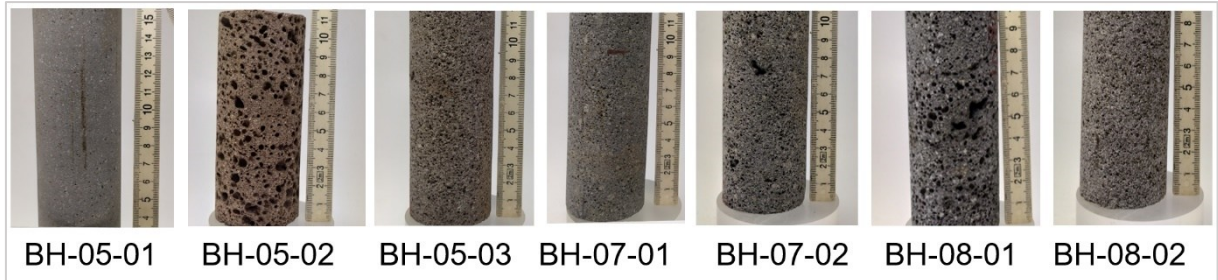


Fig. 7 Plugs of basalts from the Helguvík site, with various porosity and from different depth (modified after Stavropoulou et al., 2023)

We specify here that the drilling method at Helguvík was destructive (down-the-hole hammer drilling), no borehole cores from the five wells mentioned above were retrieved before injection, and no overcoring after injection has been performed at present date.

At the EPFL lab the hydromechanical characteristics of basalts were tested both before and after exposure to CO<sub>2</sub>-enriched fluid. The flow properties of the basaltic samples were tested using the experimental setup illustrated in Chapter 2.4.6 and Fig. 15. 3D x-ray computed tomography (XRCT) combined with pore network modelling was used to determine how mineralization affects the material's pore space. Additional measurement of the pore size range of the material has been performed using the Mercury Intrusion Porosimetry (MIP) method.

Using a scanning electron microscopy facility (QEMSCAN QUANTA 650F), the University of Geneva lab contributed by characterizing the mineralogical composition of the basalt, and measuring the porosity by difference between grain and bulk density.

A detailed description of the activities carried out in the project is reported in the section 2.4.6.

## 2.4 Methods

### 2.4.1. Feasibility study for time-lapse CO<sub>2</sub> migration monitoring (WP2)

Geophysical and geochemical time-lapse surveys are a crucial component of the DemoUpStorage pilot project. A feasibility study was performed both to prove the usability of the cross-hole seismic method for monitoring an in-situ CO<sub>2</sub> mineral storage experiment and to determine the optimal experimental setup for Helguvík. A seismic cross-hole survey that uses transit times of seismic waves between two wells to invert for the underlying velocity structure can provide the best spatial resolution for such an endeavour compared to surface or surface-to-well based surveys. The travel time differences between a baseline survey conducted before and after the injection can image the velocity anomaly caused by dissolutions and precipitations of minerals. The feasibility of imaging subsurface velocity anomalies has been investigated with the aid of wave propagation forward modelling methods, detailed in Junker et al. (submitted Aug 2025 to g3). The velocity anomaly was simulated with amplitudes of 0.1% to 5%, respectively to examine the setup's sensitivity. To learn more about the extension of the area that can be imaged with an acceptable resolution, forward scenarios with wells spaced 25 m, 50 m, 75 m and 100 m apart were examined. The results were decisive for the positioning of the geophysical monitoring well CMB-03 at 30 m from the injection well in Helguvík (Junker et al., 2022). A numerical study on the velocity changes expected by carbonate precipitation on basalts were also conducted and are detailed in (Junker et al., submitted Aug 2025). Using the MATLAB toolbox mTex (Bachmann et al., 2010) the range velocity variation due to mineralization was estimated. mTex enables the calculation of seismic velocities of mineral aggregates based on the stiffness tensors and the relative volumetric fractions of the mineral components. In this case the averaged volumetric mineral fractions of the core samples



provided by Carbfix and analysed at EPFL were used as input, and the effects of pore saturation was incorporated on the stiffness tensor (Li & Zhang, 2011; Gassmann, 1951).

#### 2.4.2. Geophysical Monitoring (WP2)

To monitor the background seismicity and seismicity potentially induced by the injection operations, a small backbone network consisting of five Lennartz 5s seismometers was installed in September 2022 around the injection site (Fig. 8). From June 10th to July 15th, 2023 the seismic array was supplemented with 43 3-component nodal geophones (type SmartSolo IGU-16HR 3C) that were buried at a shallow depth around the site for passive seismic imaging.

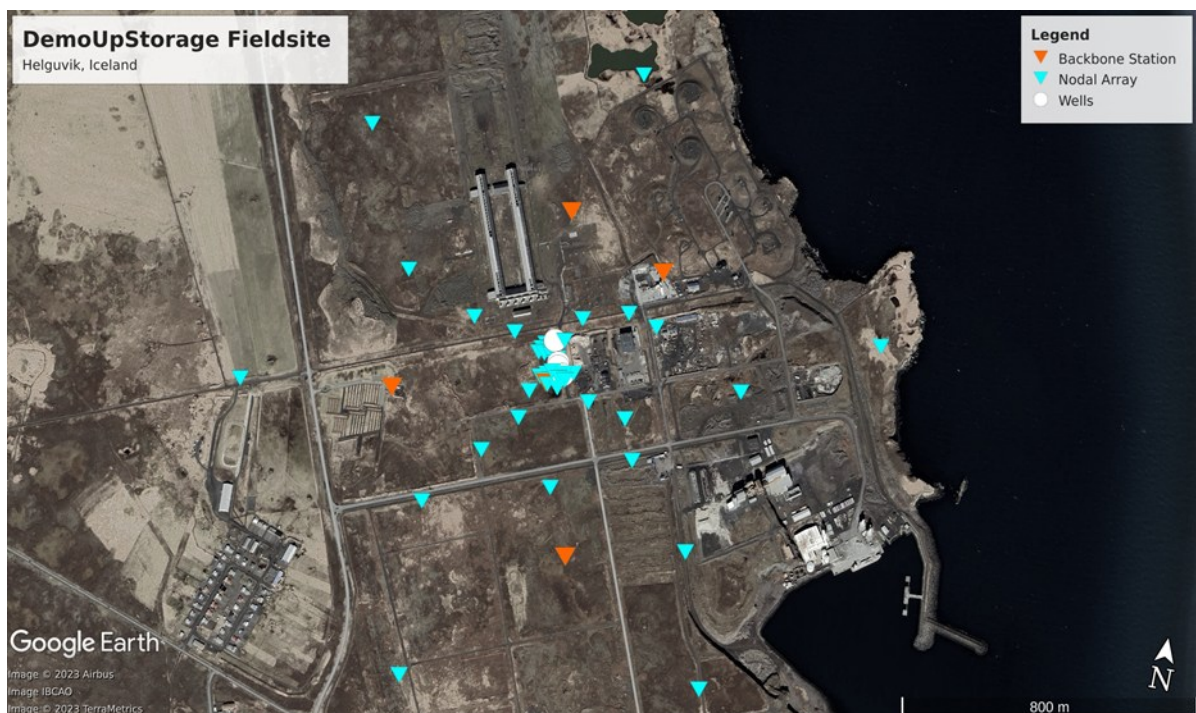


Fig. 8 Location of the wells and of the seismic stations. The backbone stations shown are in orange and the deployment locations of the nodal array for the baseline measurements are in light blue. Please note that one of the backbone stations is placed just in the middle of the nodal array.

Active seismic measurements were conducted as baseline in June and August 2023 (details in Junker et al., 2025). Seismic cross-hole between CBI-01 and CBM-03 (Fig.9a), was performed using a P-wave sparker source. The sparker shots were recorded with by the hydrophone chain with 2 m spacing in CBI-01 between 226 m and 404 m depth. Fiber optics (FO) hanging inside CBM-01 were used in parallel to the hydrophone chain as recording units. DAS measurements were carried out using the FEBUS-A1 interrogator, using a gauge length of 2 m, channel spacing of 0.8 m and a sampling rate of 1 kHz. The FO cable was lowered to the bottom of borehole CBI-1, and was kept in place by a weight attached to the bottom. This ensured that the hydrophone cable could move freely beside the FO cable. The potential of using DAS in this setting is that it can measure each shot along the full length of the borehole, whereas the hydrophone chain needs to be moved and manifold shots are needed to cover the full borehole. However, due to the lack of coupling of the FO to the bedrock, the sparker shots were not measured by the DAS. Unfortunately, we noticed strong interference between FO and hydrophone, compromising the data quality, therefore we decided to dismantle the FO installation after June 2023. Additionally, we performed a refraction seismic profile along the road parallel to the boreholes using a 370 Kg concrete weight as a seismic source. (Fig. 9b). 14 surface weight drops were recorded on FO and on 15 surface nodes that were placed in a line between CBI-01 and CBM-03. Due to the generally



high noise level of the pilot site, next to the industrial area and to the high dumping ground for building rubble, the signal-to-noise ratio was unsatisfactory. The waves could not penetrate the underground at the depth we were interested to, they illuminated only the shallow levels. A further analysis of these data is still pending.

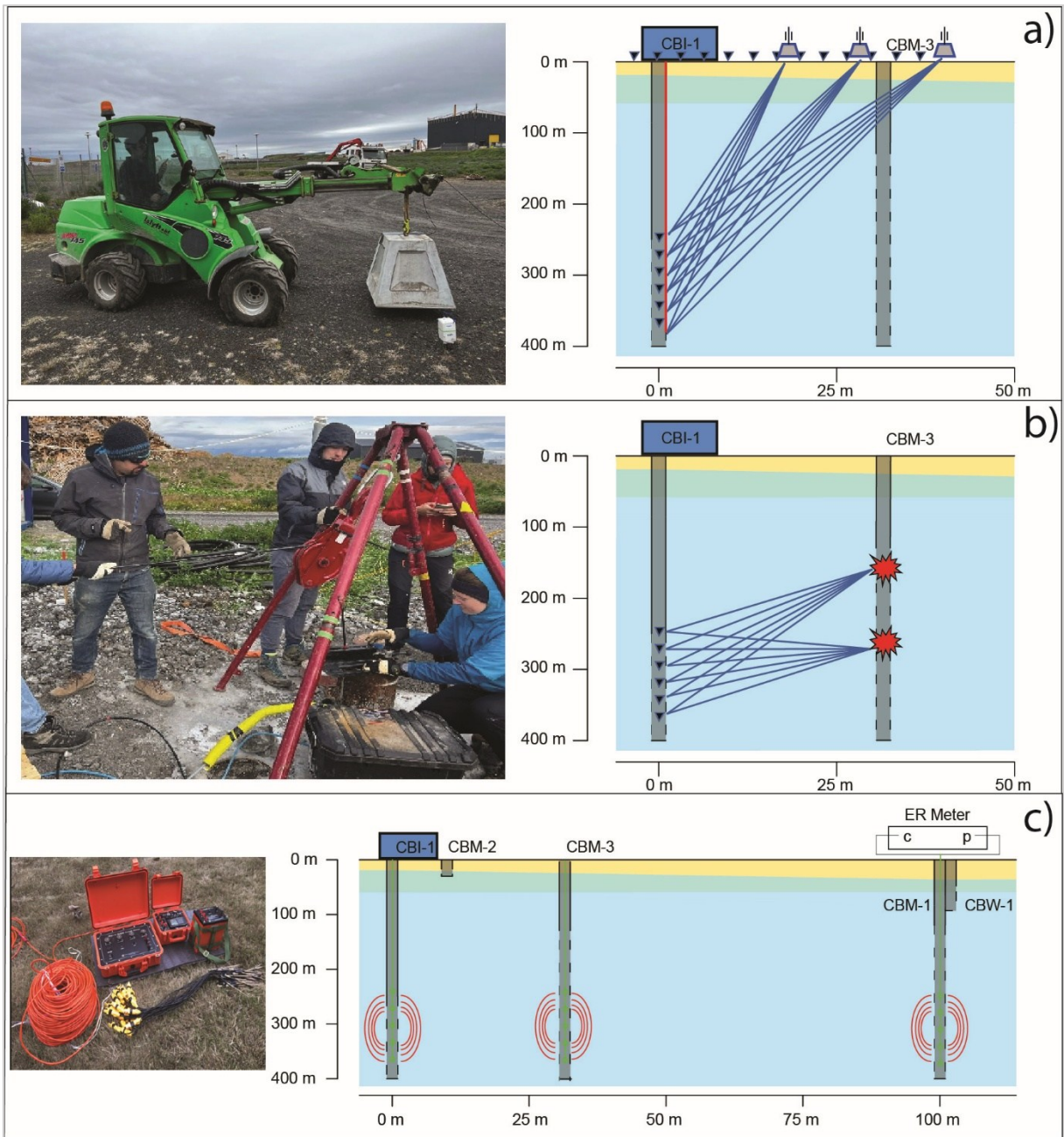


Fig. 9: schematic of seismic and electrical resistivity surveys. a) refraction and vertical seismic profile, black triangles are the hydrophones, red line is the Fiber optic, b) crosshole seismic with sparker lowered at different position in the boreholes; c) electrical resistivity performed in all boreholes and left for long term measurements in CMB-03

In parallel to seismic measurements, single-hole electrical resistivity tomography (ERT) was performed in CBI-01, CBM-01 and CBM-03 with a 24-electrode chain covering the whole open-hole sections (Fig. 9c). A Geolog Geotom MK8E1000 ERT system was used in different classical configurations (Wenner,



Schlumberger and Dipole-Dipole). After the measurement campaign in August 2023, we placed the electrode chain at 314m to 360m depth in CBM-03, for continuous measurement. The cross-hole seismic survey and the single-hole electrical resistivity survey were repeated in September 2024, 8 months after the start of the injection and with 137t CO<sub>2</sub> injected. The single-hole electrical resistivity survey was successful and produced reliable measurements. However, we were only able to repeat a small fraction of the cross-hole seismic survey due to a technical failure of the hydrophone chain.

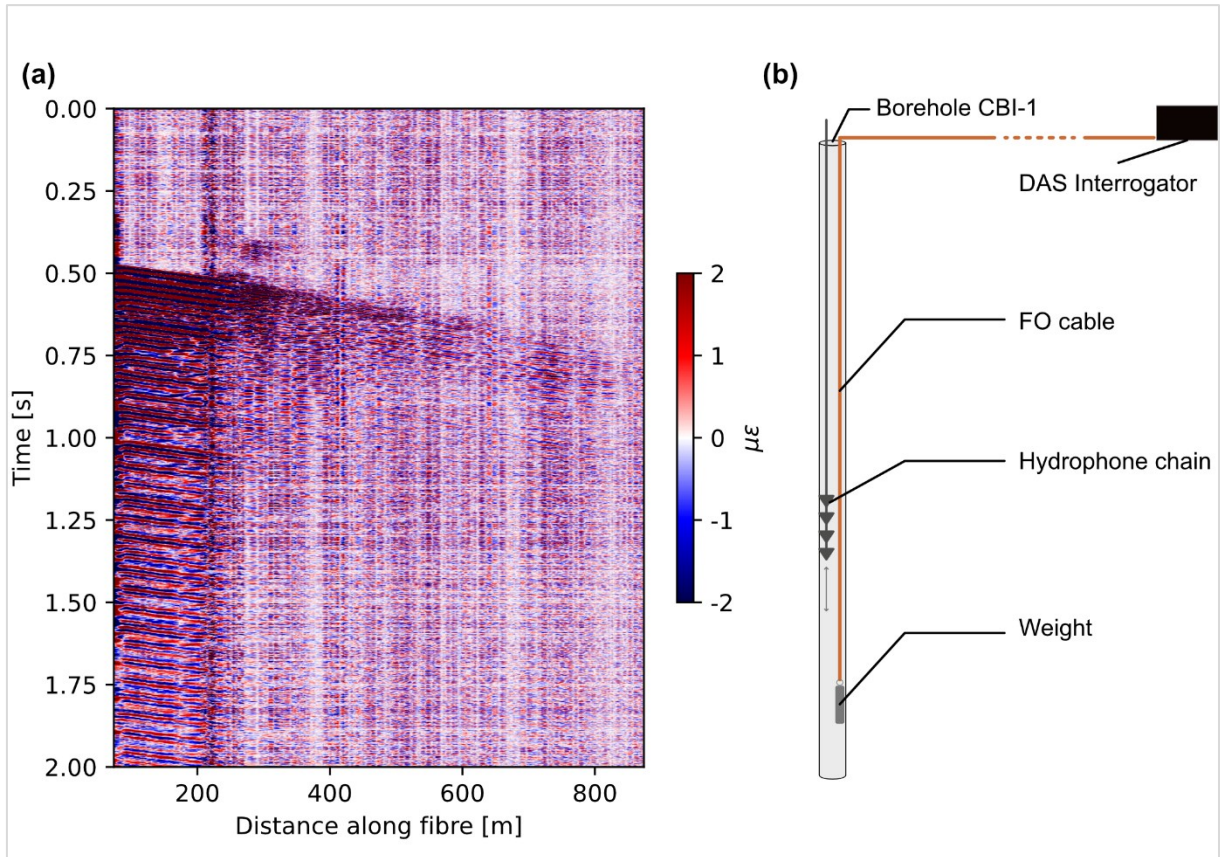


Fig. 10: FO data and experimental layout of the DAS acquisition in borehole CBI-1. (a) Raw DAS data from borehole CBI-1 showing a hammer shot in the vicinity of the borehole. (b) Experiment sketch (not to scale) for the fibre-optic (FO) measurement setup, where the DAS cable was lowered to the bottom of the borehole and kept in place by a weight, so that the hydrophones may move freely.

#### 2.4.3. Dissolved gases monitoring (WP2).

The monitoring of gases dissolved in underground-water was a crucial component of the timelapse monitoring. We wanted to evaluate the transport and retention of CO<sub>2</sub> in the subsurface by monitoring changes in the partial pressures of dissolved gas species over time. The portable mass spectrometer miniRuedi, equipped with a novel gas-equilibrium membrane-inlet (GE-MIMS; Brennwald et al., submitted Oct 2025) was connected to the shallow CBM-02 intercepting the freshwater aquifer, and to the deep CBM-03 and -01 boreholes, intercepting the deep reservoir targeted for CO<sub>2</sub> mineralization. The CO<sub>2</sub>-enriched fluid was artificially labelled with He as an inert gas tracer, and the partial pressures of CO<sub>2</sub>, He, and other, naturally abundant gases (He, Ar, Kr, O<sub>2</sub>, N<sub>2</sub>, CO<sub>2</sub>, and CH<sub>4</sub>) dissolved in the groundwater were monitored using GE-MIMS over one year. (Fig. 11), capturing a period of c.a. three month before the injection start and the subsequent 9 months of injection. The installation of the spectrometer for continuous monitoring in the boreholes CMB-02 and CMB-03 was carried out in June 2023. To prevent freezing of the tubes transporting water to the mass spectrometer, two trenches c.a. 60 cm deep were excavated from the wells to the container, and the tubes, together with electric cables,



protected by PVC tubes were buried in the trenches (Fig. 12). In October 2023, the deep borehole CBM-01, 100 m away from the injection well, was also connected to the spectrometer.

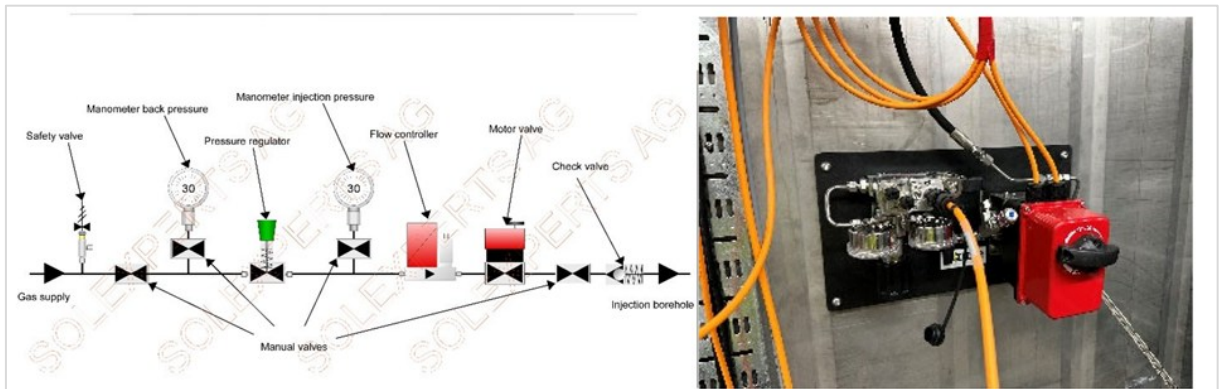


Fig. 11: Helium board layout (© Solexpert A.G). The board is mounted in the Carbfix container and connected with the CO<sub>2</sub> mixing unit.

e

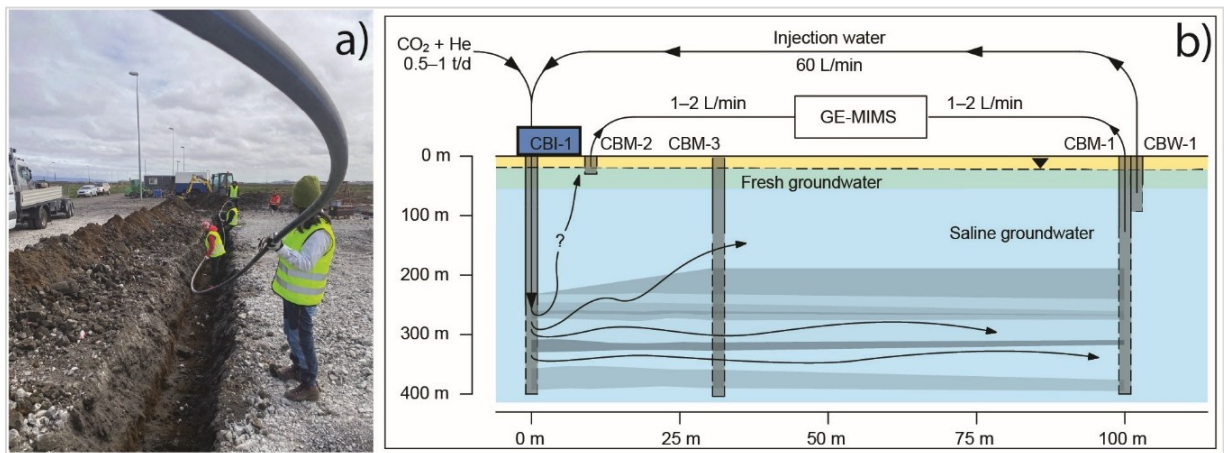


Fig. 12: Installation of the mass spectrometer and Ge-MIMS system. a) The trenches for burying water tubes and electrical cables extend from the Carbfix container to CMB-03 and CMB-01; b) schematic of the GE-MIMS connection to the aquifers at the test site, with pumping and injection rates (modified after Brennwald et al., submitted Oct 2025).

#### 2.4.4. Rock typing (WP3)

To characterise the quality of the reservoir and forecast its behaviour, a rock typing was accomplished at the GE-RGBA Group, Department of Earth Sciences, University of Geneva. This was achieved by combining high-resolution mineralogical, geochemical, and petrophysical investigations. The heterogeneities of the storage interval control CO<sub>2</sub> mineralisation, injectivity, and subsurface fluid movements. The rock typing was first carried out on five of the core plug collections that were tested in EPFL for flow properties, and specifically from the boreholes HB-05, HB-06, and HB-07. The plugs were selected aiming at targeting different field locations of variable pore structure. The plugs were cylindrical, having a height of 7.6 cm and a diameter of 3.9 cm (Fig. 12). Thin sections were then prepared from the core plugs for textural analyses. Petrographic description under an optical microscope was performed on the



thin sections of the core plugs. Moreover, six stubs containing about 50 grams of leftover material have been retrieved for geochemical analysis through the X-ray Fluorescence method (XRF). Additionally, drill cuttings obtained from CBM-01 and CBM-03 boreholes (Fig. 13), sampled approximately every 5 m, were analysed. Forty-five samples from CBM-01 and from CBM-03 were selected for quantitative petrographic analysis using the FEI QEMSCAN® Quanta 650F electron microscopy facility. Mineral phase identification based on back-scattered electron (BSE) imaging and Energy-Dispersive X-ray Spectroscopy (EDS) defined the relative proportion of the minerals composing the rock (modal composition). From the modal composition, adding density values to each mineral species, QEMSCAN calculates grain density, bulk density, and 2D porosity derived by computing the cumulative areas of empty spaces within the perimeter of individual cutting fragments.

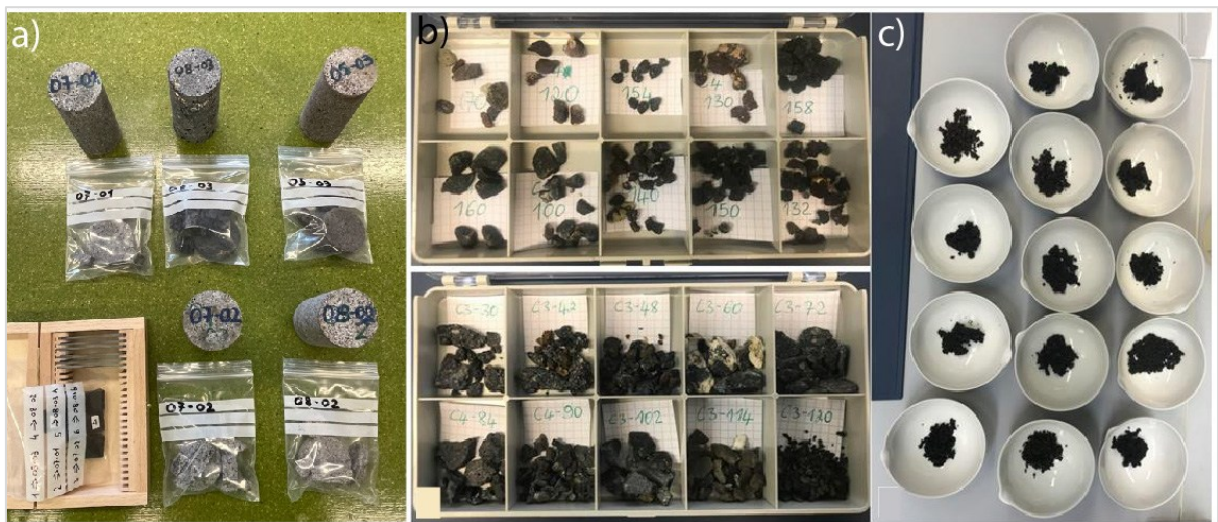


Fig. 13: Overview of samples used for the compositional, textural and rock property analysis of basalt samples. a) Plugs from boreholes HB-05, HB-07 and HB-08 received from Carbfix analysed both at EPFL and Geneva. B) Drill cuttings from boreholes CBM-03 and CBW-01. (a) used for polished thin sections and QEMSCAN analyses; used for XRF and LA-ICP-MS analyses (From Kemgang, 2024).

To assess the reliability of 2D porosity data from QEMSCAN, porosity ( $\phi$ ) and permeability ( $K$ ) on the core plugs with a length of 7.6 cm and a diameter of 3.9 cm were measured using an AP-608 Automated pulse decay Porosimeter-Permeameter with Nitrogen gas at the University of Geneva. The 3D porosity of each core was also measured at EPFL using XRCT images of an average resolution of 50  $\mu\text{m}$  (details below). Additional measurement of the pore size range of the material has been performed using the Mercury Intrusion Porosimetry (MIP) method at EPFL (Stavropoulou et al, 2024).

From the samples selected for the QEMSCAN analysis, approximately 13 to 14 g of cuttings samples were used for Loss of Ignition (LOI) measurements and subsequent X-ray fluorescence (XRF) and Laser ablation inductively coupled plasma mass spectrometry (LA-ICP-MS) for geochemical analyses. Both XRF for whole rock major elements determination and LA-ICP-MS for trace elements were performed at the Faculty of Geosciences and Environment, University of Lausanne (analytical details in Moscarillo et al., in preparation).

#### 2.4.5. Reservoir modelling (WP3)

The creation of a subsurface database of the CO<sub>2</sub> injection location at Helguvík is a key step before the creation of a 3D geological reservoir model (Fig. 14; Tab. 1). The Petrel software (SLB; version 2023) was used for this purpose. In Petrel, a high-resolution topographic map of the injection site and locations of the boreholes and the available well logs (Fig. 13; Tab. 1). The dataset from all the logged boreholes was included. It is also important to stress that the televiewer image was not available along the entire length of the boreholes, and there are some sections of the borehole with poor image quality. For a more reliable reservoir characterisation, we added to our database important drilling data from the HB-



05, HB-06, and HB-07 boreholes, including lithology and optically determined porosity logs (Davis, 2022).

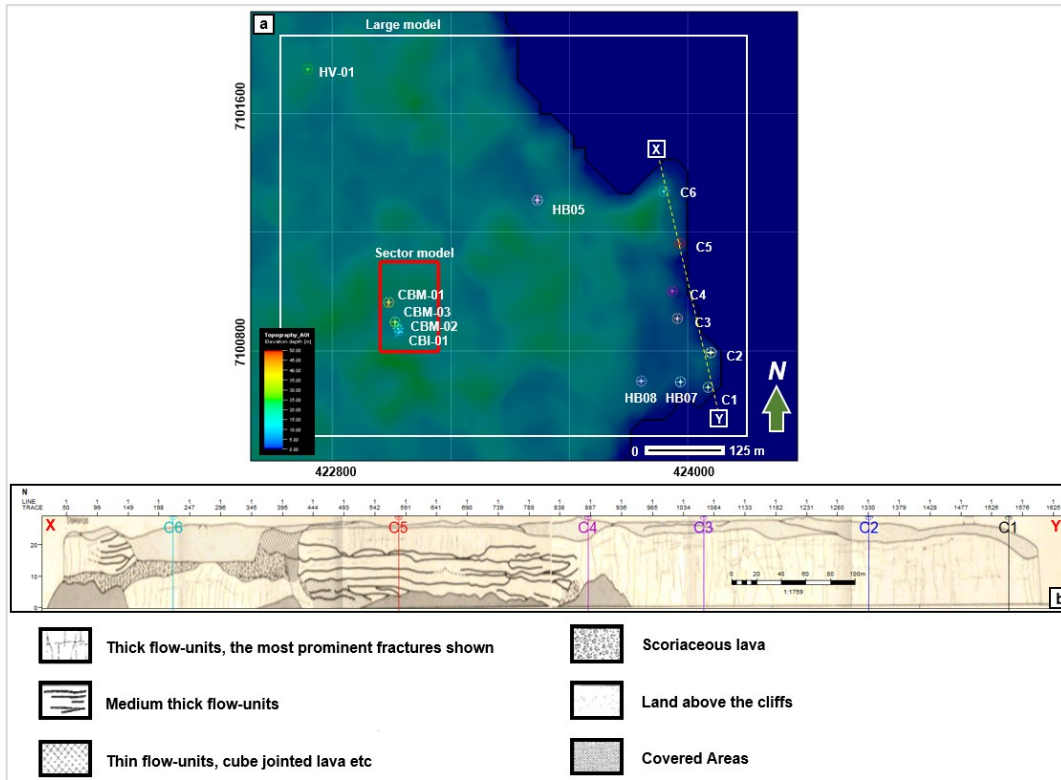


Fig. 14 Subsurface database. (a) Location of the study area using the ASTER Digital Elevation Map, showing two modelling boundaries, a large (white square) and a sector model (red square). The boreholes CBI-01, CBM-02, CBM-03 and CBM-01, the pseudo boreholes(C1-C6), and HB05, HB07, HB08 and HV-01. (b) Cross-section of the outcrop profile digitised from Vikingsson et al. (1982) and corresponding pseudo-boreholes generated (from Kengang 2024).

Table 1. The available well logs (Litho denote lithology, while  $\Phi$  is porosity)

Borehole	Depth (m)	Log Types	Cuttings/Core	Comments	Source
CBI-01	0-420	Gamma, Televiewer	N/A	N/A	ISOR
CBM-02	0-37	N/A	N/A	N/A	ISOR
CBM-03	0-420	Litho	Cuttings	N/A	ISOR
CBM-01	0- 420	Litho, Neut, Dens, Temp, Cond, Res, Televiewer, Caliper, Self-potential	Cutting	N/A	ISOR
HB-05	0-60	Litho, $\Phi$	core	$\Phi$ derived from core photos optical analysis	Vikingsson and Kristinsson, 1982; Davis, 2022
HB-07	0-60.25	Litho $\Phi$	core	$\Phi$ derived from core photos optical analysis	Vikingsson and Kristinsson, 1982; Davis, 2022
HB-08	0- 60.1	Litho $\Phi$	core	$\Phi$ derived from core photos optical analysis	Vikingsson and Kristinsson, 1982; Davis, 2022



#### 2.4.6. Flow properties characterization and validation of processes (WP4)

The flow properties of seven basaltic samples from boreholes HB-05, HB-07 and HB-08 were tested at the Laboratory for Soil Mechanics in EPFL, using the experimental setup illustrated in Fig. 15 (details in Stavropoulou et al., 2024). The samples, subjected to 5 MPa confining pressure and 25°C temperature, were saturated with synthetic saline water similar to the composition used by Voigt et al., 2021. Permeability and hydraulic conductivity were measured with the constant head method (Darcy, 1856, Renard et al., 2001) by applying a  $\Delta P$  of 1 MPa. The samples were then injected with saline water enriched in CO<sub>2</sub>. The salinity was significantly higher than the one in the field (about 5 times higher) in order to accelerate the mineralization processes (Aradóttir et al., 2012) and test multiple samples within the timeframe of DemoUpStorage. The exposure time (1 to 3,5 months) was chosen based on the results of Voigt et al. (2021). The flow properties were then re-assessed at the same initial experimental conditions.

Because mineralization is expected to change the pore structure, all cores were scanned with x-ray tomography (50  $\mu\text{m}/\text{px}$ ) before and after CO<sub>2</sub> exposure. Using the open source openPNM software (Gostick et al., 2016), pore network simulations were executed to reproduce the experimental flow results and better understand the impact of mineralization on the pore structure of the material. The porous space is simulated by considering a network of pores (spheres) connected by throats (cylinders). A double-scale porosity is considered: micro (< 50  $\mu\text{m}$ ) and macro (> 50  $\mu\text{m}$ ). The fluid flow is then simulated using the Hagen-Poiseuille equation and the net flow rate is obtained by Darcy law for a single-phase laminar flow simulation.

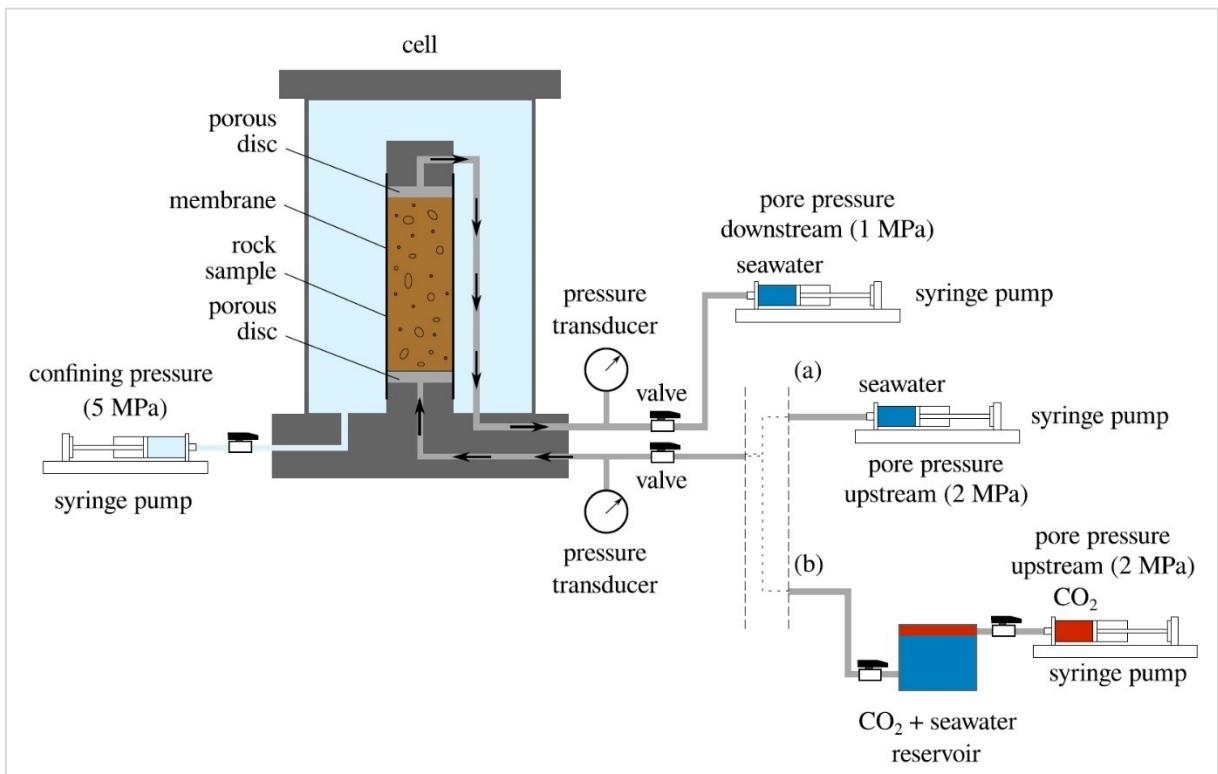


Fig. 15. Experimental setup for flow characterisation, (a) CO<sub>2</sub>-rich seawater injection and (b) long-term CO<sub>2</sub>-rich seawater exposure (from Stavropoulou et al., 2024)

#### 2.4.7. Independent investigation of societal acceptance (WP 5)

An evaluation of societal acceptance of the Swiss public towards CCTS/CCUS chains, particularly concerning the transport and storage of Swiss CO<sub>2</sub> abroad, began with a literature review, that identified four major research gaps. First, although existing studies have examined public perceptions of CCS



technologies and their associated risks and benefits, little is known about the extent to which people are willing to accept certain risks when they believe the benefits outweigh them. Second, while previous research indicates that public understanding of CCS remains limited, it is still unclear what specific information individuals require to make informed decisions about supporting these technologies. Third, most studies have investigated general attitudes toward CCS rather than focusing on clearly defined and concrete technological pathways. Fourth, although some recommendations emphasize the importance of providing both technical information and addressing public concerns, there remains a lack of best practices and guidelines for designing effective and accessible communication for diverse audiences.

Based on these gaps, the study addressed two main research questions in relation to the CCTS/CCUS pathways envisioned in DemoUpCARMA and DemoUpStorage:

- What are the Swiss public's levels of familiarity, support, perceived risks and benefits, and acceptance regarding the two CCTS/CCUS pathways?
- How can clear and effective communication be designed to inform the public about CCTS/CCUS in ways that reflect their preferences and informational needs?

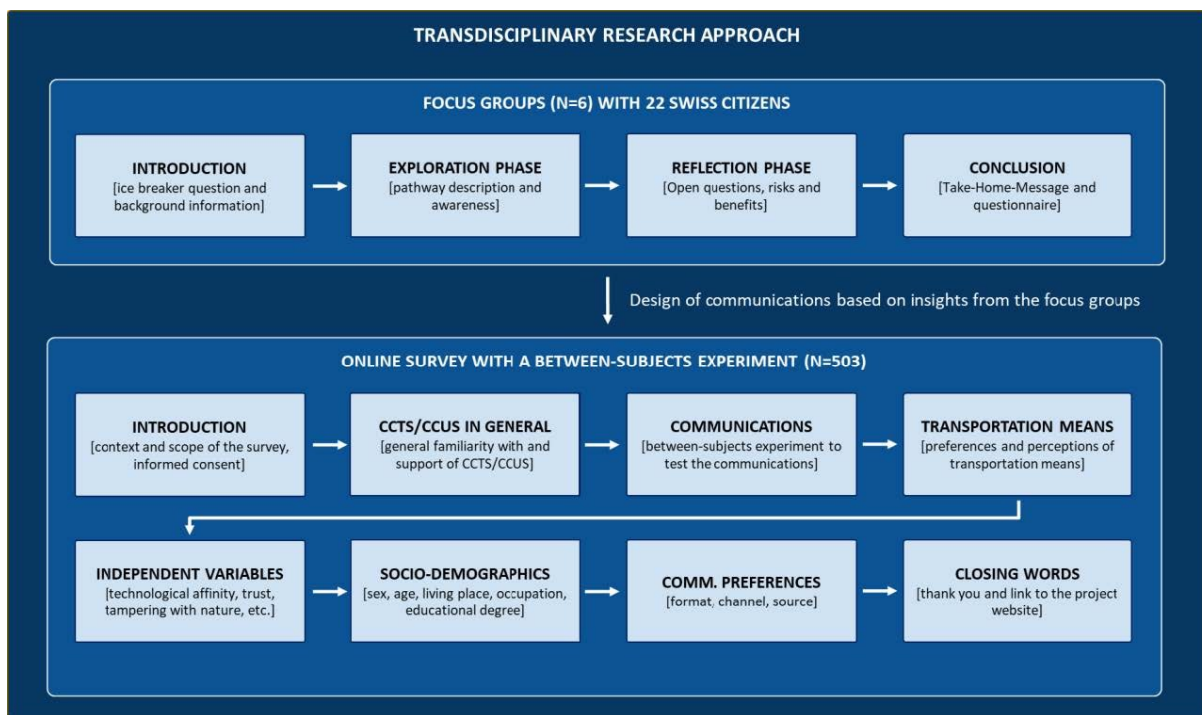


Fig. 16: Overview of the research procedure on societal acceptance of CCTS/CCUS: focus groups and survey (from Dallo et al., 2024).

To answer these questions, a transdisciplinary approach (Fig. 16) was adopted, by collaborating with scientists from various disciplines and engaging the general public. This approach enabled to integrate the latest research findings from the DemoUpCARMA project, address research questions from multiple scientific perspectives, and incorporate public viewpoints. To engage the public, in-person focus groups and an online survey were conducted. These methods provided both in-depth insights into people's perceptions and evidence-based guidance for designing effective communication strategies. The focus groups helped to prepare communication products (an infographic, a Q&A, a LinkedIn post, and a written text). These communications were then tested with a between-subjects experiment in an online survey, which means that participants were randomly assigned to one version of the communication product but had to answer the same questions (details reported in Deliverable D5.6, Dallo et al., 2024). The results of this study are reported in chapter 2.8.5.



#### 2.4.8. Injection (Carbfix)

After initial tests in 2023, the CO<sub>2</sub> injection started on January 15th, 2024, and continued with multiple interruption till September 2024. By September 1st, 2024, 137 t of CO<sub>2</sub> had been injected at an average rate of 4.14 t/week. This is below the planned rate of 20t/week which could not be reached due to various technical challenges in the CO<sub>2</sub> supply chain.

## 2.5 Results

### 2.5.1. Feasibility study for time-lapse CO<sub>2</sub> migration monitoring (WP2)

The sensitivity of crosshole seismic surveys for monitoring CO<sub>2</sub> mineralization was evaluated (Junker et al., submitted Agu 2025) prior to the drilling and measurement campaigns. Forward and inverted modelling of time-lapse crosshole seismic data for different interwell distances (25–100 m) showed that velocity anomalies as small as 1% of the initial p-wave velocity ( $v_p$ ) can be detected. Resolution decreases with greater distance, and fine-scale features blur, but anomalies remain identifiable. Velocity increases of 1% are the minimum detectable signal due to the limited sampling rate of crosshole seismic surveys (in the order of 50 kHz). Higher-density receiver and source arrays improve anomaly definition, particularly for shallow and thin layers. The minimal tested anomaly of a mineralized zone of 5–10 m radius and 25 m thickness was still resolved by a coarse receiver spacing of 8 m and a source spacing of 4m. In our simulations, this velocity anomaly was resolved in all cases of tested interwell distances (25m to 100m). For actual time-lapse seismics, several factors need to be accounted for: First, the seismic attenuation of the volcanic strata might be stronger than assumed in our models. This increases scattering of the seismic waves emitted from the sparker and limits the detectability range. In the case of the Helguvik site, we were able to pick first arrival travel times in the crosshole seismic data for source-receiver distances up to 100 m. The maximal distance is of course dependent also on local site conditions (e.g. strata, noise field), orientation of the source-receiver pair (due to seismic anisotropy) and also the source strength and frequency content. Further considerations need to be made when seismic monitoring is planned: First, a high ray path coverage in the area of interest is key for resolving any velocity anomaly. Second, the chosen interwell distance is a trade-off between the subsurface area investigated and the seismic resolution that can be achieved. Thus, additional information (e.g. the location and thickness of high-permeable layers) may support the design of the monitoring strategy. Third: the survey design also depends on the resolution that shall be reached in the seismic monitoring. In our case, we were able to achieve a 1m x 1m resolution in the inversion with 1m source and 2m receiver spacing at 30m interwell distance. Further investigations would need to show whether a similar result could also be achieved at larger interwell distances and which source and receiver spacing should be used there.

Rock physics modelling was used to quantify the expected magnitude of seismic velocity changes resulting from CO<sub>2</sub> injection into basaltic formations. Two primary processes induced by CO<sub>2</sub>-enriched water injection affect the seismic velocities of the basaltic host rock. Initially, the low pH of the CO<sub>2</sub>-saturated water promotes the dissolution of primary minerals, leading to an increase in pore volume and a corresponding decrease in seismic velocity (e.g., Snæbjörnsdóttir et al., 2018; Gassmann, 1951). This dissolution releases divalent cations such as Fe<sup>2+</sup>, Mg<sup>2+</sup>, and Ca<sup>2+</sup> into the pore fluid, which progressively raises the pH. Under these more alkaline conditions, often occurring at some distance from the injection point, these cations react with dissolved CO<sub>2</sub> to precipitate carbonate minerals within the pore space. The resulting reduction in porosity enhances the rock's stiffness, thereby increasing its seismic velocity. These processes were simulated using the mTex rock physics modelling toolbox, assuming different shapes of pores (spheroidal and penny-shaped cracks). Fig. 17a illustrates the seismic P-wave velocity ( $V_p$ ) of basalt as a function of porosity and calcite content. An increase in porosity, representing host-rock dissolution, is expressed as a shift parallel to the y-axis (arrow "host-rock dissolution" in Fig. 17b) when no pre-existing calcite is present. If, however, calcite or other carbonate minerals are already present prior to CO<sub>2</sub> injection, the acidic injected fluid is likely to dissolve them as well, resulting in a



velocity trajectory that deviates up to 45° anticlockwise from the vertical (arrow “calcite dissolution” in Fig. 17b).

Assuming an initial porosity of 8.5% and no pre-existing calcite, the minimal velocity increase of 1% found in the synthetic crosshole seismic study, translates to a minimum carbonate precipitation of about 17 kg  $\text{CaCO}_3/\text{m}^{-3}$  of rock volume (yellow arrow in Fig. 17a). As fluid flow effects are not considered in this simulation, the result should be regarded as an order-of-magnitude estimate. To further assess the plausibility of this threshold, we estimated the expected velocity changes for the Hellisheidi site based on the masses of host rock dissolved and secondary minerals precipitated, reported by Snæbjörnsdóttir et al. (2018) for the Carfix pilot injection of 175t  $\text{CO}_2$ . The resulting average velocity increase of  $\Delta V_p = 0.54\%-1.70\%$  supports the conclusion that, depending on the pore-shape, crosshole seismic imaging of  $\text{CO}_2$  mineralization processes is feasible under realistic field conditions.

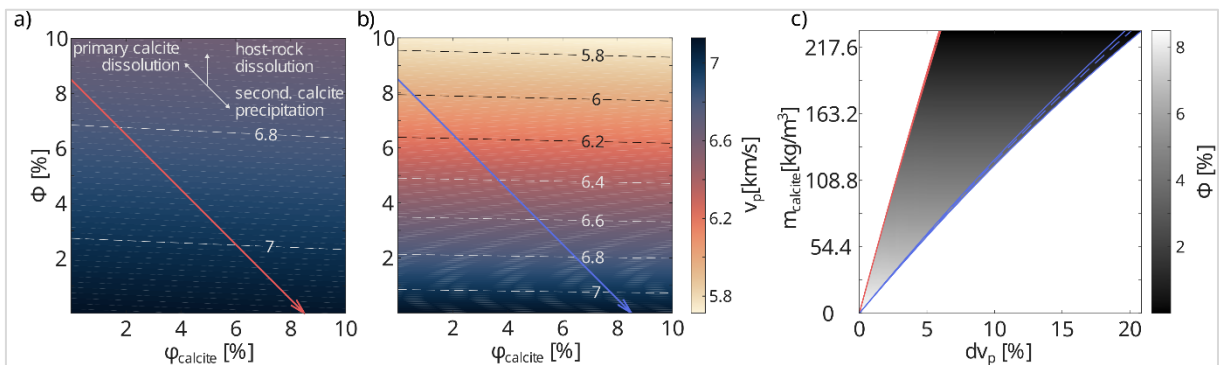


Fig. 17: Results of numerical simulation on p-waves ( $V_p$ ) velocity variations. a)  $V_p$  as a function of porosity and calcite content, b) possible pathways of velocity variations. The grey circular section indicates potential evolution paths for the first phase of the injection (mineral dissolution) between the two extremes of the pure dissolution of preliminary calcite and the pure dissolution of other minerals of the host rock, if no preliminary calcite is present (modified after Junker et al., submitted Agu 2025).

Based on the synthetic seismic modelling mentioned above, and assuming that 95% of the injected  $\text{CO}_2$  mineralizes, the mass of  $\text{CO}_2$  that needs to be injected before a detectable velocity anomaly is caused by the mineralization of  $\text{CO}_2$  accounts to 33 t – 106 t of  $\text{CO}_2$ . However, those numbers need to be interpreted very carefully as those calculations are neglecting any fluid dynamical and geochemical effects. It is unlikely that all secondary minerals precipitate in a perfectly uniform distribution around the injection well. A more detailed assessment of when a time-lapse seismic survey should be done earliest would require substantial reactive transport modelling.

## 2.5.2. Geophysical Baseline Characterization (WP2)

The seismic noise characterization (Fig. 18a; Junker et al., 2025) indicates elevated anthropogenic noise levels in the 7–15 Hz frequency band, exhibiting a pronounced day–night cycle. Network sensitivity estimates suggest a detection threshold of approximately ML 0.8 during daytime and ML 0.4 at night. Beamforming analysis (e.g., Rost & Thomas, 2002; Fig. 18b, c) within the same frequency range identifies dominant noise sources located from the northeast to the south of the study area, with stronger and more spatially extensive sources on working days. These directions coincide with nearby industrial facilities. A preliminary seismic catalogue, compiled from the five backbone stations, reveals artificial events likely associated with industrial machinery, as well as regional seismicity originating from the Trans-Tensional Zone of the Reykjanes Peninsula and the Reykjanes Ridge (Sæmundsson et al., 2020), but no evidence of local natural seismicity. Nevertheless, microseismic events below the current detection threshold cannot be excluded. Attempts to use the anthropogenic noise field for ambient noise



tomography and extraction of a 1-D S-wave velocity model were discontinued due to insufficient data quality.

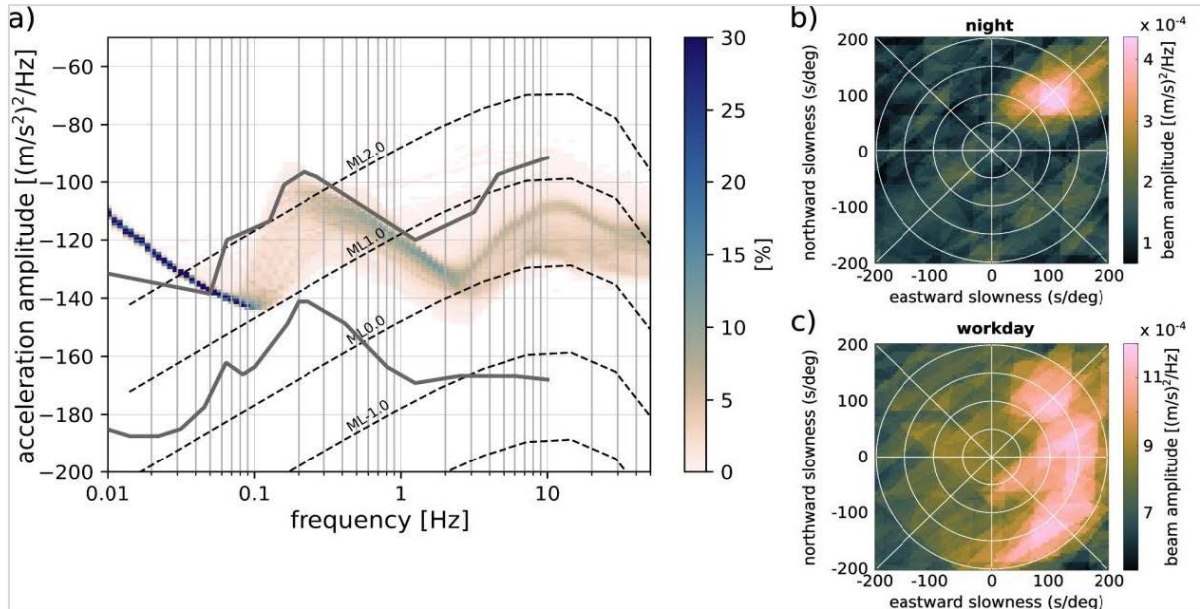
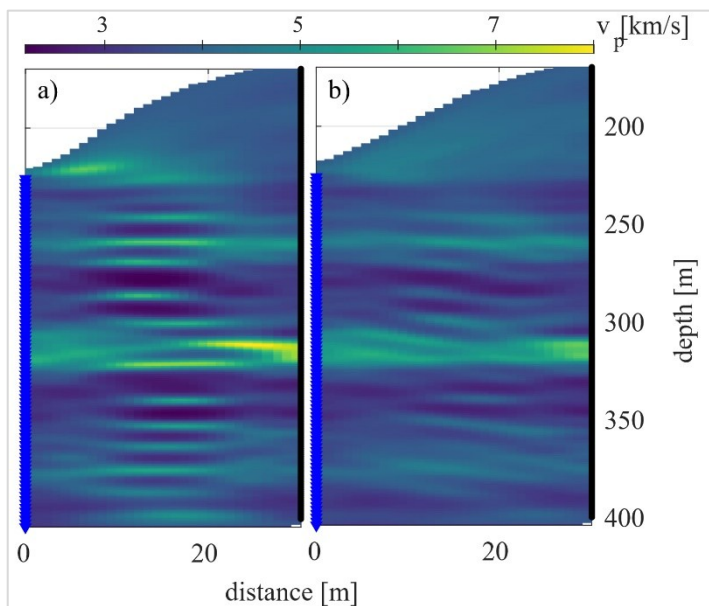


Fig. 18: Probabilistic Power Spectral Density (PPSD) plot of the vertical component of one of the backbone stations (DC01) 50m from the injection borehole. The thick grey lines show the lower and upper noise levels of a worldwide noise model (Peterson 1993). The dashed lines represent the S-wave source spectra for theoretical local earthquakes of different local magnitudes  $ML$  (Brune, 1970-1971). b) and c) show the beamforming results using the ambient noise recording of the nodal array for a representative hour in the night (June 30, 2023, 03:00 to 04:00) and during a workday (June 30, 2023, 14:00 to 15:00). Note the different amplitude scales for day and night (from Junker et al., 2025).



The crosshole seismic data were processed using in-house MATLAB-based software developed by Lanz et al. (1998). The resulting seismic tomogram (Fig. 19) reveals sub-horizontal layering with pronounced velocity contrasts. P-wave velocities range from 2.6  $km/s$  to 6.6  $km/s$ , consistent with values reported from other travel-time tomography studies in southeast Iceland (Grab et al., 2015). Individual layers exhibit thicknesses between 13  $m$  and 40  $m$ , with boundary undulations of up to 10  $m$  across the 30  $m$  distance between wells CBI-01 and CBM-03.

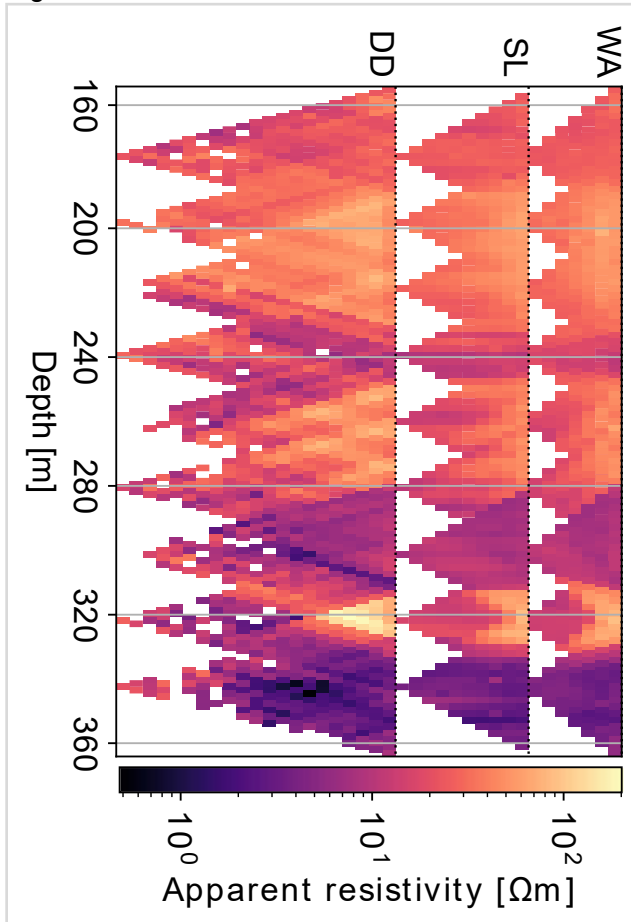
Fig. 19: Seismic tomography before a) and after b) weak anisotropy removal. The inverted  $v_p$  model highlights sub-horizontal layers with high velocity contrast.

The inverted ERT data (Fig. 20) indicate an apparent resistivity of approximately 40  $\Omega m$  from 160m (note that from 0 to 160 m the well was cased and no resistivity could be measured) down to around



240 m. Below this depth, a zone with resistivity values near  $10 \Omega\text{m}$  appears. At depths exceeding 250 m, two low-resistivity zones (ranging from  $0.5 \Omega\text{m}$  to  $10 \Omega\text{m}$ ) are observed, separated by a high-resistivity layer at approximately 300 m depth, exhibiting apparent resistivities up to  $207 \Omega\text{m}$ .

The subsurface structure revealed by the electrical resistivity and seismic velocity tomographies depict eight sub-horizontal continuous units with distinct P-wave velocity and electrical resistivity ( $\rho$ ). Both parameters strongly depend on rock porosity (e.g., Archie, 1942; Gassmann, 1951), and (even if in minor proportion) on clay minerals content. Although the different stratigraphic layers show varying mineralogical compositions and glass fractions, we do not expect significant variations originating from those two parameters as i) various studies (e.g. Carlson 2014, Miller & Stewart 1990) and also our rock-physics modelling have shown that  $V_p$  variations are governed by porosity and as ii) the solid rock matrix is, with the exception of clay minerals, expected to be non-conductive (e.g. Archie, 1942).



Although the different stratigraphic layers show varying mineralogical compositions and glass fractions, we do not expect significant variations originating from those two parameters as i) various studies (e.g. Carlson 2014, Miller & Stewart 1990) and also our rock-physics modelling have shown that  $V_p$  variations are governed by porosity and as ii) the solid rock matrix is, with the exception of clay minerals, expected to be non-conductive (e.g. Archie, 1942).

The neutron porosity log in CBM-01 agrees with the porosity distribution as indicated by resistivity and velocity. By applying a P-wave velocity/porosity relation known in literature (Navarro et al., 2020), the mean porosity of each unit was calculated. The permeability was derived for each layer by applying the porosity/permeability relation proposed by the same study (Navarro et al., 2020).

Fig. 20 Apparent resistivities with depth in CBM-03 for the Wenner (WE), Schlumberger (SL) and Dipole-Dipole configuration

### 2.5.3. Rock typing (WP3)

Through drill cutting macroscopical analyses, optical microscope and electron microscopy a stratigraphy composed of 4 main units, subdivided into 10 different lithotypes, has been identified:

- Unit A: 0-106 m consists of light grey, medium-grained basalt associated with dark grey and very dark grey fine-grained basalt;
- Unit B: 106-242 m is an alternation of heterogeneous material, containing sandy sediment (interval 106-116 m) with fragments of shells, medium-grained basalt, scoriaceous material, medium-grained basalt, hypocrySTALLINE glassy fragments and a glassy breccia towards the bottom of the unit;
- Unit C: 242-300 m consists of breccia, associated with crystalline basalt, glass, scoria and fine-grained basalt rich in olivine. A thick deposit of fine sediment is in the interval at 273-300 m;
- Unit D: from 300-420m is a homogeneous crystalline basalt and light grey dense basalt with minor sedimentary layers.



The vertical distribution of the various minerals has implications for the dielectric and elastic properties of the whole rock; therefore, it is of paramount importance in the interpretation of geophysical observations. Fig. 21 illustrates the results of the mineralogical detection by QEMSCAN and the subdivision into lithological units. Basaltic glass is a main component of the rocks (38% and 27% on average in CMB-03 and CMB-01 respectively), together with plagioclase (33% in CMB-03 and 28% in CMB-01). Pyroxene (augite) varies from 11% in CMB-01 to 18% in CMB-03. Olivine decreases with depth from c.a. 10% at the top to 1% at the bottom of the sequence. Various Na-Ca-K zeolites occur filling vacuoles and open spaces are abundant in both boreholes mainly from 150 to 300 m depth. Chemical analyses reveal a content of  $\text{Fe}_2\text{O}_3$  around 13% and while MgO and CaO vary between 6 to 12%.

The 2D matrix porosity measured using QEMSCAN indicates a large variability in the first 200 m (ca. 8.9%) and a decrease towards greater depth (c.a. 4.5%)

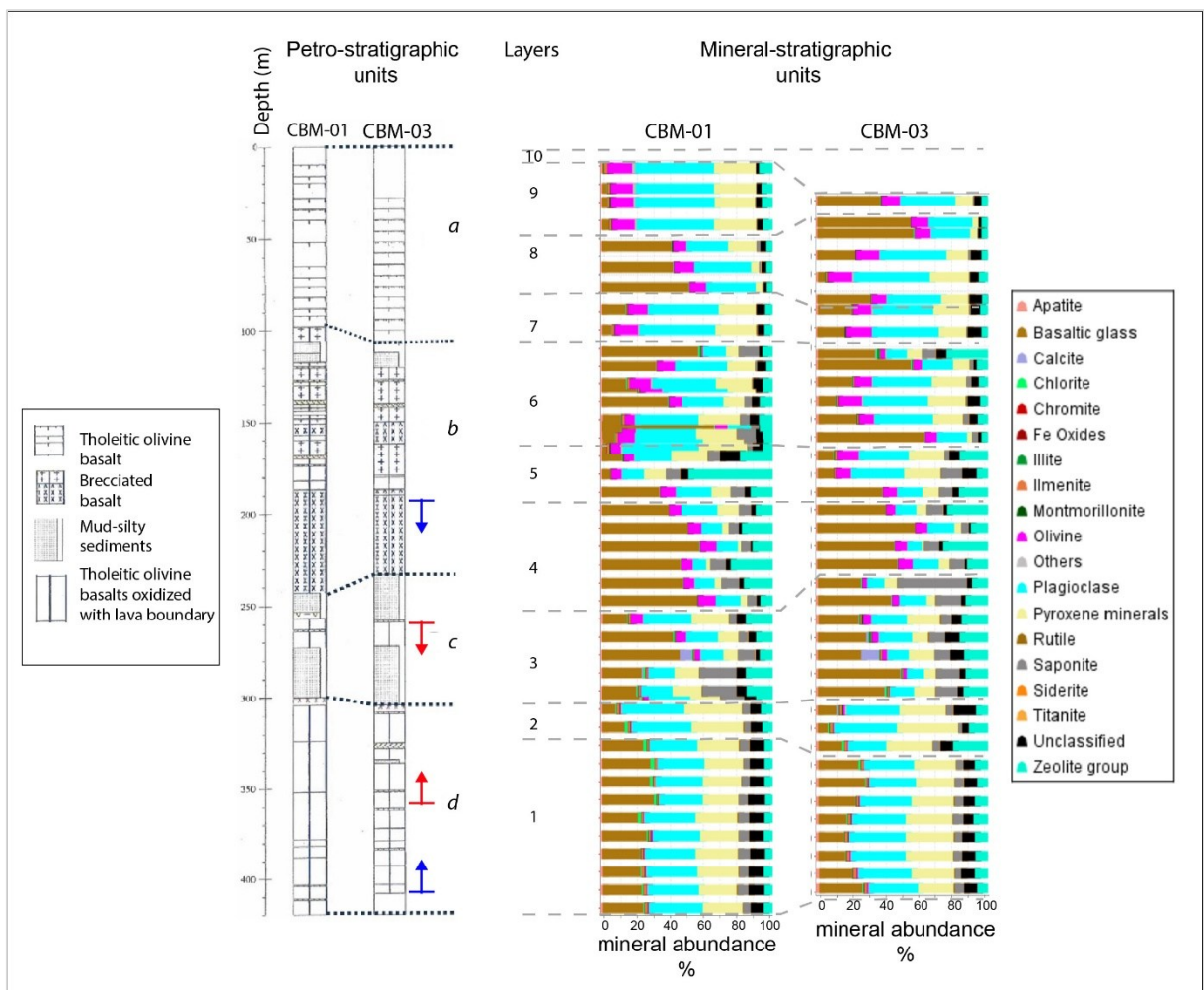


Fig. 21: Stratigraphic subdivision based on petrographic description in boreholes CBM-01 and CBM-03 compared with the results of modal mineralogical composition from QEMSCAN, validated by optical thin section analysis. The correlation between the different units highlights the lateral change in thickness of the different units (from Moscariello et al., in prep); note that layer 10 corresponds to soil, of which no samples were available. The red arrows indicate the top and bottom of the borehole section shown in fig 29 and the blue arrows represent the section in fig. 33.

#### 2.5.4. 3D Geological Model (WP3)

A 3D conceptual geological model of the pilot site at Helguvík, incorporating the stratigraphy was derived from CBM-01 and CBM-03 (Fig. 22). Two modelling boundaries comprising of a larger boundary



incorporating pre-existing wells HB05, HB08, HB07, in addition to the pilot site CarbFix wells and a smaller sector model incorporating on the CarbFix wells were defined (Fig. 23). Importantly, the large boundary captures the cliffs and outcrop exposure which will enable an understanding of the fracture system and possible near-surface lithofacies. The geological characteristics such as strata and bed geometry of the cliff's outcrops have been drawn from offshore and reported in an ISOR report (Vikigsson and Kristinsson, 1982).

The geological layering of the site (sector model) was performed using CBM-03 and CBM-01 borehole as control points. Based on the integration of the cuttings and QEMSCAN results, the Helguvík site was eventually subdivided into 10 subsurface layers named progressively Layer 1 – 10 and likewise from oldest to youngest based on their distinct reservoir properties (Fig. 23 and 24). The 10th layer was undefined because no cuttings were available for characterisation (Fig. 23 and 24).

The characterization and estimation of reservoir volume in basaltic units is not well constrained compared to sedimentary basins (Raza et al., 2022; Andrews, 2023). In order to estimate the storage capacity for Helguvík site, a modelling boundary was set to those of the smaller sector model indicated in Fig. 23 and 24 and following the approach of Andrews (2023):

*Volume (V) = Area of sector model \* thickness of the storage interval at the Helguvík site*

*Net Pore Volume = V \* Porosity ( $\phi$ )*

where the porosity was measured on borehole cuttings both as 2D porosity using both conventional petrographic microscopy and QEMSCAN and 3D porosity using conventional core analysis (porosity and permeability, see Fig. 23). 2D QEMSCAN porosity is presented as function of depth in the Helguvík Site in Fig. 22.

In order to estimate the potential CO<sub>2</sub> storage capacity within our modelling area, we assumed storage within the layers 1 to 3 corresponding to Units C and D in Fig. 21 where the main basaltic facies have been described. Using the equation from Vishal et al. (2021), the total CO<sub>2</sub> storage capacity can be estimated using the equation below:

$$MCO_2 = V * \phi * ECO_2$$

Where:

*MCO<sub>2</sub> = Total CO<sub>2</sub> storage potential in Tonnes*

*V = Volume of the basalt formation (Area \* Thickness)*

*$\phi$  = Average porosity, and*

*ECO<sub>2</sub> = Storage efficiency or the CO<sub>2</sub> storage per unit pore volume.*

According to Snæbjörnsdóttir et al. (2014) the storage per unit volume for the Reykjanes and Hellisheiði system in Iceland is in the order of 18.8 kg/m<sup>3</sup> and 43.8 kg/m<sup>3</sup>. Both values were used as lower and upper limit for ECO<sub>2</sub>. The estimate of the storage potential is strongly dependent on the extent of the modelling area adopted since the thickness of the storage unit does not vary greatly. In this study an area of 500 m by 350 m has been used together with an average useable thickness of 185 m. A probabilistic distribution of the static CO<sub>2</sub> storage capacity was derived using Monte Carlo simulations with 10,000 iterations (Tables 2 and 3). The estimated cumulative static storage capacity percentiles for the study area for scenario 1 (matrix porosity only) range between P10 = 3.8E+04 Tonnes; P50 = 8.8E+04 Tonnes and P90 = 1.6E+05 Tonnes (Table 2; Fig. 26). However, for scenario 2, considering a possible increase in porosity of 0 - 10% arising from possible reasonable fracture contribution, the static CO<sub>2</sub>



storage capacity now ranges between P10 = 4.7E+04 Tonnes; P50 = 1.3E+05 Tonnes and P90 = 2.6E+05 Tonnes (Table 3; Fig. 27).

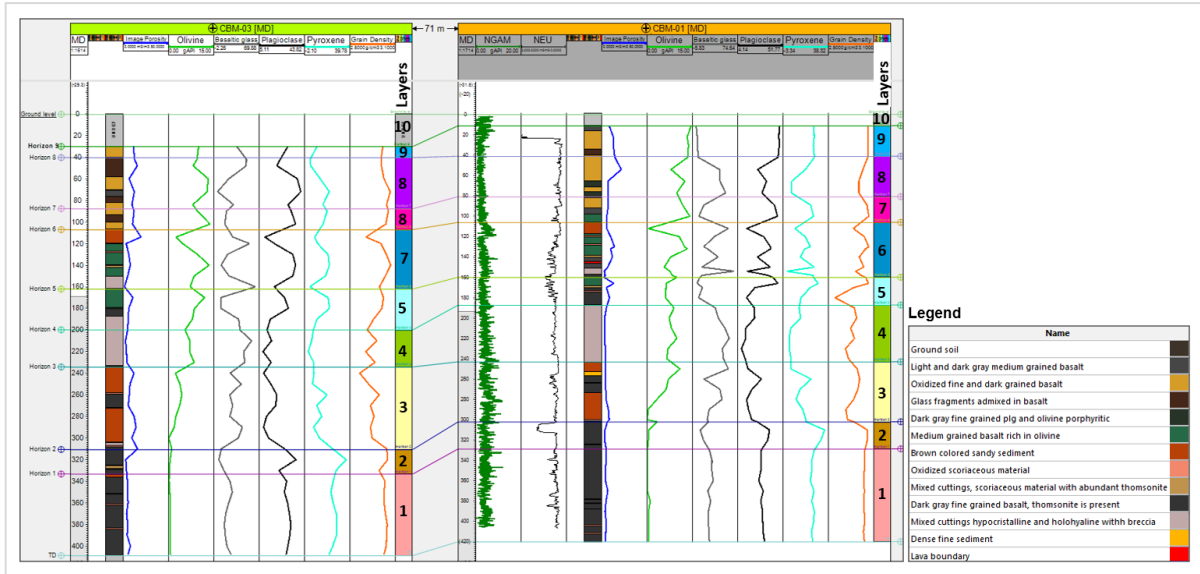


Fig. 22: Correlation panel between CBM-03 (left) and CBM-01 (right). Layers with similar reservoir characteristic (mineralogy, density, porosity and lithology) were correlated (From Kengang 2024 Master thesis).

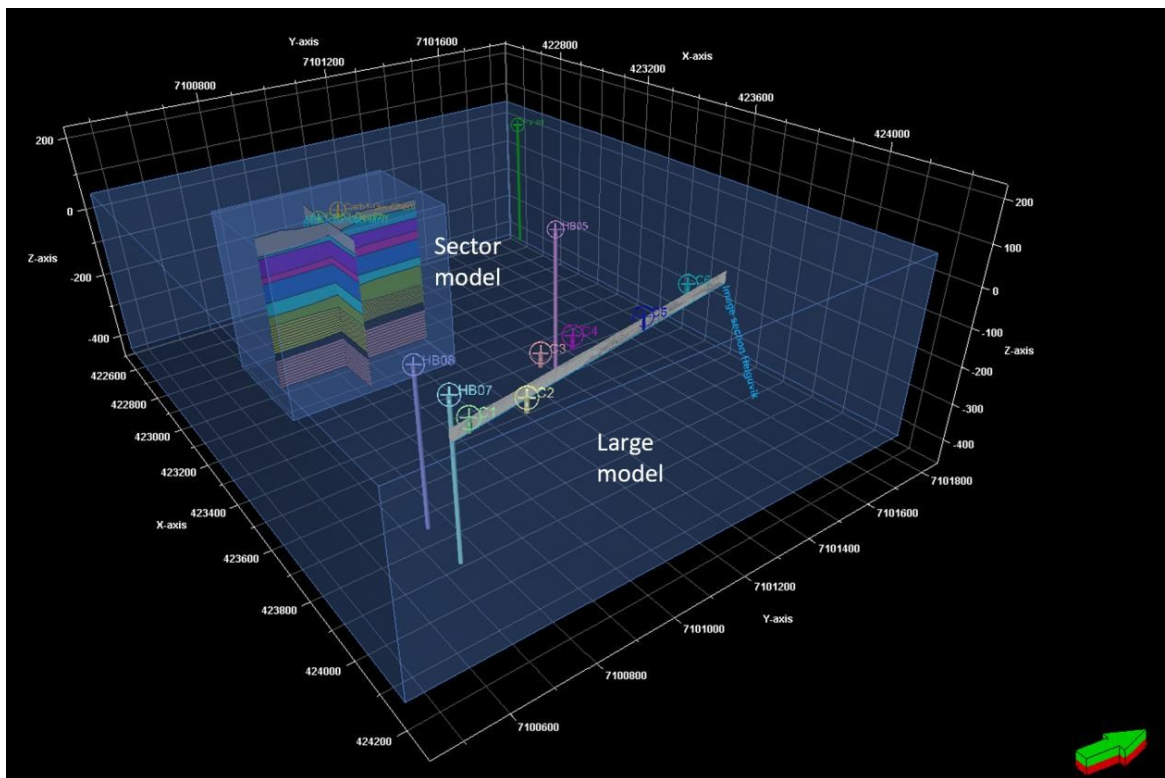


Fig. 23: 3D conceptual reservoir model of the Helguvík site encompassing the small-scale sector model, outcrop and pseudo boreholes along the cliff and other boreholes in Helguvík (from Kengang, 2024, master thesis)

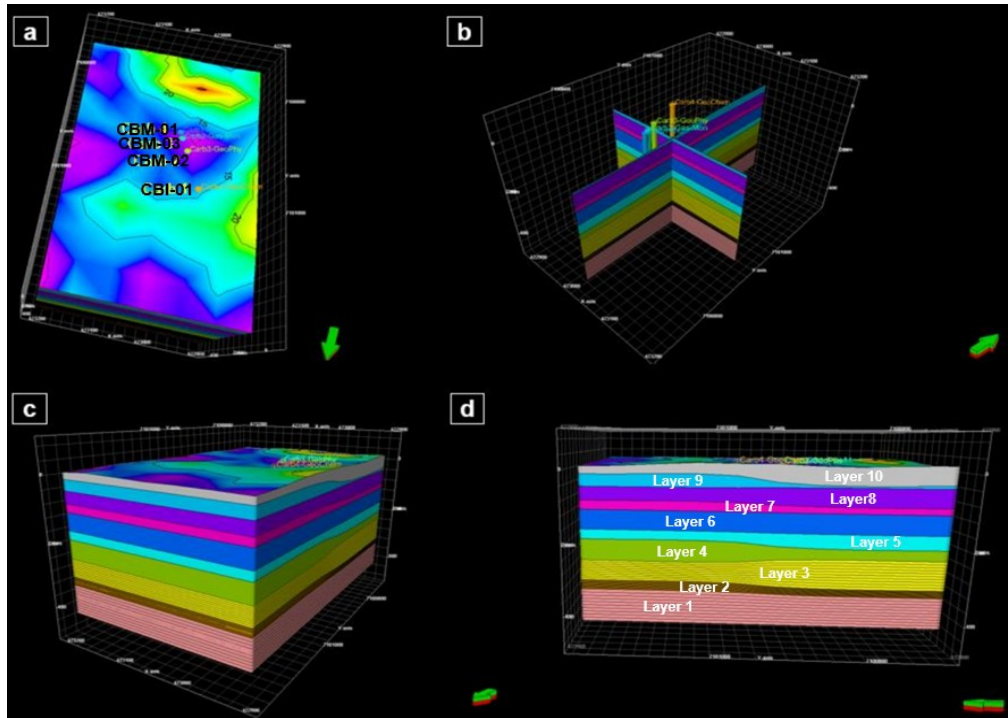


Fig. 24: Geological model of the Helguvík storage site. (a) a view from the top of the model showing the four principal boreholes (b) internal architecture of the model. (c) and (d) external architecture of the model, showing the 10 main layers in the model (from Kemgang 2024, master thesis).

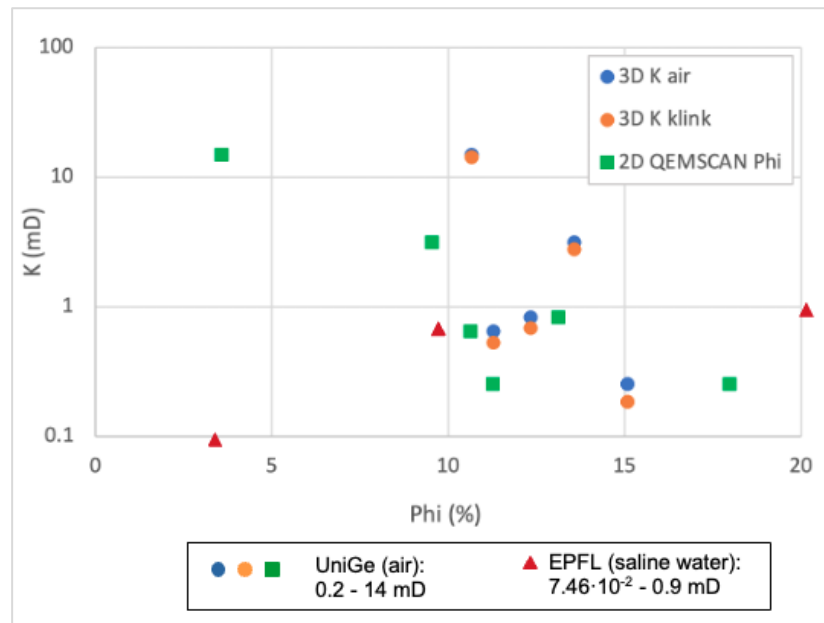


Fig. 25: Porosity and Permeability cross plot using conventional core analysis (Helium injection) on core plugs from HB wells.



Table 2: Parameters used for estimating CO<sub>2</sub> storage potential within the sector model.

Parameters	Value / Source	Standard deviation
Area	175 000 m <sup>2</sup>	35000 m <sup>2</sup> (20%)
Thickness (Layers 1 to layer 3)	185 m (controlled by well data)	5 m
Average Matrix Porosity	3 - 16% (from thin-section and QEM-SCAN)	-
ECO <sub>2</sub>	18.8 – 43.8 kg/m <sup>3</sup>	-
MCO <sub>2</sub>	P10 = 3.8E+04 Tonnes; P50 = 8.8E+04 Tonnes and P90 = 1.6E+05 Tonnes	

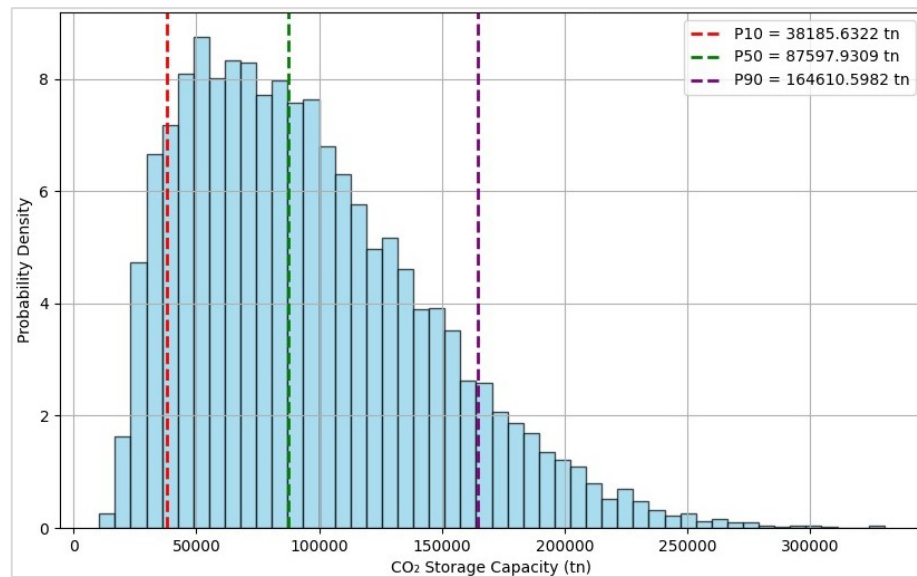


Fig. 26: Probabilistic-based static CO<sub>2</sub> storage capacity estimate for the study area- scenario 1 (matrix porosity only).

Table 3: Parameters used for estimating CO<sub>2</sub> storage potential within the sector model.

Parameters	Value	Standard deviation
Area	175 000 m <sup>2</sup>	35000 m <sup>2</sup> (20%)
Thickness (Layers 1 to layer 3)	185 m (controlled by well data)	5 m
Average Matrix Porosity	3 - 16% (from thin-section, QEMSCAN and Conventional Core Analysis*)	-
Average Fracture Porosity (Additional)	0 - 10% (from outcrop observation and bore hole image)	-
ECO <sub>2</sub>	18.8 – 43.8 kg/m <sup>3</sup>	-
MCO <sub>2</sub>	P10 = 4.7E+04 Tonnes; P50 = 1.3E+05 Tonnes and P90 = 2.6E+05 Tonnes	

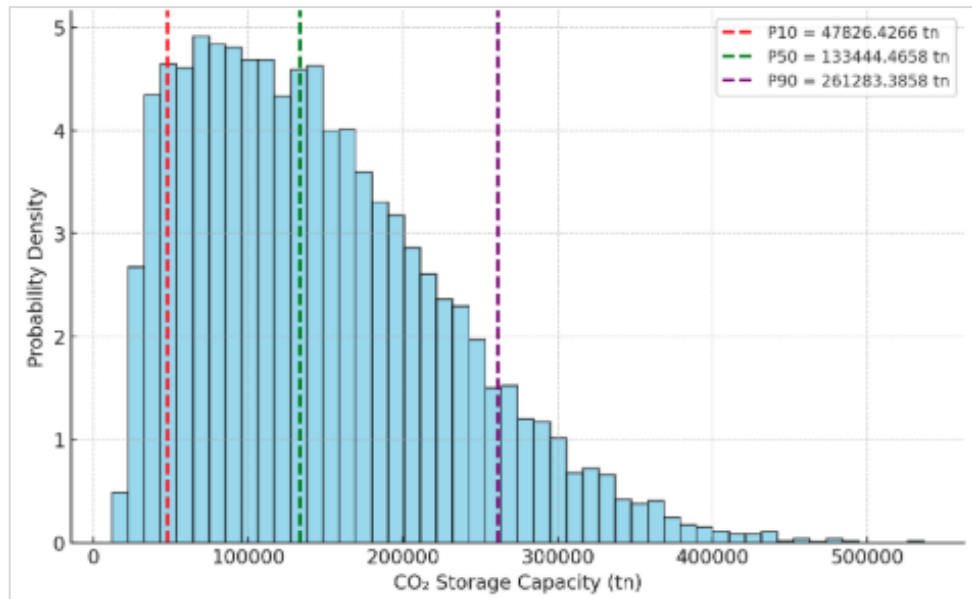


Fig. 27: Probabilistic-based static CO<sub>2</sub> storage capacity estimate for the study area (scenario 2, considering a possible increase in porosity of 0 - 10%).

#### 2.5.5. Dissolved gases monitoring (WP2)

From June 2023 to September 2024, the miniRuedi system continuously monitored dissolved gas concentrations (He, Ar, Kr, N<sub>2</sub>, O<sub>2</sub>, and CO<sub>2</sub>) in the CBM-02 and CBM-01 wells. The data reveal clear differences between the two wells in temperature, total dissolved gas pressure, and gas composition.

At the shallow observation well CBM-2, the partial pressures of He, CO<sub>2</sub>, and other gas species remained within the typical range of natural background levels, exhibiting only minor fluctuations over the monitoring period. A slight increase in CO<sub>2</sub> partial pressure was observed from November to April, followed by a decrease during the summer months. This seasonal variation is attributed to reduced ventilation of respired CO<sub>2</sub> from the unsaturated zone caused by snow cover and soil freezing during the cold season. Aside from these small natural variations, the partial-pressure time series at CBM-2 show no detectable changes in He or CO<sub>2</sub> that could be linked to the injected fluid. These observations indicate minimal upward migration of the injected CO<sub>2</sub> near the injection borehole and suggest effective CO<sub>2</sub> retention within the aquifer.

At the deep extraction well CBM-01, the initial partial pressure of He is slightly higher than that measured in water from CBM-2. This minor excess likely reflects the accumulation of terrigenous helium in the deeper, older groundwater. Over the course of the observation period, the He partial pressure increased steadily, reaching more than ten times its initial value. In contrast, the partial pressures of atmosphere-derived gases (Ar, Kr, and N<sub>2</sub>) remained close to their natural background levels and displayed similar temporal trends, with fluctuations of approximately  $\pm 50\%$  relative to their mean values. These correlated variations are interpreted as reflecting variable mixing between groundwater components with differing dissolved gas concentrations.

The pronounced increase in He from spring 2024, shown in Fig. 28 at borehole CBM-01 indicates the arrival of He-labelled injection water at CMB-1. In contrast, the CO<sub>2</sub> partial pressure remains low and varies in parallel with the natural background levels of atmosphere-derived gases (Ar, Kr, and N<sub>2</sub>). This pattern suggests that the CO<sub>2</sub> detected at CBM-01 is primarily of natural origin rather than originating from the injected CO<sub>2</sub>. By the end of the monitoring period, the CO<sub>2</sub>/He partial-pressure ratio had



decreased over three orders of magnitude lower than that of the injected fluid. This strong retardation of CO<sub>2</sub> at CBM-01 is consistent with the expected retention of CO<sub>2</sub> within the aquifer.

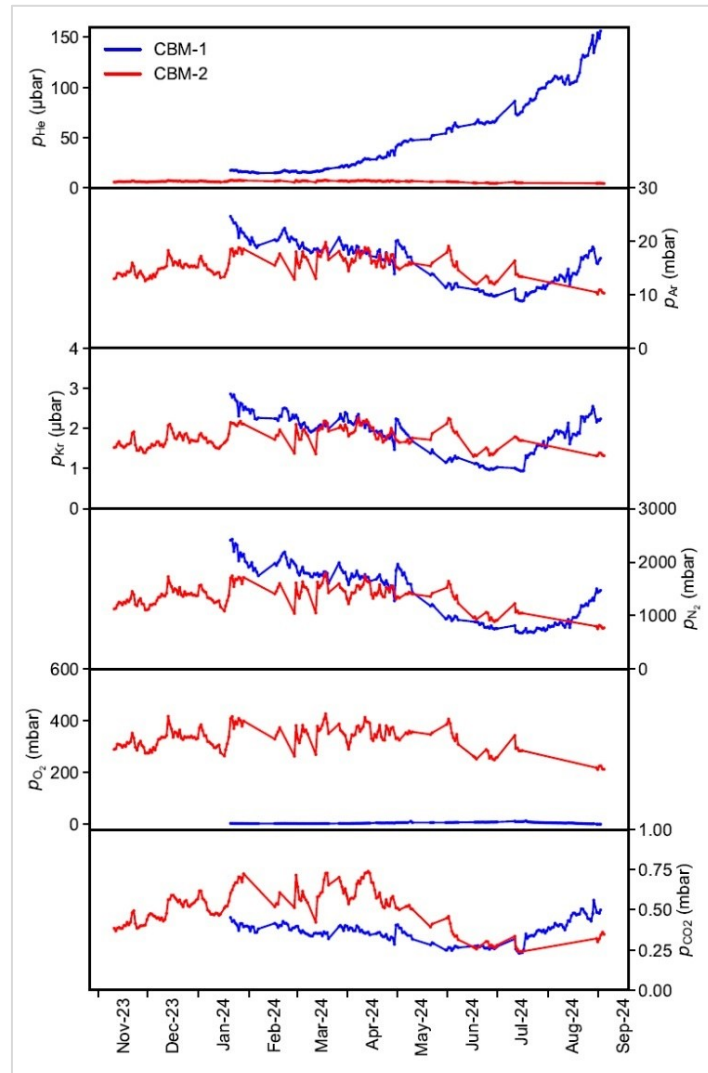
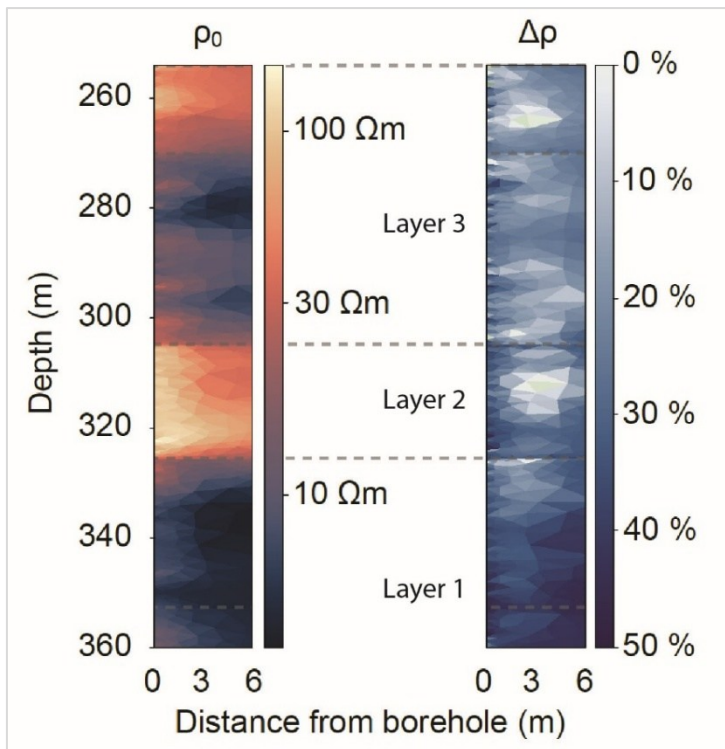


Fig. 28: Partial pressures of dissolved He, Ar, Kr, N<sub>2</sub>, O<sub>2</sub> and CO<sub>2</sub> observed at boreholes

### 2.5.6. Timelapse Electrical Resistivity Imaging (WP2)

Continuous ERT measurements at CBM-03 showed a stable resistivity distribution before injection, with only minor random fluctuations. This stability persisted throughout the injection period during available measurements. The likely reason is that the electrode chain was located within the lower high-permeability layer, while most injected fluid entered the upper high-permeability layer (layer 4 of Fig.21 and Fig.24). Repeated single-hole ERT surveys in August 2024 across all three wells were compared with those from August 2023. Fig. 29 shows the relative resistivity changes between 2024 and 2023. However, an interpretation of these variations is not straight forward as electrical subsurface resistivity



strongly depends on temperature and as the injection of cold, CO<sub>2</sub> charged water (~15°C) led to a cooling at reservoir depth of approximately 40°C. Thus, for a proper interpretation of the data, a temperature correction is needed (Hayashi et al, 2004; Keller et Frischknecht 1965). As we had only reliable temperature logs for the CBI-01 well available, we limit the ERT time-lapse analysis to this profile (Fig. 29).

Fig. 29: ERT Timelapse: Relative changes in electrical resistivity between Summer 2023 ( $\rho_0$ ) and August 2024 ( $\Delta\rho$ ) in borehole CBI-1.  $\rho_0$  is the initial electrical resistivity determined before CO<sub>2</sub> injection.  $\Delta\rho$  is the relative change of the electrical resistivity one year after the start of the injection. Modified after Brennwald et al. (submitted Oct 2025). Please note that the boundary between layer1 and 2 is slightly shallower than in the Mineral-stratigraphy (c.a.5 m) this can be attributed to errors in the recovery depth of the cuttings.

The inverted resistivity variations agree with the baseline resistivity structure and the porosity model retrieved from the baseline geophysical data: the strongest electrical resistivity decreases (up to 50% relative to the baseline) locate in the highly permeable layers (layer 1 and upper part of layer 3). The lower permeable layers (2 and lower part of layer 3) show resistivity decreases less than 25%. We attribute this pattern to the permeability distribution of the subsurface and the geochemical processes related to the CO<sub>2</sub> injection: Most of the injected water enters the formation in layers C and E, replacing the local groundwater with higher conductive, CO<sub>2</sub> charged injection water. Further, the injected, acidic water dissolves minerals in the host-rock and thus increases its porosity. Consequently, the resistivity of the reservoir further decreases.

We do not see any resistivity increases that could be attributed to a precipitation of secondary minerals but we do not expect such variations in the vicinity of the injection well but further away from the injection point. Unfortunately, we do not have electrical resistivity or seismic time-lapse data in these parts of the reservoir.

#### 2.5.7. Flow properties characterization and validation of processes (WP4)

Table 4 summarises the flow measurements and the porosity variations by XRCT before and after different exposure times. Hydraulic conductivity and porosity before and after exposure are plotted in Fig. 30 (Stavropoulou et al., 2023). Initial hydraulic conductivity and permeability of the tested basalt cores ranged between approximately  $10^{-10}$ – $10^{-7}$  m/s and  $10^{-17}$ – $10^{-14}$  m<sup>2</sup>, respectively. These values align with those reported for natural basalts in similar hydrogeological settings (e. g. Saar and Manga, 1999). After exposure to CO<sub>2</sub>-rich seawater for periods between one and 3.5 months, variable changes in flow behaviour were observed among the seven samples. Four cores (05-01, 05-03, 07-01, and 07-02) exhibited negligible variation in hydraulic conductivity ( $K_i/K_f \approx 1$ ), while three cores (05-02, 08-02, and 08-03) showed significant decreases, by up to one order of magnitude. These latter samples also displayed the most evident signs of porosity loss, suggesting precipitation of secondary minerals within the pore network.



Table 4: Experimental results before and after exposure to CO<sub>2</sub>

Sample	CO <sub>2</sub> exposure (days)	Pre-CO <sub>2</sub>			Post-CO <sub>2</sub>		
		K (m/s)	K (m <sup>2</sup> )	ϕ (%)	K (m/s)	k (m <sup>2</sup> )	ϕ (%)
05-01	33	8.35 10 <sup>-10</sup>	8.64 10 <sup>-17</sup>	3.2	8.55 10 <sup>-10</sup>	8.85 10 <sup>-17</sup>	3.9
05-02	28	1.06 10 <sup>-17</sup>	1.09 10 <sup>-14</sup>	19.0	7.35 10 <sup>-8</sup>	7.60 10 <sup>-15</sup>	19.0
05-03	31	6.02 10 <sup>-8</sup>	6.23 10 <sup>-15</sup>	10.8	5.59 10 <sup>-8</sup>	5.78 10 <sup>-15</sup>	10.4
07-01	28	1.51 10 <sup>-8</sup>	1.56 10 <sup>-15</sup>	7.8	1.65 10 <sup>-8</sup>	1.70 10 <sup>-15</sup>	10.3
07-02	85	1.58 10 <sup>-8</sup>	1.64 10 <sup>-15</sup>	9.8	1.79 10 <sup>-8</sup>	1.85 10 <sup>-15</sup>	11.0
08-02	110	1.83 10 <sup>-7</sup>	1.90 10 <sup>-14</sup>	9.8	1.81 10 <sup>-8</sup>	1.88 10 <sup>-15</sup>	8.3
08-03	60	1.65 10 <sup>-9</sup>	1.71 10 <sup>-16</sup>	6.5	7.32 10 <sup>-10</sup>	7.57 10 <sup>-17</sup>	5.2

The flow properties of the cores before and after exposure to CO<sub>2</sub>-rich seawater were measured in the lab using the experimental setup presented in Fig. 15 (details in Stavropoulou et al., 2024).

X-ray computed tomography (XRCT) performed for the three samples that show decrease in hydraulic conductivity revealed an overall reduction in macro-porosity of up to 1.5 % at 50 µm resolution. Fig. 30 summarizes the results. In sample 08-02, porosity decreased from 9.8 % to 8.3 % after 110 days of CO<sub>2</sub> exposure, and in 08-03 from 6.5 % to 5.2 % after 60 days. No measurable porosity change was detected in 05-02 despite a decrease in hydraulic conductivity, indicating that sub-resolution micro-porosity contributed significantly to flow reduction. The observed permeability decline therefore suggests that mineral precipitation primarily affected fine pore structures rather than the larger, XRCT-resolvable pores.

To interpret the hydraulic results, pore-scale simulations were performed on 3D networks derived from XRCT data. The original tomographic reconstructions showed poor connectivity between visible pores (> 50 µm). To model flow realistically, a dual-porosity concept was adopted: macroporosity represented by the XRCT-resolved voids and microporosity (< 50 µm) corresponding to the unresolved matrix porosity inferred from mercury intrusion porosimetry. Micropores were implemented as connecting throats between macropores, with diameters determined iteratively to reproduce experimental conductivities.

Numerical simulations of pore-pressure propagation across the reconstructed pore networks revealed distinct structural modifications following CO<sub>2</sub> exposure. Fig. 31 visualizes a pressure front propagating through the samples, before and after exposure. In samples 08-02 and 08-03, the post-exposure pressure fields displayed irregular fronts and localised zones of increased gradient, suggesting partial pore clogging. In 08-02, mineralisation produced “finger-like” pressure patterns, whereas in 08-03, a confined region of higher pressure indicated reduced connectivity. These features point to spatially heterogeneous mineral deposition and evolving permeability anisotropy within the basalt matrix.

In sample 05-02, a pre-existing micro-fissure acted as a preferential flow path before CO<sub>2</sub> injection but disappeared in the post-exposure image, implying fissure infilling or closure. This observation is consistent with a localised accumulation of mineral precipitates along fracture surfaces.



Chemical analyses of the pore fluid, particularly for sample 08-02, corroborated the physical evidence of mineralisation. The electrolytic conductivity of seawater decreased from 47.65 mS/cm (initial) to 44.99 mS/cm after circulation through the basalt core, and further to 28.30 mS/cm after 110 days of exposure to CO<sub>2</sub>-rich seawater. The observed reduction in ionic strength indicates precipitation of solid carbonate phases within the pore space. Concurrently, solution pH increased from initially acidic values to 6.6 (seawater + basalt) and 7.2 (seawater + CO<sub>2</sub>), supporting carbonate formation. These geochemical shifts, together with the measured reduction in permeability, strongly suggest that carbonation reactions occurred within the micro-porous regions of the basalt.

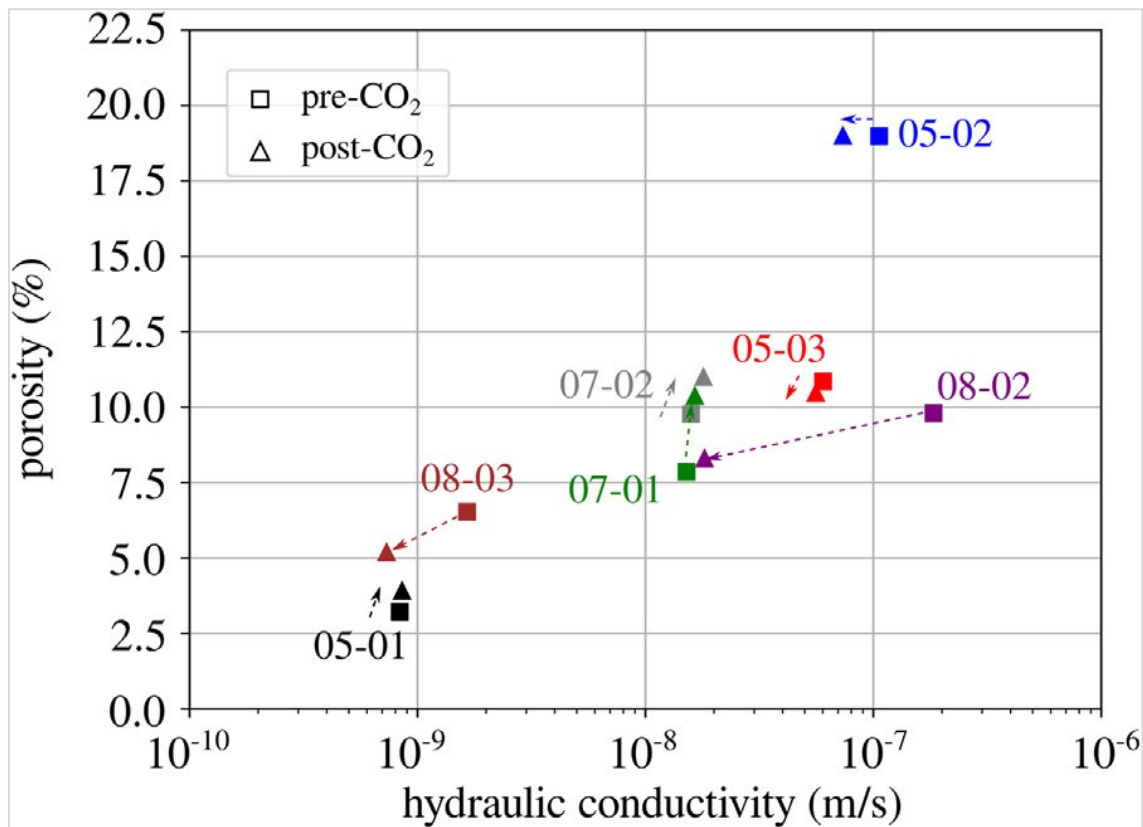


Fig. 30: Porosity and hydraulic conductivity before and after CO<sub>2</sub> exposure (from Stavropoulou et al., 2024)

In summary, across all experiments, the onset of CO<sub>2</sub>-induced mineralisation produced measurable hydromechanical effects within one to two months of exposure. Flow reduction was most pronounced in samples with higher initial olivine content and longer exposure durations. Pore-network analyses indicate that macro-porosity remained largely unchanged, while micro-porosity underwent significant constriction. These observations are consistent with, but do not yet conclusively demonstrate, carbonate mineral precipitation within the pore space. Further confirmation will require a more detailed characterization of the fluid chemistry beyond bulk indicators such as conductivity and pH, together with micro-textural and mineralogical analyses (e.g., thin-section observations) to directly identify carbonate phases and their spatial distribution.

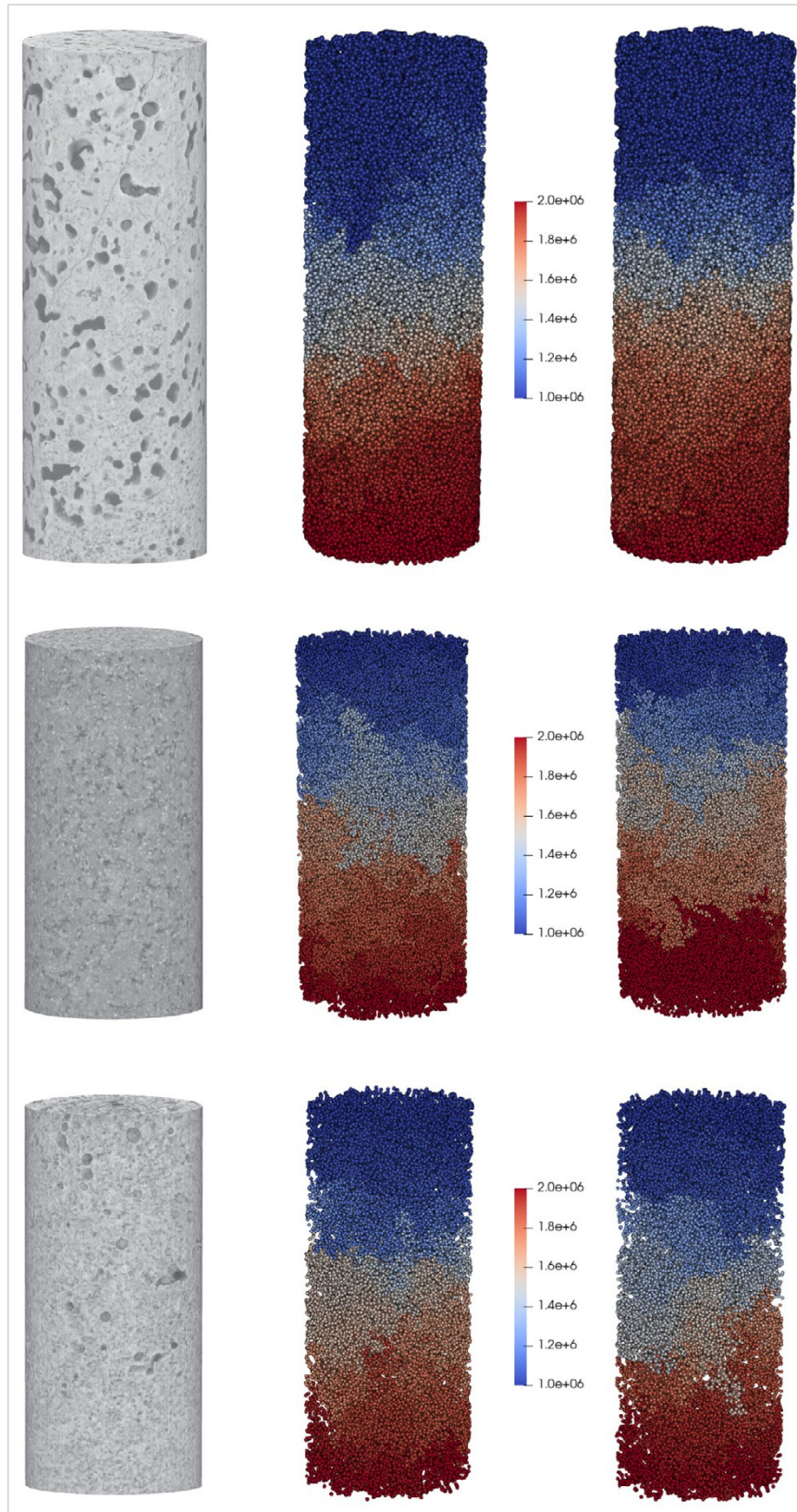


Fig. 31 Pore pressure propagation before and after CO<sub>2</sub> exposure (from Stavropoulou et al.,2023)



## Societal Acceptance

The results of the societal acceptance studies are detailed in the Deliverable 5.3 and in the paper Dallo et al., 2024. We summarize here the main aspects.

Both the focus groups and the nationwide online survey (n=503) showed low public familiarity with CCTS/CCUS technologies. Most Swiss participants had not heard of these technologies. When familiar, knowledge was superficial and often based on limited media exposure or academic contexts. Participants expressed a strong interest in learning more, particularly about the energy efficiency, CO<sub>2</sub> balance, costs, and safety of the processes.

Overall acceptance and support for CCTS/CCUS were moderate but generally positive, especially when linked to climate change mitigation. The Swiss pathway (CO<sub>2</sub> storage in recycled concrete in Switzerland developed in DemoUpCARMA) received significantly higher acceptance than the Icelandic pathway (CO<sub>2</sub> transport and storage in basalt abroad).

Acceptance drivers included:

- High concern about climate change.
- Greater trust in involved institutions (science, industry, government).
- Better understanding of the information provided.
- Higher educational level and younger age groups.

Barriers to acceptance included:

- Low knowledge, concerns about long-term safety and costs,
- Doubts about fairness when exporting Swiss CO<sub>2</sub> for storage abroad.

Perceptions of risks and benefits were pathway-specific and often reflected general uncertainty rather than detailed technical evaluation. Perceived risks included environmental harm (e.g., leakage, induced earthquakes, energy use, pollution), social concerns (fairness of exporting CO<sub>2</sub>, health effects, lack of control), and economic issues (high investment costs, fossil fuel lock-in). Perceived benefits included reduced CO<sub>2</sub> emissions, climate mitigation potential, technological innovation, and creation of local jobs.

Participants generally saw CCTS/CCUS as part of a broader portfolio of climate measures, not as a standalone solution.

About the influence of transportation on the perception of risks and benefits, pipelines and trains were considered the most suitable and secure transport means; trucks were the least preferred.

The origin of CO<sub>2</sub> influenced acceptance: participants preferred domestic capture and storage over transporting CO<sub>2</sub> abroad. For the Icelandic pathway, participants emphasized that local acceptance in Iceland is an ethical precondition.

A between-subjects experiment compared four communication formats (infographic, Q&A, LinkedIn post, written text). Infographics were the most effective and preferred format, they increased understanding, attention, and acceptance. Participants favoured concise, visually supported, and transparent information from trusted sources such as universities or public agencies. Preferences for communication channels included official websites, print media, and scientific outlets; social media was less trusted.

The study highlighted a key pattern across demographics: younger individuals showed higher support.

Trust in science correlated positively with acceptance and perceived benefits.

## 2.6 Discussion

### 2.6.1. Combined Geophysical and Geochemical Monitoring (WP2)

The combination of dissolved-gas monitoring, electrical resistivity tomography (ERT), and seismic modelling demonstrates the feasibility of multi-scale geophysical monitoring for tracing reactive fluid



migration and mineral precipitation in situ. Together, these studies advance understanding of both the short-term dynamics of injected CO<sub>2</sub> and the long-term detectability of its mineral trapping.

Fig. 32 and 33 summarize the porosity and permeability distribution in the subsurface of the pilot site with the layering identified in the rock typing, logs, cross-hole seismic and electrical resistivity data. We carried out a detailed geophysical characterisation of the prospect using cross-hole seismic and single hole electrical resistivity measurements. We complemented the interpretation of the data using well logs and mineralogical data derived from drill cuttings. Based on laboratory analyses of cuttings, we found that the target reservoir intersects four main lithological units that can be subdivided into ten layers. The dependence of both parameters (resistivity and velocity) on porosity explains the excellent agreement between seismic velocity and electrical resistivity. We use the seismic data to derive a rough porosity and permeability model of the subsurface which shows two potential preferential layers for fluid flow at 270 m to 300 m and 320 m to 350 m. This agrees well with the spinner test performed in the injection well which identifies the main inflow zones into the formation at 285 m and 335 m

Complementary seismic modelling (Junker et al., submitted *Agu* 2025) further indicates that mineral precipitation associated with CO<sub>2</sub> conversion to calcite may increase P-wave velocities by up to 38% for complete pore infill (only order of magnitude indication). Time-lapse crosshole seismic tomography could, therefore, detect even subtle ( $\geq 1\%$ ) velocity changes corresponding to partial mineralization. This threshold is well within the expected range for early-stage carbonation reactions (Adam et al., 2013; Bellezza et al., 2024), highlighting the high sensitivity of seismic methods for continuous monitoring. However, the modelling also emphasizes that survey geometry, inter-well spacing, and volcanic heterogeneity critically constrain resolution, underscoring the need for site-specific acquisition design.

Although we had difficulties with establishing long-term ERT time-series with daily resolution, we could successfully image the timelapse difference across the open-hole sections of the CBI-01 injection well (Fig. 29 and Fig. 32). The time lapse indicated the strongest resistivity decreases of up to 50% within high-permeability layers near the injection borehole consistent with basalt, or secondary minerals (e.g. pre-existing calcite) dissolution by acidic CO<sub>2</sub>-rich fluids. In contrast, resistivity remained stable or increased slightly in lower-permeability zones, where we do not expect large fluid movements. Such spatially contrasting trends support the conceptual model of a reaction front: near-well dissolution supplying cations for downstream carbonate formation. These patterns correspond closely to those predicted by reactive transport simulations (Aradóttir et al., 2012; Wu et al., 2021). However, the interpretation of the ERT data is not trivial as two main factors may influence the resistivity: First, changes in the electrical resistivity of the fluid and second variations in pore-space. The decrease in electrical resistivity close to CBI-01 could be caused by an increase in porosity, caused through dissolution of minerals in the host-rock or by the replacement of local groundwater by more conductive, injected water or through a combination of both. A distinction of those two processes solely by resistivity is not possible. A clear interpretation of the underlying geochemical process is also not trivial there as next to secondary mineral precipitation could also be caused by changes in the pore-fluid-chemistry.

The GE-MIMS measurements by Brennwald et al. (submitted *Oct* 2025) indicate strong CO<sub>2</sub> retardation relative to the He-labelled injection fluid. The lack of detectable CO<sub>2</sub> or He in the overlying freshwater aquifer (CBM-2) confirms effective hydrological confinement and minimal upward migration, suggesting some retention of the injected CO<sub>2</sub> within the target formation. It should be noted, however, that these observations are based on a relatively short measurement period and on injections involving comparatively small CO<sub>2</sub> volumes; longer-term monitoring and larger-scale injections will be required to fully assess retention and migration behaviour.

The combined application of GE-MIMS/miniRuedi and ERT at Helguvík demonstrates the complementarity of in situ dissolved-gas tracing and resistivity imaging. GE-MIMS/miniRuedi provides continuous temporal resolution of reactive gas dynamics at well locations, while ERT supplies spatial constraints on evolving porosity and fluid distribution. When integrated with seismic tomography, these methods together can characterize the entire sequence of CO<sub>2</sub> migration, dissolution, and mineralization, from meter- to decameter-scale. This multi-method approach represents a significant advance over purely geochemical monitoring, offering real-time verification of subsurface carbon fixation processes.

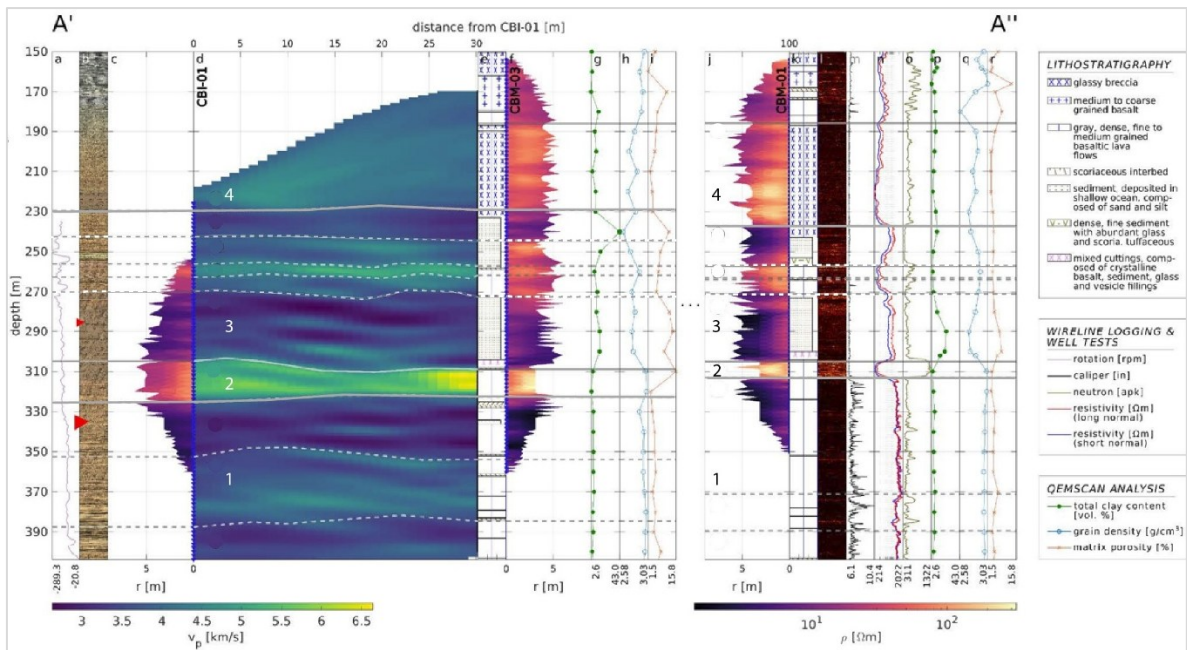


Fig. 32: Geophysical baseline characterization results with logging information along the borehole axis of CBI-01, CBM-03 and CBM-01. The ERT inversion results are shown as radial plots next to the respective boreholes in logarithmic scale (c, f and j). The crosshole seismic tomography is shown between CBI-01 and CBM-03 (d). We also show the rotational rate of the spinner test in CBI-01 (a) with the identified main inflow zones shown as red arrows in (b), the optical televiewer log for CBI-01 (b), the acoustic televiewer (l), caliper (m) and electrical resistivity (n) logs for CBM-01, lithostratigraphic interpretation by ISOR (e, k), QEMSCAN derived total clay mineral content (g, p), porosity (h, q) and density (i, r) derived from the drill cuttings for CBM-03 and CBM-01. The solid-gray lines indicate lithological unit boundaries and the dashed lines further divisions of the units into layers (from Junker et al., 2025)

The experiences done at Helgavik with the multiparameter monitoring setup provided several important lessons for future CO<sub>2</sub> mineral storage monitoring. Passive seismic monitoring based on ambient noise interferometry proved less effective than anticipated, mainly due to insufficient and unstable noise sources, limiting its ability to resolve time-lapse changes in the reservoir. Similarly, the deployment of fiber-optic (FO) sensing inside the well did not deliver the expected sensitivity, likely due to imperfect coupling with the formation. For future projects, behind-casing FO installations should be considered, as they are expected to significantly improve mechanical coupling and data quality, particularly for distributed acoustic sensing applications. More generally, the results highlight the importance of prioritizing monitoring techniques that ensure strong formation coupling and sustained signal quality over long periods.

These insights could help expand the existing Carbfix monitoring concept by promoting refined testing followed by a selective integration of geophysical methods, emphasizing permanently installed sensors, improved coupling strategies, thereby enhancing the robustness and interpretability of monitoring data at both pilot and industrial scales. Furthermore, the continuous dissolved gas measurements tested in this project have the potential to complement existing sampling and continuous geochemical measurements used at Carbfix sites. However, practical issues, mainly related to clogging of filters and membranes, reduced the availability of measurements and required frequent on-site maintenance, which would need to be improved to increase robustness and costs-effectiveness.

## 2.6.2. Rock typing (WP3)

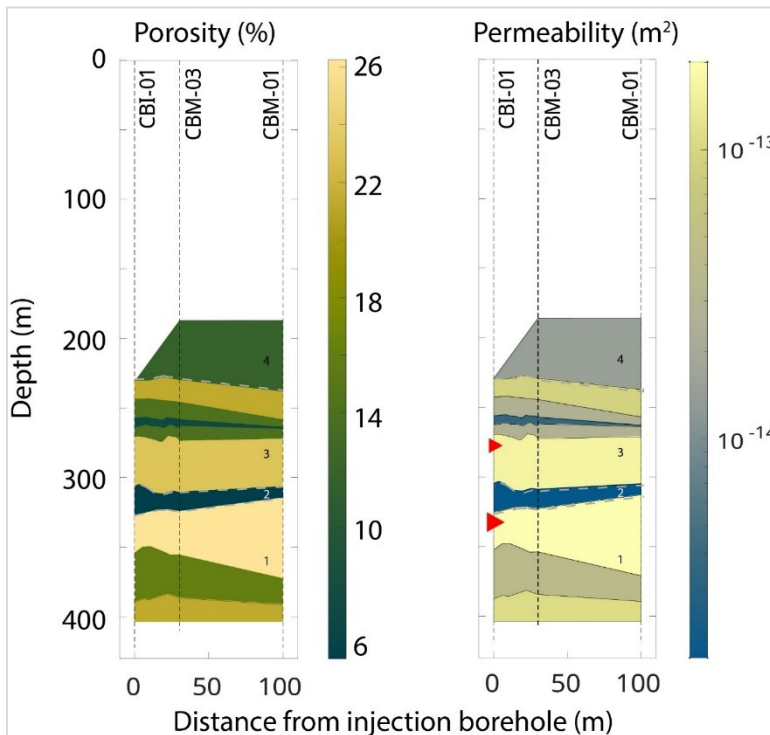
The integration of mineralogical, geochemical, and geophysical datasets from the Helgavik pilot site provides a coherent framework for understanding the heterogeneity and storage potential of basaltic reservoirs for in-situ CO<sub>2</sub> mineralization. The QEMSCAN-based mineral and chemical stratigraphy allowed for the identification of ten discrete mineral-stratigraphic units, revealing strong vertical and lateral



variations in mineral composition, porosity, and density even over short interwell distances (~70 m). Such heterogeneity plays a key role in determining the spatial distribution of permeability and reactive surface area, parameters that ultimately control the rate and extent of CO<sub>2</sub> mineralization.

The V<sub>p</sub> – porosity and V<sub>p</sub>-permeability relationship of Navarro et al. (2020) were used to obtain an estimation of distribution in situ. Note that we select to estimate the porosity starting from seismic velocities instead of the electrical resistivity measurements as those are only weakly dependent on the clay content of the rock and should therefore give a more robust estimate compared to the electrical resistivity measurements. Porosity measurements from lab analyses on cuttings were compared. For the upper 200 m the results are in good agreement with the porosity calculated through V<sub>p</sub> (Junker et al. 2025, Fig. 33), of 10 to 12%. Below 300m porosities calculated from V<sub>p</sub> are between ~14% and 26%, significantly higher than the matrix porosity. This reflect an area of high fracturing, which is detected also by the caliper log in all boreholes.

In situ porosity is expected to be higher than the 2D matrix porosity from laboratory because it includes also the contribution of the fracture porosity. The observed differences between matrix porosity derived from QEMSCAN (typically <10%) and higher connected porosities inferred from well logs and core analyses (Moscariello et al., 2023; Junker et al., 2025) highlight the importance of fracture networks in fluid flow and mineral trapping. Total porosity in basaltic reservoirs reflects both matrix and fracture contributions, with fractures serving as the primary conduits for reactive fluid transport. This dual-porosity system suggests that mineralization will likely localize along fracture planes where permeability and reactive surface area are greatest (Stavropoulou et al., 2023). The lateral variability in porosity and density within



the Helguvik reservoir correlates well with the seismic velocity and electrical resistivity variations observed by Junker et al. (2025).

Fig. 33: Cross-section porosity and permeability distribution through the study site with the layering identified in the cross-hole seismic and electrical resistivity data. The colour indicates the porosity and permeability estimated using the seismic velocities (Navarro et al. 2020). The numbers in the graphs indicate the layers as in fig 21, and the dotted grey lines represent their boundaries. Please note that both layer 1 and layer 3 could be subdivided further in sublayers based on the porosity and permeability. The red arrows indicate the main inflow zones from the well into the formation identified in the spinner test (modified from Junker et al., 2025).

### 2.6.3. Flow properties characterization and validation of processes (WP4)

The experimental and numerical findings demonstrate that exposure of basaltic material to CO<sub>2</sub>-rich seawater induces measurable alterations in flow properties within relatively short time scales, ranging from one to three months. The observed reduction in hydraulic conductivity and permeability—up to one order of magnitude in some cores—points to the onset of mineral precipitation within the pore network. This behavior is consistent with previous studies showing that carbonation reactions in basalt can occur rapidly under aqueous CO<sub>2</sub> conditions, often within months (Matter et al., 2016; Voigt et al., 2021). The



efficiency of such reactions highlights the strong reactivity of basaltic minerals, particularly olivine and pyroxene, when exposed to acidified CO<sub>2</sub>-bearing fluids (Snæbjörnsdóttir et al., 2018).

XRCT analyses and pore-network simulations confirm that permeability reduction is primarily controlled by micro-porosity (< 50 μm) rather than macro-scale voids. The dual-porosity modelling approach suggests that visible pores (> 50 μm) play a minor role in maintaining connectivity, whereas the unresolved micro-pore system governs effective flow through the matrix. Reductions of up to 43 % in micro-porosity were required to reproduce post-exposure permeability, despite only minor decreases in total porosity (≤ 1.5 %). This finding indicates that basalt permeability is strongly dependent on micro-scale connectivity and that even small reductions in fine-pore volume can cause substantial decreases in transmissivity. Fig. 34 shows a micro fissure evolution before and after exposure to CO<sub>2</sub>. It is noticeable that there is a reduction in aperture of the fissure. The results thus underscore the importance of microstructural analyses in assessing long-term injectivity of basaltic reservoirs.

The emergence of heterogeneous pressure fronts and localized flow “fingers” in post-exposure simulations highlights the spatially variable nature of mineralization. Such patterns likely arise from feedback between local flow velocity, reactive surface area, and mineral precipitation rates—processes also described in reactive transport simulations of CO<sub>2</sub>-basalt systems (Wu et al., 2021). The partial closure of a micro-fissure observed in sample 05-02 further illustrates that mineral deposition can effectively seal small fractures, enhancing containment but potentially impeding further CO<sub>2</sub> migration.

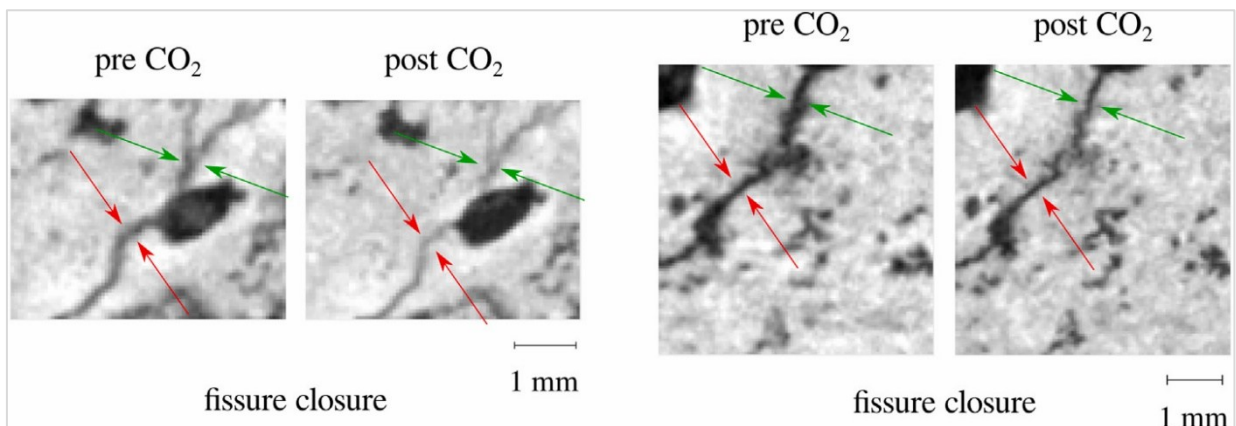


Fig. 34. Magnified locations showing micro-fissure evolution of sample 05-02 before and after CO<sub>2</sub> exposure (from Stavropoulou et al., 2024).

Geochemical evidence supports these microstructural observations. The decrease in electrolytic conductivity of the pore fluid and the concomitant pH increases after CO<sub>2</sub> exposure potentially indicate removal of dissolved ions through carbonate precipitation. Similar trends were reported in earlier basalt–CO<sub>2</sub>–water experiments (e.g. Gislason et al., 2014; Matter et al., 2009). These results confirm that dissolution of primary silicate phases releases Ca<sup>2+</sup>, Mg<sup>2+</sup>, and Fe<sup>2+</sup>, which subsequently form stable carbonates such as calcite, magnesite, and siderite. The coupling of dissolution and precipitation processes therefore leads to a dynamic competition between permeability enhancement and clogging, depending on local chemical equilibria and transport rates.

The observed differences between samples also reflect mineralogical control: olivine-rich basalts (e.g., 08-02 and 08-03) exhibited stronger permeability reduction than plagioclase-dominated ones (e.g., 05-02), consistent with the higher reactivity of mafic minerals (Liu et al., 2019). This suggests that although olivine-bearing basalts favor rapid mineralization and permanent CO<sub>2</sub> fixation, they also risk faster pore clogging. In practical terms, this trade-off implies that effective injection strategies should prioritize fractured or highly permeable zones, ensuring sustained flow while still promoting mineral trapping (Ratouis et al., 2022).

Overall, these results emphasize that CO<sub>2</sub> mineralization in basalts is governed by micro-scale processes that dictate macroscopic flow behavior. Understanding the coupled hydraulic, chemical, and



structural evolution of these rocks is therefore essential for predicting reservoir performance and designing safe, efficient large-scale CO<sub>2</sub> storage operations.

#### 2.6.4. Societal Studies (WP5)

The design of the DemoUpStorage graphics benefited from the user testing conducted in the context of DemoUpCARMA. The processes relevant to DemoUpStorage were included in the tested info-graphic. The DemoUpCARMA main infographic was evaluated with the general public through six focus groups involving 22 citizens and a between-subjects experimental survey (N = 503) carried out in 2022 and 2023 (Dallo et al., 2023). The mixed-methods approach revealed important insights into public familiarity, acceptance, and communication needs.

Overall, the Swiss public showed very limited knowledge of the technologies. Most participants were unfamiliar with the concepts but expressed interest in learning more, particularly about efficiency, safety, and climate benefits. This low familiarity, paired with curiosity, indicates that public attitudes are still forming and can be shaped through early, transparent communication.

The study found moderate but positive acceptance and support for CCTS/CCUS, driven largely by climate-related motivations rather than detailed technical understanding. The Swiss concrete pathway received higher support than the Icelandic storage option, mainly because it was perceived as local, controllable, and fairer. Key drivers of acceptance were trust in science and government, climate concern, and understanding of the information provided. Conversely, uncertainty about risks and scepticism toward institutional motives reduced support. These findings reaffirm the importance of trust and transparency for technological acceptance.

Participants associated CCTS/CCUS with both environmental and ethical risks, such as leakage, high energy use, and exporting Swiss CO<sub>2</sub> abroad. However, they also recognized significant potential benefits, notably in climate change mitigation and innovation. Overall, CCT(U)S was viewed as a complementary measure within the transition to net zero, not as a substitute for renewable energy or efficiency efforts.

A key contribution of this research is its experimental assessment of communication tools. The between-subjects survey demonstrated that infographics significantly improved comprehension, perceived credibility, and acceptance compared to text-heavy formats such as written descriptions or social media posts. Participants preferred concise, visual, and trustworthy information delivered by recognized institutions (e.g., universities or government agencies). This confirms the importance of user-centred communication design in shaping public understanding of complex technologies. Moreover, preferences for information channels varied: while traditional and institutional sources were trusted, social media was viewed with scepticism, despite its potential for outreach.

The evaluation further revealed two misconceptions of particular importance for the DemoUpStorage infographics. The first concerned the storage concept. Some thought that the CO<sub>2</sub> is mixed with seawater and then simply released into the oceans, instead of stored in a geological reservoir. The second misconception was that some participants did not realise that the CO<sub>2</sub> is captured in Switzerland and transported to Iceland; they assumed instead that it was captured directly from the air.

The findings collectively suggest that Switzerland is at an early stage of societal engagement with CCTS/CCUS. The public is not opposed but seeks reassurance regarding safety, equity, and environmental effectiveness. Acceptance will likely depend on transparent governance, co-creation of communication materials, and inclusion of local and cross-border ethical considerations. Furthermore, building trust through credible institutions and demonstrating tangible benefits (e.g., climate impact, job creation) will be essential for long-term legitimacy.

From a policy perspective, the results highlight that social acceptance cannot be assumed and must be actively cultivated. As Switzerland explores CCTS/CCUS as part of its net-zero strategy, public engagement should be integrated early into project planning, not only as a communication exercise but as a participatory process enabling citizens to voice concerns and preferences.



### 3 Conclusions and outlook

The Helguvík pilot site in Iceland provides a rare, high-resolution case study that bridges laboratory-scale reactivity, reservoir characterization, field monitoring, and public perception, addressing both the technical and social dimensions required for scaling carbon mineralization as a durable climate mitigation strategy. The integrated geological, geochemical, geophysical, and societal investigations conducted within the DemoUpCARMA and DemoUpStorage projects durable, safe, efficient, and economically viable CO<sub>2</sub> mineral storage in basaltic aquifers, with a particular emphasis on advancing and benchmarking monitoring strategies suitable for mineral storage. The results achieved allow a partial but meaningful assessment of the initially defined objectives.

Petrophysical and mineralogical analyses (Moscariello et al., in preparation) and borehole logging revealed a complex stratigraphy, with alternating high- and low-permeability basaltic layers. These variations, largely controlled by lithological facies, fracture density, and secondary alteration, govern the distribution of effective porosity and reactivity across the reservoir. Such heterogeneity enhances both the capacity and containment of CO<sub>2</sub> mineral storage by promoting localized dissolution–precipitation reactions while confining reactive fluids within low-permeability boundaries. The observed dual-porosity behaviour, matrix micro-porosity coupled with fracture-dominated permeability, was further analysed by Stavropoulou et al. (2023), whose experiments on CO<sub>2</sub>-rich seawater-basalt interactions demonstrated rapid secondary mineral precipitation (potentially carbonate) within micro-pores, leading to measurable permeability reduction within weeks. Mineralisation can impact the flow properties of the basaltic material, mainly by reduction of the micro-porosity. Successful implementation of the technology at large scales requires injection in locations of high porosity, ideally in fractured zones where flow can be ensured and mineralisation will not result in pore clogging (Stavropoulou et al., 2023.). Laboratory findings confirm that basalt-hosted systems can rapidly immobilize CO<sub>2</sub>, by using saline water as injected fluid.

Geophysical monitoring results (Junker et al., 2025) reinforce this observation. Electrical resistivity tomography (ERT) captured spatial variations that could be linked to fluid injection, and basalt dissolution, caused by acidic CO<sub>2</sub> rich fluids. These responses close to the injection borehole align well with theoretical reactive transport models. Due to the lack of reliable temperature logs, we were not able to reliably interpret the electrical resistivity changes around the CBM-01 and CBM-03 monitoring wells. Theoretical reactive transport models suggest that secondary minerals precipitate at a certain distance from the injection point. Consequently, we would expect a resistivity increase in those areas. However, it also needs to be noted that single-hole ERT measurements have a limited penetration depth (in our case approximately 5m, see red shaded areas around the wells in Fig. 5). Thus, it might be desirable in a future project to employ crosshole ERT measurements in combination with permanent temperature logging (e.g. through FO based distributed temperature sensing). The integration of miniRuedi mass spectrometry (Brennwald et al., submitted Oct 2025) further validated the geophysical measurements by providing direct, continuous tracking of dissolved gases. The strong He signal and the pronounced retardation of CO<sub>2</sub> relative to the tracer suggested some in-aquifer CO<sub>2</sub> retention and no upward migration, affirming the system's containment integrity. To be noted that our results relate to the short-term observation period, and should not be extrapolated blindly to long term storage / containment.

When dealing with heterogeneous reservoirs, whether belonging to clastic depositional environments or to carbonate settings, the understanding of lateral variability and compositional heterogeneity is essential for predicting the CO<sub>2</sub> storage potential and the possible occurrence of mineralization-driven sequestration processes. This study, carried out on basaltic rocks, poorly represented in the Swiss subsurface, highlights the value of a multiscale and multidisciplinary integrated approach which could be transferred to Swiss subsurface case studies. The interpretation of geophysical investigations used to establish the baseline at the onset of the project and geochemical continuous monitoring throughout the duration of the project, requires a fundamental understanding of the compositional and architectural characteristics of the reservoir. Consequently, mineralogical and geochemical analyses of core and cutting materials represent a primary prerequisite, a *conditio sine qua non*, for the successful design, implementation, and long-term assessment of CO<sub>2</sub> storage projects.



Numerical seismic modelling performed by Junker et al., (submitted *Agu* 2025) demonstrated that variations in P-wave velocity as small as 1 % could, in principle, be detected with the monitoring array installed in the Helguvík boreholes.

The simulations showed that CO<sub>2</sub>-induced mineral precipitation and fluid substitution generate elastic contrasts within the resolvable range of high-frequency crosshole, confirming the strong diagnostic potential of seismic methods for tracking carbonation processes. However, field verification could not be achieved because of technical failures of the hydrophone chain during the survey period. Moreover, the injected CO<sub>2</sub> was far beyond the threshold of detectability (two orders of magnitude higher than the injected CO<sub>2</sub>). Despite these setbacks, the modelling outcomes underline that, once operational reliability is ensured, time-lapse seismic monitoring can provide quantitative constraints on porosity evolution and mineralization fronts, complementing ERT and gas-tracer observations in future campaigns.

From an operational standpoint, these findings underscore a central duality: rapid mineralization enhances storage security but simultaneously reduces reservoir permeability through pore clogging. Optimizing this balance will be essential for large-scale deployment. Strategic targeting of permeable fracture zones, combined with controlled flow regulation and monitoring, can sustain injection efficiency while maximizing mineral trapping. The combined methodologies developed at Helguvík, linking mineralogical, hydrological, and geophysical diagnostics, provide a transferable framework for the design and surveillance of future basalt storage operations in both onshore and offshore environments.

Beyond technical feasibility, the societal studies led by Dallo et al. (2024) highlight that public trust, transparent communication, and equitable governance are indispensable for the acceptance of CO<sub>2</sub> mineral storage, even if transported abroad for storage. The Swiss public currently shows limited knowledge but cautious openness toward CCTS/CCUS technologies. Acceptance and support are strongly conditioned by trust, perceived benefits, and communication quality. Clear, transparent, and visually accessible communication, particularly via infographics, can significantly enhance understanding and acceptance. The results suggest that domestic, tangible pathways (like CO<sub>2</sub> mineralization in concrete) are more acceptable than international storage schemes, which raise ethical and environmental concerns. The findings emphasize that social legitimacy is contingent not only on scientific robustness but also on participatory engagement and the visibility of environmental benefits. Demonstration projects such as DemoUpCARMA and DemoUpStorage serve as critical platforms for fostering dialogue between scientists, policymakers, and local communities, and could transform perception of carbon storage from a high-risk intervention to a publicly endorsed climate solution.

The experience matured within the DemoUpStorage suggests that CO<sub>2</sub> mineral storage in basalts could represent a scientifically mature, verifiable, and publicly compatible pathway for permanent carbon sequestration. With respect to the project objectives, the demonstration of controlled CO<sub>2</sub> injection and effective hydraulic confinement at the Helguvík site was achieved. The absence of detectable CO<sub>2</sub> or tracer signals in the overlying freshwater aquifer during the monitoring period confirms effective short-term containment and supports the safety objective. In addition, the project successfully demonstrated the operability of an integrated, multidisciplinary monitoring concept, combining borehole- and surface-based geophysics with continuous dissolved-gas monitoring.

Other objectives were only partially met. While hydromechanical changes and tracer retardation consistent with CO<sub>2</sub>-rock interaction were observed, direct, spatially resolved evidence of carbonate precipitation at field scale remains below the detection limits of the applied geophysical methods for the injected CO<sub>2</sub> volumes and observation period. As a result, the project could not conclusively image mineralization fronts in situ. Nevertheless, the results meaningfully constrain the conditions under which such monitoring approaches may become effective and provide valuable bounds on sensitivity and detectability.

A general appraisal of the applied methods indicates that geophysical techniques offer clear advantages in terms of spatial coverage and non-invasive monitoring, but their effectiveness is strongly dependent on injected volumes, sensor coupling, and survey geometry. Dissolved-gas monitoring proved to have the potential to be a robust and cost-effective complement if practical issues can be solved, providing direct insights into CO<sub>2</sub> transport and retention processes, albeit without direct mineralogical confirmation. Where field-scale results remain inconclusive within the time-scale of this project, existing



laboratory experiments consistently demonstrate rapid carbonate precipitation in basaltic systems, supporting the interpretation that mineralization is occurring. Regarding monitoring suitability and certification purposes, the project shows that no single method can currently satisfy all efficiency, cost, and robustness criteria. Instead, tiered monitoring strategies appear most promising, combining low-cost continuous measurements (e.g. chemistry, dissolved gases) with targeted geophysical surveys deployed when detectability thresholds are likely to be exceeded. Such an approach balances operational costs with the need for defensible, auditable evidence of containment and long-term storage.

Finally, the project provides important insights into the transfer of knowledge across technology readiness levels (TRLs). Laboratory experiments clearly demonstrate rapid mineralization and porosity reduction, but their translation to field-scale observables remains challenging due to scale effects, heterogeneity, and limited injected volumes. This project represents a critical intermediate step, identifying where laboratory-derived expectations remain valid and where additional scaling, longer monitoring periods, and higher injection volumes are required to bridge the gap between experimental proof and industrial deployment.

Overall, while not all objectives could be conclusively met within the project scope, the results substantially advance the understanding of monitoring limits, methodological trade-offs, and design requirements for future CO<sub>2</sub> mineral storage projects. These insights provide a solid foundation for refining monitoring concepts, improving monitoring strategies, and supporting the next generation of pilot and commercial-scale storage initiatives in Switzerland and beyond.

Pilot and demonstration projects are an essential step beyond the purely academic setting, and as we argued in Becattini et al. (2024), DemoUpCarma and DemoUpStorage together have been exemplary in breaking new ground in many respects. In our assessment, the projects have had a substantial impact on the generation of know-how and on stimulating interest within industry for CO<sub>2</sub> capture and storage solutions, and they have produced valuable new knowledge on CO<sub>2</sub> storage in seawater-basalt systems. At the same time, while the results clearly demonstrate technical feasibility at pilot scale and significantly advance understanding, the most critical proof points required for commercial-scale implementation, particularly direct, field-scale confirmation of mineralization and long-term performance, could not yet be fully established within the scope of this project.

. In our assessment, the projects' overall impact on advancing both the state of the art and the state of practice in CCTS in Switzerland and internationally remains substantial, even if some key questions necessarily remain open. We are particularly encouraged that the DemoUpCarma/Storage chain has been taken up by Swiss industry, building on an agreement between the Swiss and Icelandic governments. The site we built together with Carbfix, and the knowledge we acquired, will therefore continue to be used. We also believe that, without the nucleus of DemoUpCarma/Storage, the Switzerland-based CITru project ([www.citru.ethz.ch](http://www.citru.ethz.ch)) which aims to store up to 10'000 tons of CO<sub>2</sub>, would not have been possible

## 4 National and international cooperation

Information on activities with other actors in Switzerland and/or abroad. Please use only the predefined format styles, insert text from other documents unformatted (right mouse button, [Insert options] -> [Insert text only])

A major objective of DemoUpStorage was to increase national and international collaboration on CCS, and this goal was fully achieved. DemoUpStorage connected key Swiss players with expertise in geological CO<sub>2</sub> storage—ETH Zurich, EPFL, EAWAG, and the Universities of Bern, Geneva, and Neuchâtel—into a network. The continued activity of this network in CITru and the BFE SWEET NetZero project ACHIEVE demonstrates that DemoUpStorage has kick-started a sustainable and highly important effort. Other CO<sub>2</sub>-storage projects—e.g., targeting dissolved CO<sub>2</sub> storage in shallower formations in



Switzerland, such as the Forsthaus project in Bern—likewise benefit from this network. As part of the project, we were able to educate several young PhD students and postdocs who can now lead CCS efforts in Switzerland. By presenting our work in peer-reviewed publications and at workshops and meetings, and by engaging with our international partners, we have put Switzerland firmly on the international map of countries active in geological CO<sub>2</sub> storage—something that was not the case before DemoUpCarma. The findings from the partner project DemoUpCARMA clearly show that the Swiss public cares about public acceptance in Iceland and has a preference of taking care of its CO<sub>2</sub> self-responsible. Consequently, when envisioning CO<sub>2</sub> storage abroad, social justice and its perception should also be considered. In addition, it is important to ensure that foreign initiatives for CO<sub>2</sub> storage adhere to comparable standards for project governance, particularly regarding stakeholder involvement and information policies.

## 5 Publications and other communications

Peer review publications:

Brennwald, M.S., Junker, J.S., Wang, C., Kipfer, R., Obermann, A., Voigt, M., Zappone, A. On-site dissolved-gas analysis and electric-resistance tomography as new tools to trace CO<sub>2</sub> mineral sequestration in aquifers. Submitted to *International Journal of Greenhouse Gas Control*, Oct. 2025

Dallo, I., Marti, M., Kuratle, L.D., Ly, C., Zeller, S., & Zaugg, S. (2024) Social perspectives of carbon capture, transportation, utilization, and storage in Switzerland. *Energy Research & Social Science* 114, 103588, <https://doi.org/10.1016/j.erss.2024.103588>.

Junker, J.S., Obermann, A., Voigt, M., Maurer, H., Eruteya, O. E., Moscariello, A., Wiemer, S. & Zappone, A. (2025). Geophysical Characterization of the in-situ CO<sub>2</sub> Mineral Storage Pilot Site in Helguvík, Iceland. *International Journal of Greenhouse Gas Control*, 1421, 104320. <https://doi.org/10.1016/j.ijggc.2025.104320>.

Junker, J.S., Maurer, H., Zappone, A., Wu, S.-M., Obermann, A., Feasibility of Crosshole Seismic Tomography for Monitoring In-Situ CO<sub>2</sub> Mineral Storage in Basalts: A Rock Physics- and Seismic Modelling Study, submitted to *Gcube*, Aug 2025.

Stavropoulou, E., Griner, C., & Laloui, L. (2024) Impact of CO<sub>2</sub>-rich seawater injection on the flow properties of basalts. *International Journal of Greenhouse Gas Control*, 134, 104128. <https://doi.org/10.1016/j.ijggc.2024.104128>.

Conference papers and Abstracts

Annan, P., Van der Net, A., Stavropoulou, E., Madonna, C., & Zappone, A. (2025). Microstructural controls on reactive flow and CO<sub>2</sub> mineralization in basalts: A  $\mu$ CT, SEM, and modelling approach. *World CCUS Conference 2025*, 1, 1–5. <https://doi.org/10.3997/2214-4609.202522137>

Brennwald, M. S., Junker, J. S., Kipfer, R., Obermann, A. C., Voigt, M., Wang, C., & Zappone, A. (2025). Noble gas tracing of CO<sub>2</sub> injection fluids for carbon capture and storage (CCS) using the miniRUEDI. *Goldschmidt 2025 Conference, Prague*. <https://conf.goldschmidt.info/goldschmidt/2025/meetingapp.cgi/Paper/28019>

Junker, J., Obermann, A., Brennwald, M., Voigt, M., Maurer, H., Wiemer, S., & Zappone, A. (2025). Geophysical and geochemical methods for in-situ CO<sub>2</sub> mineral storage site characterization and monitoring. *World CCUS Conference 2025*, 1, 1–5. <https://doi.org/10.3997/2214-4609.202522030>

Junker, J., Obermann, A. C., Maurer, H., Wiemer, S., & Zappone, A. (2025). Geophysical methods for characterizing and monitoring the in-situ CO<sub>2</sub> mineral storage site in Helguvík, Iceland—Field



experiments and modelling results. *EGU General Assembly 2025*. <https://doi.org/10.5194/egusphere-egu25-3040>

Junker, J. S., Obermann, A., Zappone, A., Maurer, H., & Wiemer, S. (2024). Geophysical site characterization and monitoring of CO<sub>2</sub> mineralization in basaltic complexes, Helguvík, Iceland. *EGU General Assembly 2024*. <https://doi.org/10.5194/egusphere-egu24-9061>.

Stavropoulou, E., & Laloui, L. (2023). CO<sub>2</sub> storage in basalts: The impact of mineralization on the hydromechanical response of the material. *Proceedings of the 9th International Congress on Environmental Geotechnics (ICEG)*, Chania, Greece.

Stavropoulou, E., Griner, C., & Laloui, L. (2024). Hydromechanical impact of carbon mineralization in basalts. *EGU General Assembly 2024*. <https://egusphere-egu24-20615>.

Zappone, A., Brennwald, M., Junker, J., Moscariello, A., Obermann, A., Voigt, M., Stavropoulou, E., & Wiemer, S. (2025). Storing Swiss CO<sub>2</sub> in Icelandic basalt: The DemoUpStorage geophysical monitoring project. *EAGE Workshop on Carbon Capture and Storage (CCS) in Basalts 2025*, 1, 1–3. <https://doi.org/10.3997/2214-4609.202570008>

Zappone, A., Wiemer, S., & the DemoUpStorage Team. (2023). The DemoUpStorage project: Monitoring mineral carbonation in Icelandic basalts. *EGU General Assembly 2023*. <https://doi.org/10.5194/egusphere-egu23-14256>

Wiemer, S., Zappone, A., Rinaldi, A. P., Gunatilake, T., Junker, J., Obermann, A., Becattini, V., & Mazzotti, M. (2024). Storing Swiss CO<sub>2</sub> in Iceland and Switzerland: Insights from DemoUpCARMA and beyond. *1st Caprock Integrity & Gas Storage Symposium*, St-Ursanne, Switzerland. [www.cigss.ch](http://www.cigss.ch).

## 6 References

Adam, L., Van Wijk, K., Otheim, T., & Batzle, M. (2013). Changes in elastic wave velocity and rock microstructure due to basalt–CO<sub>2</sub>–water reactions. *Journal of Geophysical Research: Solid Earth*, 118(8), 4039–4047. <https://doi.org/10.1002/jgrb.50302>

Andrews, G.D., (2023). Geological carbon storage in northern Irish basalts: prospectivity and potential. *Frontiers in Climate*, 5, p.1207668.

Aradóttir, E. S., Sigurdardóttir, H., Sigfússon, B., & Gunnlaugsson, E. (2011). Carbfix: A CCS pilot project imitating and accelerating natural CO<sub>2</sub> sequestration. *Greenhouse Gases: Science and Technology*, 1(2), 105–118. <https://doi.org/10.1002/ghg.18>

Aradóttir, E. S. P., Sonnenthal, E. L., Björnsson, G., & Jónsson, H. (2012). Multidimensional reactive transport modelling of CO<sub>2</sub> mineral sequestration in basalts at the Hellisheidi geothermal field, Iceland. *International Journal of Greenhouse Gas Control*, 9, 24–40. <https://doi.org/10.1016/j.ijggc.2012.02.006>

Archie, G. E. (1942). The electrical resistivity log as an aid in determining some reservoir characteristics. *Transactions of the AIME*, 146(1), 54–62. <https://doi.org/10.2118/942054-G>

Aming, K., Offermann-van Heek, J., Sternberg, A., Bardow, A., & Ziefle, M. (2020). Risk–benefit perceptions and public acceptance of carbon capture and utilization. *Environmental Innovation and Societal Transitions*, 35, 292–308. <https://doi.org/10.1016/j.eist.2019.05.003>

Bachmann, F., Hielscher, R., & Schaeben, H. (2010). Texture analysis with MTEX: Free and open-source software toolbox. *Solid State Phenomena*, 160, 63–68. <https://doi.org/10.4028/www.scientific.net/SPP160.63>

Becattini, V., Gabrielli, P., Antonini, C., Campos, J., Acquilino, A., Sansavini, G., & Mazzotti, M. (2022). Carbon dioxide capture, transport and storage supply chains: Optimal economic and environmental performance of infrastructure rollout. *International Journal of Greenhouse Gas Control*, 117, 103635. <https://doi.org/10.1016/j.ijggc.2022.103635>



- Bellezza, C., Barison, E., Farina, B., Poletto, F., Meneghini, F., Böhm, G., Draganov, D., Janssen, M. T. G., van Otten, G., Stork, A. L., Chalari, A., Schleifer, A., & Durucan, S. (2024). Multi-sensor seismic processing approach using geophones and HWC DAS in the monitoring of CO<sub>2</sub> storage at the Hellisheiði geothermal field in Iceland. *Sustainability*, *16*(2), 877. <https://doi.org/10.3390/su16020877>
- Björnsson, S., Einarsson, P., Tulinius, H., & Hjartardóttir, Á. R. (2020). Seismicity of the Reykjanes Peninsula 1971–1976. *Journal of Volcanology and Geothermal Research*, *391*, 106369. <https://doi.org/10.1016/j.jvolgeores.2018.04.026>
- Brennwald, M. S., Schmidt, M., Oser, J., & Kipfer, R. (2016). A portable and autonomous mass spectrometric system for on-site environmental gas analysis. *Environmental Science & Technology*, *50*, 13455–13463. <https://doi.org/10.1021/acs.est.6b03669>
- Brune, J. N. (1970). Tectonic stress and the spectra of seismic shear waves from earthquakes. *Journal of Geophysical Research*, *75*(26), 4997–5009. <https://doi.org/10.1029/JB075i026p04997>
- Brune, J. N. (1971). Correction to “Tectonic stress and the spectra of seismic shear waves from earthquakes.” *Journal of Geophysical Research*, *76*(20), 5002. <https://doi.org/10.1029/JB076i020p05002>
- Carlson, R. L. (2014). The Effects of Alteration and Porosity on Seismic Velocities in Oceanic Basalts and Diabases. *Geochemistry, Geophysics, Geosystems*, *15*(12), 4589–98. <https://doi.org/10.1002/2014GC005537>.
- Chatelain, Y. (2024). *Structural analysis of a highly oblique rift zone influenced by a transform fault in southwest Iceland* (Master's thesis). University of Geneva
- Darcy, H. (1856). *Les fontaines publiques de la ville de Dijon: Exposition et application des principes à suivre et des formules à employer dans les questions de distribution d'eau, etc.* V. Dalmont.
- Davis, D. A. (2022). *Investigating carbon mineralization storage potential in SW Icelandic basaltic formations* (Master's thesis). University College London.
- Furre, A.-K., Eiken, O., Alnes, H., Vevatne, J. N., & Kiær, A. F. (2017). 20 years of monitoring CO<sub>2</sub> injection at Sleipner. *Energy Procedia*, *114*, 3916–3926. <https://doi.org/10.1016/j.egypro.2017.03.1523>
- Gassmann, F. (1951). Über die Elastizität poröser Medien. *Mitteilungen aus dem Institut für Geophysik, ETH Zürich*, *17*.
- Gidden, M. J., Joshi, S., Armitage, J. J., et al. (2025). A prudent planetary limit for geologic carbon storage. *Nature*, *645*, 124–132. <https://doi.org/10.1038/s41586-025-09423-y>
- Gislason, S. R., & Oelkers, E. H. (2014). Carbon storage in basalt. *Science*, *344*, 373–374. <https://doi.org/10.1126/science.1250828>
- Gostick, J., Aghighi, M., Hinebaugh, J., Tranter, T., Hoeh, M. A., Day, H., Spellacy, B., Sharqawy, M. H., Bazylak, A., Burns, A., & Lehnert, W. (2016). OpenPNM: A pore network modeling package. *Computing in Science & Engineering*, *18*(4), 60–74. <https://doi.org/10.1109/MCSE.2016.49>
- Goertz-Allmann, B. P., Langet, N., Iranpour, K., Kühn, D., Baird, A., Oates, S., Rowe, C., Harvey, S., Oye, V., & Nakstad, H. (2024). Effective microseismic monitoring of the Quest CCS site, Alberta, Canada. *International Journal of Greenhouse Gas Control*, *133*, 104100. <https://doi.org/10.1016/j.ijggc.2024.104100>
- Grab, M., Zürcher, B., Maurer, H., & Greenhalgh, S. A. (2015). Seismic velocity structure of a fossilized Icelandic geothermal system: A combined laboratory and field study. *Geothermics*, *57*, 84–94. <https://doi.org/10.1016/j.geothermics.2015.06.004>
- Gislason, S. R., Broecker, W. S., Gunnlaugsson, E., Snæbjörnsdóttir, S. Ó., Mesfin, K. G., Alfredsson, H. A., et al. (2014). Rapid solubility and mineral storage of CO<sub>2</sub> in basalt. *Energy Procedia*, *63*, 4561–4574. <https://doi.org/10.1016/j.egypro.2014.11.489>
- Global Carbon Council. (2024). *Guidance for geological CO<sub>2</sub> storage (GCCM006 Guidance v. 1.1)* (p. 61). Global Carbon Council



- Gunnarsson I., Aradóttir E. S., Oelkers E. H., Clark D. E., Amarson M. P., Sigfússon B., Snæbjörnsdóttir S. Ó., Matter J. M., Stute M., Júlíusson B. M. and Gíslason S. R. (2018). The rapid and cost-effective capture and subsurface mineral storage of carbon and sulfur at the CarbFix2 site. *International Journal of Greenhouse Gas Control*, 79, 117–126.
- Hayashi, M. (2004). Temperature–electrical conductivity relation of water for environmental monitoring and geophysical data inversion. *Environmental Monitoring and Assessment*, 96(1–3), 119–128. <https://doi.org/10.1023/B:EMAS.0000031719.83065.68>
- Jobin, M., & Siegrist, M. (2020). Support for the deployment of climate engineering: A comparison of ten different technologies. *Risk Analysis*, 40(5), 1058–1078. <https://doi.org/10.1111/risa.13462>
- Junker, J. S., Wu, S.-M., Obermann, A. C., Maurer, H., & Wiemer, S. (2022). *Seismic monitoring strategies for carbon dioxide mineralization in basalt* (Master's thesis). ETH Zürich.
- Kaven, S. H., Hickman, A. F., McGarr, A., Walter, W. L., & Ellsworth, W. L. (2014). Seismic monitoring at the Decatur, IL, CO<sub>2</sub> sequestration demonstration site. *Energy Procedia*, 63, 4264–4272. <https://doi.org/10.1016/j.egypro.2014.11.461>
- Keller, G. V., & Frischknecht, F. C. (1966). *Electrical methods in geophysical prospecting* (Monographs on Electromagnetic Waves). Pergamon Press, 519pp.
- Lanz, E., Maurer, H., & Green, A. G. (1998). Refraction tomography over a buried waste disposal site. *Geophysics*, 63(4), 1414–1433. <https://doi.org/10.1190/1.1444443>
- Li, C., & Zhang, X. (2024). Geophysical monitoring technologies for the entire life cycle of CO<sub>2</sub> geological sequestration. *Processes*, 12(10), 2258. <https://doi.org/10.3390/pr12102258>
- Li, H., & Zhang, J. (2011). Elastic moduli of dry rocks containing spheroidal pores based on differential effective medium theory. *Journal of Applied Geophysics*, 75(4), 671–678. <https://doi.org/10.1016/j.jappgeo.2011.09.012>
- Liu, D., Agarwal, R., Li, Y., & Yang, S. (2019). Reactive transport modeling of mineral carbonation in unaltered and altered basalts during CO<sub>2</sub> sequestration. *International Journal of Greenhouse Gas Control*, 85, 109–120. <https://doi.org/10.1016/j.ijggc.2019.04.006>
- Matter, J., & Kelemen, P. B. (2009). Permanent storage of carbon dioxide in geological reservoirs by mineral carbonation. *Nature Geoscience*, 2, 837–841. <https://doi.org/10.1038/ngeo683>
- Matter, J. M., Stute, M., Snæbjörnsdóttir, S. Ó., Oelkers, E. H., Gíslason, S. R., Aradóttir, E. S., Sigfússon, B., Gunnarsson, I., Sigurdardóttir, H., Gunnlaugsson, E., Axelsson, G., Alfredsson, H. A., Wolff-Boenisch, D., Mesfin, K., de la Reguera Taya, D. F., Hall, J., Dideriksen, K., & Broecker, W. S. (2016). Rapid carbon mineralization for permanent disposal of anthropogenic carbon dioxide emissions. *Science*, 352(6291), 1312–1314. <https://doi.org/10.1126/science.aad8132>
- McGrail, B. P., Spane, F. A., Amonette, J. E., Thompson, C. R., & Brown, C. F. (2014). Injection and monitoring at the Wallula Basalt Pilot Project. *Energy Procedia*, 63, 2939–2948. <https://doi.org/10.1016/j.egypro.2014.11.316>
- Miller, S. L.M., Stewart, R.R. (1990). Effects of Lithology, Porosity and Shaliness on P- and S-Wave Velocities from Sonic Logs. *Canadian Journal of Exploration Geophysics*, 26(1–2), 94–103.
- Myer, E. M., & Arnaldsson, A. (2019). *Kísilverksmiðja Stakksbergs í Helguvík: Líkanreikningar til mats á áhrifum grunnvatnstöku* [Technical report]
- Navarro, J., Teramoto, E. H., Engelbrecht, B. Z., & Kiang, C. H. (2020). Assessing hydrofacies and hydraulic properties of basaltic aquifers derived from geophysical logging. *Brazilian Journal of Geology*, 50(4). <https://doi.org/10.1590/2317-4889202020200013>
- Oelkers, E. H., Gíslason, S. R., & Matter, J. (2008). Mineral carbonation of CO<sub>2</sub>. *Elements*, 4, 333–337. <https://doi.org/10.2113/gselements.4.5.333>



- Oltra, C., Sala, R., Solà, R., Di Masso, M., & Rowe, G. (2010). Lay perceptions of carbon capture and storage technology. *International Journal of Greenhouse Gas Control*, 4(4), 698–706. <https://doi.org/10.1016/j.ijggc.2010.02.001>
- Panzer, F., Zechar, J. D., Vogfjörð, K. S., & Eberhard, D. A. J. (2016). A revised earthquake catalogue for South Iceland. *Pure and Applied Geophysics*, 173(1), 97–116. <https://doi.org/10.1007/s00024-015-1115-9>
- Peterson, J. R. (1993). Observations and modeling of seismic background noise. *USGS Open-File Report* (No. 93-322). <https://doi.org/10.3133/ofr93322>
- Ratouis, T. M. P., Snæbjörnsdóttir, S. Ó., Voigt, M. J., Sigfússon, B., Gunnarsson, G., Aradóttir, E. S., & Hjörleifsdóttir, V. (2022). Carbfix-2: A transport model of long-term CO<sub>2</sub> and H<sub>2</sub>S injection into basaltic rocks at Hellisheiði, SW-Iceland. *International Journal of Greenhouse Gas Control*, 114, 103586. <https://doi.org/10.1016/j.ijggc.2022.103586>
- Raza, A., Glatz, G., Gholami, R., Rost, S., & Thomas, C. (2002). Array seismology: Methods and applications. *Reviews of Geophysics*, 40(3). <https://doi.org/10.1029/2000RG000100>
- Renard, P., Genty, A., & Stauffer, F. (2001). Laboratory determination of the full permeability tensor. *Journal of Geophysical Research: Solid Earth*, 106(B11), 26443–26452. <https://doi.org/10.1029/2001JB000243>
- Rezvani Khalilabad, M., Axelsson, G., & Gislason, S. R. (2008). Aquifer characterization with tracer test technique: Permanent CO<sub>2</sub> sequestration into basalt, SW Iceland. *Mineralogical Magazine*, 72(1), 121–125. <https://doi.org/10.1180/minmag.2008.072.1.121>
- Sæmundsson, K., Sigurgeirsson, M. Á., & Friðleifsson, G. Ó. (2020). Geology and structure of the Reykjanes volcanic system, Iceland. *Journal of Volcanology and Geothermal Research*, 391, 106501. <https://doi.org/10.1016/j.jvolgeores.2018.11.022>
- Sánchez-Pastor, P., Obermann, A. C., Reinsch, T., Ágústsdóttir, T., Gunnarsson, G., Tómasdóttir, S., Hjörleifsdóttir, V., Hersir, G. P., Ágústsson, K., & Wiemer, S. (2021). Imaging high-temperature geothermal reservoirs with ambient seismic noise tomography: A case study of the Hengill geothermal field, SW Iceland. *Geothermics*, 96, 102207. <https://doi.org/10.1016/j.geothermics.2021.102207>
- Snæbjörnsdóttir, S. Ó., Wiese, F., Fridriksson, T., Ármannsson, H., Einarsson, G. M., & Gislason, S. R. (2014). CO<sub>2</sub> storage potential of basaltic rocks in Iceland and the oceanic ridges. *Energy Procedia*, 63, 4585–4600. <https://doi.org/10.1016/j.egypro.2014.11.491>
- Snæbjörnsdóttir, S. Ó., & Gislason, S. R. (2016). CO<sub>2</sub> storage potential of basaltic rocks offshore Iceland. *Energy Procedia*, 86, 371–380. <https://doi.org/10.1016/j.egypro.2016.01.038>
- Snæbjörnsdóttir, S. Ó., Gislason, S. R., Galeczka, I. M., & Oelkers, E. H. (2018). Reaction path modeling of in-situ mineralisation of CO<sub>2</sub> at the Carbfix site at Hellisheiði, SW-Iceland. *Geochimica et Cosmochimica Acta*, 220, 348–366. <https://doi.org/10.1016/j.gca.2017.09.053>
- Snæbjörnsdóttir, S. Ó., Sigfússon, B., Marieni, C., et al. (2020). Carbon dioxide storage through mineral carbonation. *Nature Reviews Earth & Environment*, 1, 90–102. <https://doi.org/10.1038/s43017-019-0011-8>
- Stavropoulou, E., Griner, C., & Laloui, L. (2024). Impact of CO<sub>2</sub>-rich seawater injection on the flow properties of basalts. *International Journal of Greenhouse Gas Control*, 134, 104128. <https://doi.org/10.1016/j.ijggc.2024.104128>
- Stauffacher, M., Muggli, N., Scolobig, A., & Moser, C. (2015). Framing deep geothermal energy in mass media: The case of Switzerland. *Technological Forecasting and Social Change*, 98, 60–70. <https://doi.org/10.1016/j.techfore.2015.05.018>
- Víkingsson, S., & Kristinsson, B. (1982). *Hólmsberg geological report* (OS-82042/VOD-25 B). Orkustofnun, Reykjavík



- Voigt, M., Marieni, C., Baldermann, A., Galeczka, I. M., Wolff-Boenisch, D., Oelkers, E. H., & Gislason, S. R. (2021). An experimental study of basalt–seawater–CO<sub>2</sub> interaction at 130 °C. *Geochimica et Cosmochimica Acta*, 308, 21–41. <https://doi.org/10.1016/j.gca.2021.05.056>
- White, D. (2013). Seismic characterization and time-lapse imaging during seven years of CO<sub>2</sub> flood in the Weyburn field, Saskatchewan, Canada. *International Journal of Greenhouse Gas Control*, 16(Supplement 1), S78–S94. <https://doi.org/10.1016/j.ijggc.2013.02.006>
- Wu, H., Jayne, R. S., Bodnar, R. J., & Pollyea, R. M. (2021). Simulation of CO<sub>2</sub> mineral trapping and permeability alteration in fractured basalt: Implications for geologic carbon sequestration in mafic reservoirs. *International Journal of Greenhouse Gas Control*, 109, 103383. <https://doi.org/10.1016/j.ijggc.2021.103383>
- Yurikov, A., Tertyshnikov, K., Yavuz, S., Shashkin, P., Isaenkov, R., Sidenko, E., Glubokovskikh, S., Barraclough, P., & Pevzner, R. (2022). Seismic monitoring of CO<sub>2</sub> geosequestration using multi-well 4D DAS VSP: Stage 3 of the CO<sub>2</sub>CRC Otway project. *International Journal of Greenhouse Gas Control*, 119, 103726. <https://doi.org/10.1016/j.ijggc.2022.103726>
- Zappone, A., Rinaldi, A. P., Grab, M., Wenning, Q., Roques, C., Madonna, C., Obermann, A., Bernasconi, S. M., Soom, F., Cook, P., Guglielmi, Y., Nussbaum, C., Giardini, D., & Wiemer, S. (2020). Fault sealing and caprock integrity for CO<sub>2</sub> storage: An in-situ injection experiment. *Solid Earth Discussions*. <https://doi.org/10.5194/se-2020-100>

